ABSTRACT

Title of Document: MICROELECTRONIC CIRCUITS FOR NONINVASIVE EAR TYPE ASSISTIVE DEVICES

Koranan Limpaphayom, Ph.D., 2009

Directed By: Professor Robert W. Newcomb
Department of Electrical and Computer Engineering

An ear type system and its circuit realization with application as new assistive devices are investigated. The auditory brainstem responses obtained from clinical hearing measurements are utilized for which the ear type systems mimicking the physical and behavioral characteristics of the individual auditory system are developed. In the case that effects from the hearing loss and disorder can be detected via the measured responses, differentiations between normal and impaired characteristics of the human auditory system are made possible from which the new noninvasive way of correcting these undesired effects is proposed. The ear type system of auditory brainstem response is developed using an adaptation of the nonlinear neural network architecture and the system for making a correction is realized using the derived inverse of neural network. Microelectronic circuits of the systems are designed and simulated showing a possibility of developing into a hearing aid type device which

potentially helps hearing impaired patients in an alternate and noninvasive useful way.

MICROELECTRONIC CIRCUITS FOR NONINVASIVE EAR TYPE ASSISTIVE DEVICES

By

Koranan Limpaphayom

Dissertation submitted to the Faculty of the Graduate School of the
University of Maryland, College Park, in partial fulfillment
of the requirements for the degree of
Doctor of Philosophy
2009

Advisory Committee:
Professor Robert W. Newcomb, Chair
Professor Pamela Abshire
Professor Nicholas Declaris
Professor Martin Peckerar
Professor Lourdes Salamanca-Riba

Dedication

This dissertation is dedicated to my family.

Acknowledgements

The dissertation could not have been completed without the valuable advices and opportunities I have received for which I am greatly grateful. First I would like to express my deepest thanks to my advisor, Professor Robert W. Newcomb, for all his guidance, advice and support. He has always been available happy to help and give suggestion for all students. I have valued all the things I have learned. His kind encouragement and generous involvement have made my graduate study away from home more pleasant. I also would like to thank Professor Martin Peckerar and Professor Pamela Abshire for many helpful suggestions, encouragement and patience in reviewing and commenting on presentations and research aspects which help me to improve and make the dissertation better. I also would like to thank Professor Nicholas Declaris for kindly consenting to join the defense and for his cheerful words. I especially would like to thank Professor Lourdes Salamanca-Riba for kindly accepting to be on the committee. I would like to express my great gratitude for all the committee members for spending their valuable time to review the dissertation. I also thank Professor Louisa Sellami for agreeing to be on the committee. I would like to thank Professor Carol Espy-Wilson for providing data of the speech signals. I also would like to thank Professor Permsarp Isipradit, for collaborating on the research, providing the data, and allowing me to make ABR measurements and participate in the hearing evaluations at the Otolaryngology clinic, King Chulalongkorn Memorial Hospital - Chulalongkorn University, Bangkok, Thailand. I have learned valuable knowledge and earned hand on experiences during the time there. I also wish to thank Professor Saowaros Asawavichianginda, for giving useful suggestions. I would like to

thank Professor Parinya Luangpitakchumpon for generously answering medical questions and to Ms. Prapapan Jaipakdee for helping me with the measurements. Also, I thank Professor Manut Utoomprurkporn, for his generous help contacting the ABR equipment manufacturers. I thank Professor Onanong Kulapatana, for help with the collaborative research and Dr. Montien Saubhayana especially for help with the collaborative research and for many suggestions. I would like to acknowledge encouragements from Yinyin Zhao, Dr. Yu Jiang, Dr. Li Wang, and Dr. Angela Hodge. I thank the graduate school for the support during the time of writing this dissertation.

Finally I would like to thank my family: father, mother, brother, and sister. Thank you all very much.

Table of Contents

List of Figures

Chapter 1

Introduction

Noninvasive means to correct hearing loss and disorder are proposed for which a new ear type system is developed with a realization of its circuit. This leads to an investigation of a new type of assistive device for the hearing impaired that helps to cancel and correct the effects from hearing disorder and potentially improves the hearing ability. In this introductory chapter, we summarize

1. overview and motivation of the research
2. main contributions
3. organization of the dissertation

1.1 Overview and Motivation

With its complex and inaccessible structure, it is a difficult task to study the internal mechanisms of the human auditory system and treat any hearing loss and disorder. Various measurements have been utilized to learn more about the function of hearing organs and the sound interpretation process inside the brain for accurate diagnosis and proper treatment. Although, direct stimulation of the specific location inside the auditory system can be done on experimental animals, noninvasive ways are much more preferable especially for humans. Noninvasive means to correct an unwanted effect from auditory damage and disorder is investigated and implemented

in this research which paves a way for a possible development of a new type of hearing aid that should be a much more effective and beneficial assistive device improving the hearing abilities of the aid users. Unlike conventional hearing aids, whose amplifying gains are adjusted over some limited sets of frequency bands or all frequency bands according to the frequency specific audiometric thresholds measured with the standard pure tone audiograms, we take into account the physical and behavioral characteristics of an individual's hearing function and hearing loss configuration and incorporate them into the hearing aid design. The idea initiated in [1]-[2] is that we create a mathematically representative ear type system descriptive of the human auditory system, particularly the auditory sensitivity and characteristics for which another ear type system inverse to this system can also be developed. As such, cascading the inverse system with the original system yields the identity output. The hearing aid, as shown in Fig. 1.1, is then composed of the connection of the ear type system with normal characteristics and the system inverse to the aid user's ear type system so that damaged parts and undesired hearing loss effects are potentially

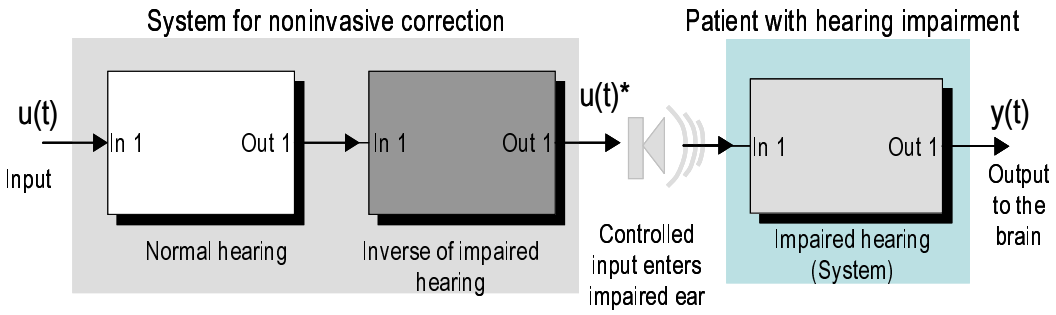

Figure 1.1. Block diagram of the proposed hearing aid technique

cancelled and corrected. To some extent, the assistive devices such as eyeglasses and contact lens exemplify the proposed correct technique in which a pair of corrective lens is used to correct defective eyesight. The lenses correct the focus of the eyes as a result people wearing eyeglasses can see as if they had normal visions.

In [2], modeling of the ear type system was made possible by using the stimulated acoustical emission signal that can be detected noninvasively in the human ears. The emitted signals are known as transiently evoked otoacoustic emission (TEOAE), also known as Kemp echoes after the first discovery by D.T. Kemp [3]. With its noninvasive property, inexpensive equipments, and fast testing time, the TEOAE is widely used as a tool to make a diagnosis and gain access into the functioning of the human auditory system from the external ear to the outer hair cells level inside the inner ear [4]. It is also effectively accepted as a reliable method for hearing loss diagnosis, hearing sensitivity evaluation and screening for both children and adults clinically used in hospitals today [5]-[9].

Here we extend the study of human auditory system functioning beyond that, for which the use of the auditory brainstem response (ABR) is investigated. The ABR is an electrical signal measured on the scalp in response to the acoustical stimulation in the ear [10]-[17]. It reflects the synchronous activity of neurons within the human auditory system and tests the functions of the cochlea, auditory nerve and brainstem auditory nervous pathways. Its waveform, Fig. 1.2, lasts about ten milliseconds and consists of five major peaks which are believed to be generated from the cochlea, and

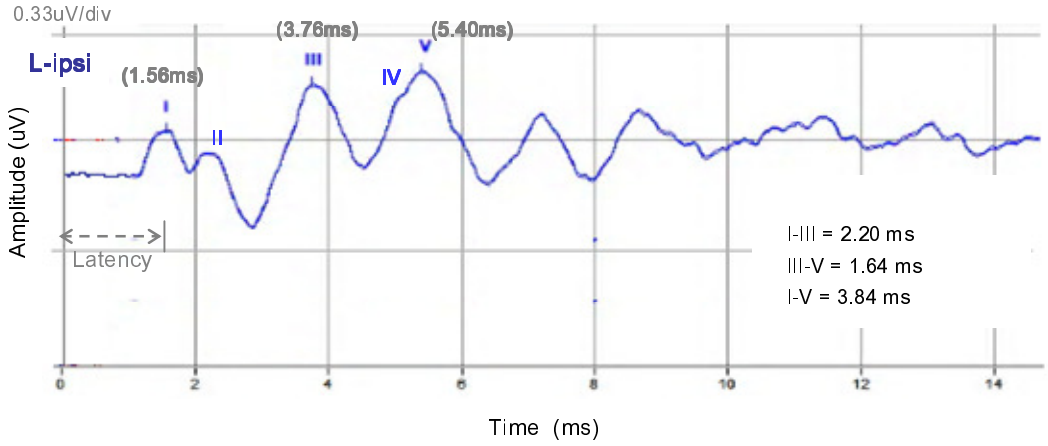

Figure 1.2. An example of the auditory brainstem response (ABR) measured from an adult with normal hearing. Latency, measured in ms, is a time occurrence of the peak of ABR waves labeled with Roman numbers I to V

along the auditory nervous pathways to the lower level of the central auditory nervous system almost at midbrain [10]. The characteristics, such as major wave latencies (I, III and V), inter-wave latencies (I-III, III-V and I-V), inter-aural wave V latencies, their amplitudes, and overall waveform morphology, are clinically used since they are generally consistent among people at adult ages with normal hearing and healthy auditory organs such that the norms can be established for hearing diagnostic and evaluation [18]-[21]. Also, these characteristics are highly affected by cochlear and retrocochlear (beyond the cochlea) pathologies which are clinically compared with the established normative criteria to identify for hearing loss and threshold and also to diagnose the disorders and tumors of the auditory system [14]-[17], [22]-[23]. The ABR is a useful tool for testing the integrity of the auditory nerve and brainstem in addition to that of the cochlea. Its special advantage over others is that the test is

objective and the measured response is also reliable regardless of the patient's awareness. This is great for newborns or anyone having a difficulty responding to a conventional pure tone audiogram. The ABR together with the Kemp echoes are therefore also acceptably used worldwide as the universal newborn hearing screening and evaluation programs [5]-[9]. The measured signals are compared against standardized response patterns to make a diagnosis for further treatment. The worldwide success of these programs allows the early intervention of any disorder so the patients can get appropriate hearing assistive devices and other hearing rehabilitation steps for better speech learning and development.

The ABR is certainly a useful tool to assess the hearing function and diagnose the hearing loss and disorder of the ear, auditory nerve and brainstem pathways. As a result, these properties are made use of in our research to develop the ear type systems that can capture the characteristics of individual auditory function via measured ABRs both from normal and impaired ears. The noninvasive technique is designed to correct the impaired ear by using the developed ear type systems from which a hearing aid type device can be implemented. From clinical applications on the use of ABR as diagnosis tools for auditory processing of normal and impaired functions [8]-[9], [12]-[17] and as monitoring indicators in the operating room [24]-[26] and from past research findings on the use of ABR with conventional hearing aids [27]-[30], changes of the characteristics of ABR from abnormal to normal and near normative criteria are shown to be associated with improved hearing ability. The method in this dissertation can hypothetically be sufficient condition for correcting

the unwanted effects from the auditory impairment and dysfunction resulting in better hearing and improved speech understanding. The final results will be very helpful for providing a novel alternate improved means of correction of the hearing impairment.

1.2 Main Contributions

The main contributions of the dissertation are summarized as follows.

- The new mathematically representative ear type system of the auditory brainstem response is developed by using the modified dynamical nonlinear neural network architecture, as shown in equations (3.1)-(3.3), for characterizing the hearing function and characteristics of the individual auditory system (see Section 3.2). Possible application of the ear type system for multichannel recording of the electrical activities measuring from the brain is given (see Section 3.4).
- The new noninvasive correction technique of effects from the hearing loss and disorder using our developed ear type systems is introduced, as per Fig. 4.1. By using the clinically measured auditory brainstem responses, assessment and determination of the auditory loss and damage are extended to the higher levels of the human auditory system such that the proposed correction technique incorporating the auditory brainstem response is more likely associated with improved speech perception (see Section 4.5.1).
- The modified technique for deriving an inverse of the dynamical nonlinear neural network with ear type system representation is given (see Section 4.2). The technique has extra advantages especially for a multilayer nonlinear

neural network with numbers of neurons and inputs-outputs whose inverse system cannot be set up by solving a reciprocal of the transfer function, by using an inverse function of a nonlinear activation function, and/or by finding an inversion of row or column vectors and matrices, particularly for a case of single input and single output with many internal neurons.

- Additional simulations and discussions on potential benefits of the proposed hearing aid compared to a conventional one are performed in Section 4.5 to show the possible validity of the proposed correction method and system to be used as a real hearing aid.
- Possible circuits for implementing the proposed method into a hearing aid are designed in Chapter 5 showing various circuit components (see Section 5.2), parameter scaling for transistorized circuits (see Section 5.1), and additional circuits with variable weight setting for alternate adjustment capability (see Section 5.2).

1.3 Organization of the Dissertation

The dissertation is organized in six chapters.

Chapter 1 introduces an overview of the concepts and motivation of the investigation of the new assistive device. This includes the use of the auditory brainstem response which leads to the proposed correction method and applications of the new type of hearing aid. The main contributions and organization of the thesis are also given, in Section 1.2 above.

Chapter 2 describes a brief explanation of basic anatomy and physiology of the human auditory system focusing on the hearing function, mechanism, and hearing loss configurations. The auditory brainstem response and the usage in hearing function assessment and hearing impairment diagnosis are introduced. The basic concept of the conventional hearing aid and a review on pertinent hearing aid researches from literatures are also given in this chapter.

Chapter 3 focuses on the methods starting with the ABR measurement and data collection. Next, modifying of the nonlinear neural network purposefully for modeling of the measured responses and setting up the ear type system is present. The discussions on system identification steps and modeling methods are then given. As an example, the method is simulated using Matlab and Simulink by using data from a hearing test of a patient with a sensorineural hearing loss. The extension of the ear type system applicable for multichannel auditory evoked potentials is also given.

Chapter 4 discusses the main scheme for noninvasive correction of auditory impairment as introduced in Fig. 1.1. A new technique is introduced for deriving a new mathematical description of the system inverse to the nonlinear neural network representative ear type system of auditory brainstem response given in Chapter 3. The technique for setting up the inverse system is also applicable to a general case of nonlinear artificial neural network architectures for other applications in which correction or certain signals are needed, such as in the model controller design or the decoding of input signals from processed signals. The results from the proposed technique are presented which can be developed into a new hearing aid. Evaluations of the potential performance are discussed by comparing between the techniques and

results presented in this dissertation and those used in other conventional hearing aids.

Chapter 5 focuses on the circuit design and realization of the developed ear type system for possible further application in hearing aid hardware implementation. The mathematical description of the system for making a correction of unwanted effects from auditory loss and damage is realized in circuits. Required parameter scaling and value shifting necessary for transistorized circuits are presented with results. Additional circuits with variable weight adjustments are also given.

Chapter 6 summarizes the dissertation and gives some open problems for future research directions.

Chapter 2

Human Auditory System, Hearing impairments, Auditory Brainstem Response and Hearing Aid

This chapter addresses brief background and literature reviews on

1. Anatomy and physiology of the human auditory system introducing the basics of hearing and hearing impairment
2. Auditory brainstem response including the basic concept and the use in hearing diagnosis
3. Hearing aids including the basic concept of the conventional hearing aid and a literature review of relevant hearing aid researches

2.1 Anatomy and physiology of the human auditory system and hearing impairment

Hearing is a very complex process involving many anatomical organs and mechanisms working together where the main simplified representations are discussed as presented in Fig. 2.1 showing the basic anatomy of the ear, the cochlea inside the inner ear, and the auditory system. The hearing function of the human auditory system consists mainly of two parts which are the sound conduction and transduction by the ear and sound interpretation by the auditory nervous system. Sound as acoustic signal enters the ear through the outer ear, hits the ear drum, which

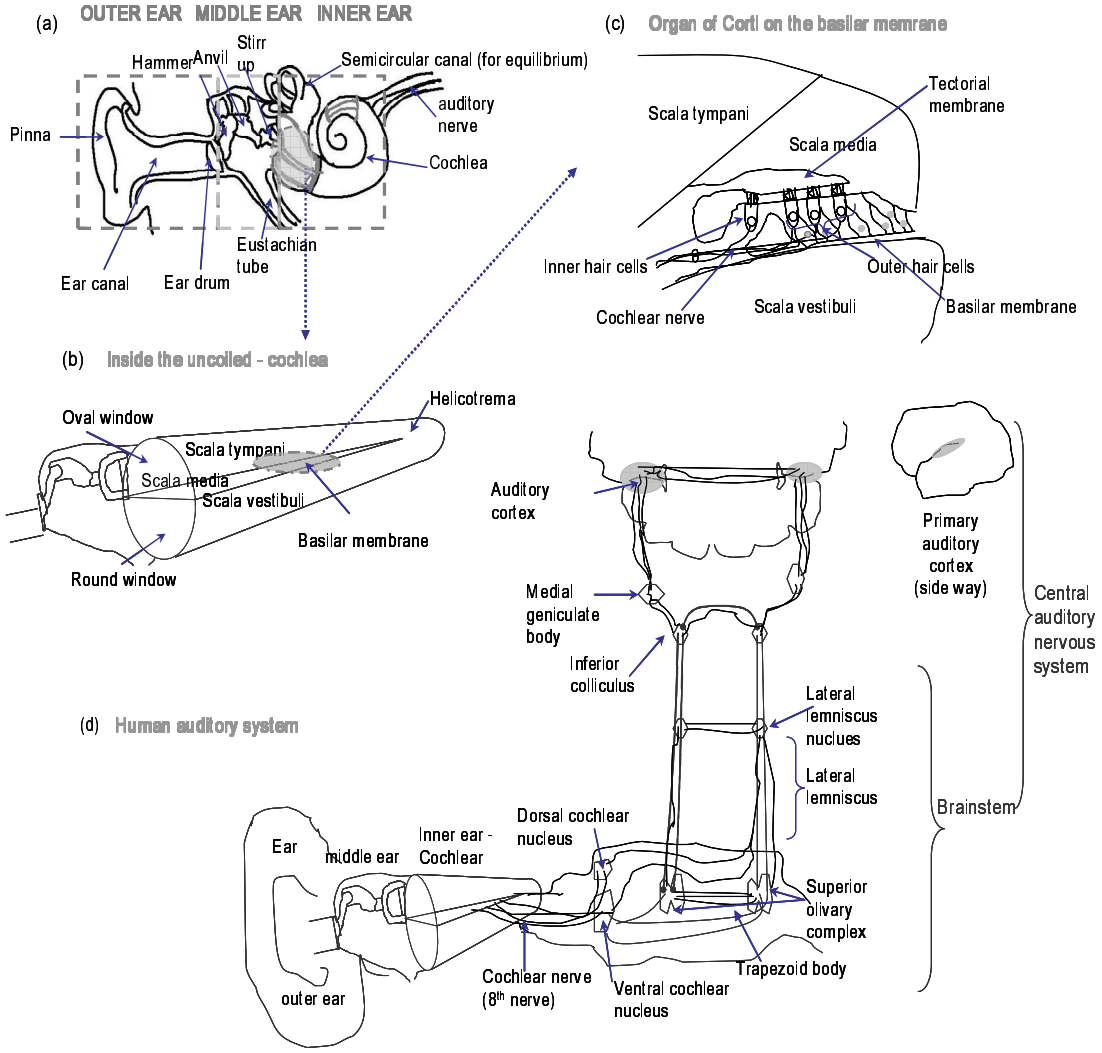

Figure 2.1. Schematic diagrams of (a) anatomy of the ear, (b) the unfolded cochlea (c) the Organ of Corti showing sensory hair cells, and (d) the main auditory nerve, nuclei, and pathways of the auditory nervous system [13,p.35-37], [16,pp.19–84], [17,pp.1–17]. Lines represent connections, not exact numbers of paths in these simplified drawings.

is also known as the tympanic membrane, separating the outer and middle ears, gets transferred by the three bones inside the middle ear into mechanical vibration of fluid inside the inner ear, and then gets transformed into the electrical neural signals by

sensory cells inside the cochlea of the inner ear. The signals are sent along the cochlear nerve, auditory nuclei, fiber, and brainstem auditory pathway to the central auditory nervous system for interpretation inside the brain. The mechanism and process underlying perception and interpretation of sound by the auditory cortex are very complicated and have been of interest in researches and clinics in order to develop neural prostheses and study neural plasticity [31]-[34]. Some of the techniques that have been utilized are, for example, techniques using electric fields such as the electroencephalographic (EEG) method, using magnetic fields such as the magnetoencephalography (MEG) method or magnetic resonance imaging (MRI) technique, and using injected radioactive chemicals such as those used in the positron emission tomography (PET) scan. They are found to be useful tools to learn more about brain activities at cortical levels [31]-[33]. The primary region of the auditory cortex, as indicated in Fig. 2.1(d), inside a brain was approximately inferred from animal testing using invasive methods because there are inevitably differences between animals and humans. With developing technologies, the noninvasive or partially invasive methods can be performed on people with confirmed brain lesions or from the brain imaging techniques, such as MRI; however, with many connections of neurons and nerve fibers within the brain, other regions of the brain can also contribute to auditory perception and speech interpretation [15,p.452], [16,p.266], [17, pp. 173-175], [35].

As we understand the basis of the hearing organs and functions, hearing loss and impairment are generated from the disorders of one or more of these organs. Here,

essential aspects of hearing impairments are discussed. Categorized by the locations of the disorders, hearing loss can be divided into four types [36]-[37].

- Conductive hearing loss where the damage is to the conduction of sound by either the outer ear or the middle ear, for example, the middle ear infection. The conductive hearing loss is usually medically or surgically treatable.
- Sensorineural hearing loss (SNHL) where the damage is to either the inner ear or the auditory nervous pathways from the inner ear to the brain. Losses resulted from the sensory organs inside the cochlea is sometimes referred to as a cochlear loss or a sensor loss and those from the auditory nervous system are referred to as a retrocochlear loss or a neural loss. The sensorineural loss is currently alleviated by using a hearing aid in the outer ear for mild to moderate cases. Permanent damage to the sensory hair cells in the cochlea in most profound cases can be alleviated by using a cochlear implant. An implanted electrode array directly stimulates the cochlear nerve bypassing the damaged sections. This is commercially available and proven to be very successful [38]-[40]. There is also a brainstem implant device [40]-[41] directly stimulating the cochlear nucleus of the brainstem for a case of damage to the cochlear nerve, such as from a removal of tumor. However, the success of this brainstem implant is limited, which may due to the tumor removal surgery during which a flow of blood supply to the cochlear nucleus can be damaged. This also leads to researches on an auditory midbrain implant [42].

- Mixed hearing loss which is the mixture of both conductive and sensorineural hearing losses. The hearing aids such as, bone-anchored types [36] or hearing aids in the tooth [43]-[44], are some of the options for assistive devices.
- Central hearing loss where the damage is to the brain mainly the central auditory nervous system of the brain. The central hearing loss is not commonly found compared to the other types. It is a case where a patient can acknowledge the presence of the sound but sometimes cannot interpret what is being said resulting in poor word recognition scores during the hearing test especially for complex speech and speech in the presence of background noise. The hearing aid is of little value in alleviating this type of loss. A speech and hearing rehabilitation and control of the environment factors may alleviate and assist the patients.

For the auditory brainstem response, the measured ABR characteristics are affected by both conductive and sensorineural hearing losses. The ABR is typically measured with an air-conducted stimulus that is affected by both losses. This is also the one used in the dissertation. However, the ABR can also be measured with a bone-conducted stimulus for a quick differentiation between the two types of losses when testing newborns or for use with ears with visible signs of severe outer or middle ear infections [15, p.460]. More discussion on the ABR signals is given in Section 2.2.

Hearing loss can also be divided according to magnitude of the hearing threshold measured with a pure tone audiogram. The pure tone audiogram is usually the first choice in testing human hearing because it is quick, easy, and cheap. It is a subjective

behavioral measurement which requires behavioral responses from the patients. Audio sine waves of commonly used frequencies fixed at 250, 500, 1k, 2k, 4k, and 6 kHz are fed into the ear to determine the lowest sound level that a person can hear or show sign of behavioral response. The audible frequency for humans with normal hearing is from 20 – 20,000Hz. The average of all audiometric thresholds are calculated as a pure tone threshold for fitting a linear analog hearing aid or as low, mid-, or high frequency thresholds for a multi-bands digital hearing aid. Hearing loss is typically categorized as normal (<25 dB HL), mild (25 – 40 dB HL), moderate (40 – 55 dB HL), moderately severe (55 – 70 dB HL), severe (70 – 90 dB HL), and profound (>90 dB HL). A unit, dB HL, is a decibels hearing level, which is calibrated from average threshold levels of adults with normal hearing at each measured audiometric frequency and also of the audiometers and the earphones. The values are then established as the reference which is usually calculated and built into the audiometer equipment with specified ear phones [36]-[37], [45]. For example, 0 dB HL corresponds to a lowest sound level that normal hearing people can hear, not an absence of sound, which also varies at each audiometric frequency: 250, 500, 1k, 2k, 4k, and 6k Hz.

For clarification, a quantification of sound level is physically measured as a sound pressure with a unit Pascal (Pa). However, the sound pressure is usually referred to a unit in decibels. Sound pressure level (dB SPL),

$$\text{dB SPL} = 20 \times \log_{10}(P/P_{ref}) \tag{2.1}$$

where P is a sound pressure in Pa and P_{ref} is the reference sound pressure = 20 uPa which is usually considered a minimum sound level that a human can hear [37], [45]. The hearing level is calculated based on the audiometric frequency, so

$$\text{dB HL at } \ldots \text{ Hz} = (\text{dB SPL})_{tester} - (\text{dB SPL})_{ref} \quad \text{at } \ldots \text{ Hz} \qquad (2.2)$$

where $(\text{dB SPL})_{ref}$ is a sound level required of a group of individuals with normal hearing and $(\text{dB SPL})_{tester}$ is a sound level required of a tester to hear. All are calculated at each of specific frequency (Hz).

The behavioral hearing threshold measurements and the ways of compensating for the loss of frequency specific sound quantification are useful; however, they may only account for a portion of the loss. The hearing loss that was considered to originate from dysfunction and pathology of the cochlea may be in part caused by the disorder of the auditory nervous system [17,pp.201-251] which cannot be clearly identified by the pure tone audiogram. Also, a requirement for a subjective decision from a patient limits its use with newborns, young children, and difficult-to-test patients. Beside the behavioral measure, additional objective auditory electrophysiologic tests, such as otoacoustic emission and auditory evoked response, are beneficial for hearing assessment and diagnosis of pathologies. Also, researches on the sound perception process and assessment of the auditory nervous system inside the brain can be accomplished by using the evoked potentials measurements such as, the ABR, to gain more insight into the physiology of the auditory system and the auditory processing functions and impairments.

2.2 Auditory brainstem response

Auditory evoked potential responses, such as, electrocochleography (ECochG), auditory brainstem response (ABR), auditory middle latency response (MLR), auditory late latency response (LLR), and others, are all useful for hearing evaluation and assessment [11]-[17], [46]. For example, ECochG is the potential response reflecting activities within the cochlea by using an electrode placed on the ear canal surface as close to the ear drum as possible or using an electrode perforating through the ear drum and resting on the round window since the signal quality depends very_much on the electrode sites. The closer the electrode is to the cochlear nerve, the better reliable signals are received. It is typically used in research on experimental animals [46], [55]. Now ECochG is only used in some cases of hearing diseases since the activities of the cochlea can also be recorded by the ABR in which the ECochG is equivalent to wave I component.

Mainly, the use of ABR is investigated in the dissertation. The auditory brainstem response (ABR), which is also known as brainstem auditory evoked potential (BAEP), or brainstem evoked response (BSER), is the most common used and well-known because it is the short latency potential (about 10 ms after stimulus) that can be easily recorded and reliably detected. Using the middle latency (MLR) or the late latency responses (LLR) would be useful as well in hearing function assessment and diagnosis, but the MLR, which reflects the activities at higher level of the central auditory nervous system, tentatively about mid-brain area with latency 10 – 50 ms after evoked stimulus, and the LLR, which reflects the activities at the

cortical area with latency 50 – 300 ms after stimulus, require very long testing and analysis time periods by a highly experienced audiologist. The MLR and LLR waveform characteristics and morphology are highly influenced by a patient's state of arousal, movement, and level of awareness [12]-[17]. Also there is tentatively much more variability within the same patient and between patients [20]-[21]. The ABR on the other hand appears to be less variable and is easier to identify. It also has received more attention, so there are many references available regarding normative data and methods for objective hearing diagnosis.

The ABR is the short latency auditory evoked potential response that lasts about 10 ms after the stimulation and consists of primary five waves customarily labeled by Roman numerals I-V [11] as shown in Fig. 2.2. Time zero represents the stimulation onset. Although, direct stimulations and invasive studies of the responses from the single nerve cells and nerve fibers in animals are possible, for human noninvasive measures are more suitable. The ABR measure is a far field recording, so the anatomical locations inside the human auditory systems that generate these waves can not be yet exactly pinpointed. Also, since the auditory system is a complex structure consisting of networks of nuclei and connections of nerve fibers, the main waves (I-V) of the ABR that are believed to be generated from the precise anatomical sites can also be contributed to from the surrounding auditory organs as well. By combining the data inferred from experimental animals and recorded from patients with confirmed site of lesions or with exposed organs during a surgery, the components of the ABR waves are believed to be generated from the corresponding

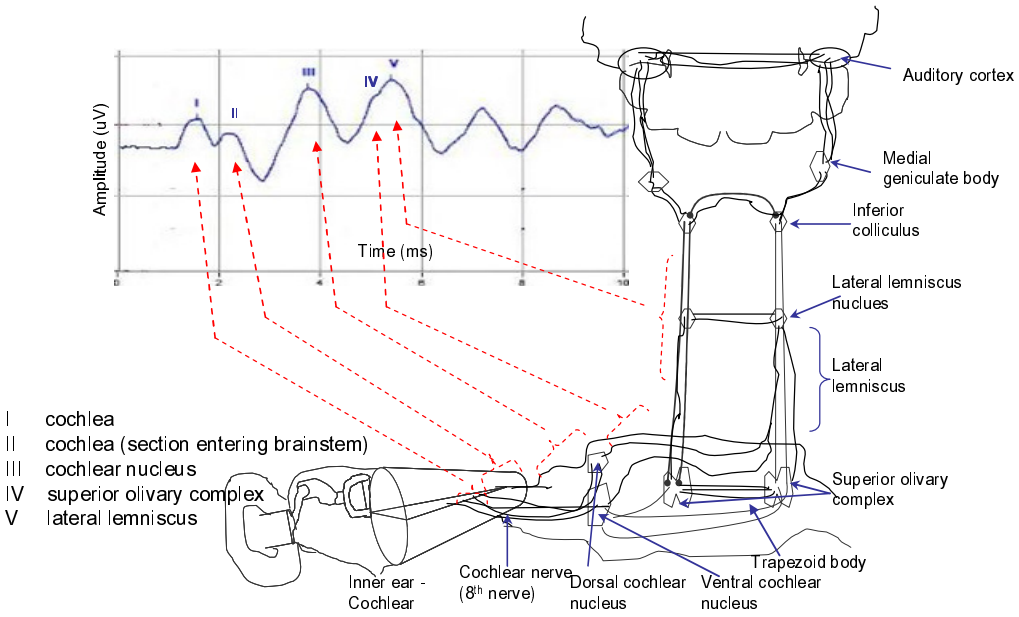

Figure 2.2. Simplified diagram of the anatomical origins of the auditory brainstem waves [10]-[11],[13,p.44],[15,p.425],[16,p.266],[17,p.175],[35]

sites in the auditory pathway as shown with dashed lines in Fig. 2.2 [10]-[11], [13, p. 44], [15, p. 425], [16, p. 266], [35].

The auditory stimulus that is used in Fig. 2.2 and in the dissertation is a click pulse, as per Fig. 2.3, which is also the most commonly used stimulus for evoking the ABR. The rectangular voltage pulses are converted into the acoustical clicks fed into the ear via an earphone. With the sharp rise and fall times, it is believed to effectively excite the synchronous activities of all auditory neurons that give rise to the easily identified and clearer signals. Its broad frequency spectrum also provides a good assessment and diagnosis of a wide working frequency region of the cochlea and auditory neurons in general. For a frequency specific response, a tone burst stimuli

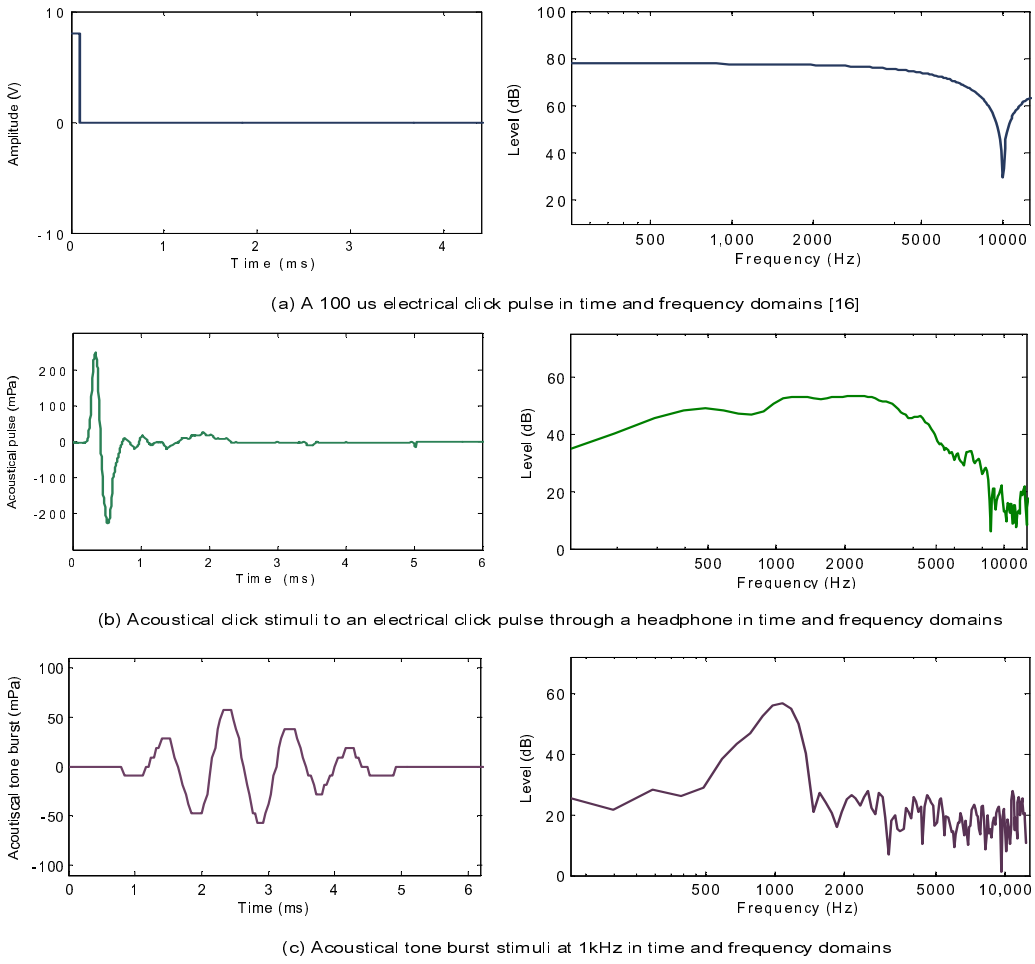

Figure 2.3. Typical used stimulus signals

can be used but the measured responses are not as clear to identify and have poor waveform morphology. Tone burst-ABR is commonly used as a quick way to compare the hearing test results with those from a pure tone audiogram by using a tone burst at the audiometric frequencies and comparing the latency of wave V of the ABR against normal limits. Wave V is the most robust and largest of all components and can be reliably identified despite the poor ABR waveform morphology [12]-[17].

The stimulus signals typically used in the ABR measurements are shown as examples in Fig. 2.3.

Amplitudes and latencies of the responses are evaluated and compared to the normative criteria that are established as a normal standard because the ABR wave characteristics of normal hearings are quite consistent in healthy adults' ears and throughout one's adulthood. There might, however, be slight variability among babies and older adults for which different sets of normative ABR characteristic criteria can be set up accordingly for more accurate results, for example, a normative data established for newborns to 6 months or for adults 60 to 70 years old. Some other environmental factors can affect the ABR characteristics, such as different ear phones, however they are typically taken into account when establishing the clinical norms. Both conductive and sensorineural hearing loss affect the response characteristics as well as the pathologies of the ear and auditory pathway such as tumors. ABR can be a much cheaper alternative for diagnosis of medium sized tumors to Magnetic Resonance Imaging. It can also be used for monitoring the auditory function in the operating room. Though, there could be limitations of the use of ABR because the signal might be absent in profound deafness cases.

The typical normal ABR waveform with click stimulus is presented in more detail in Fig. 2.4 for illustrative purpose. As common in most bioelectrical signal recording and processing techniques, repeating stimulus and averaging of the measured signals are required to reduce noise and artifacts and enhance the signal to

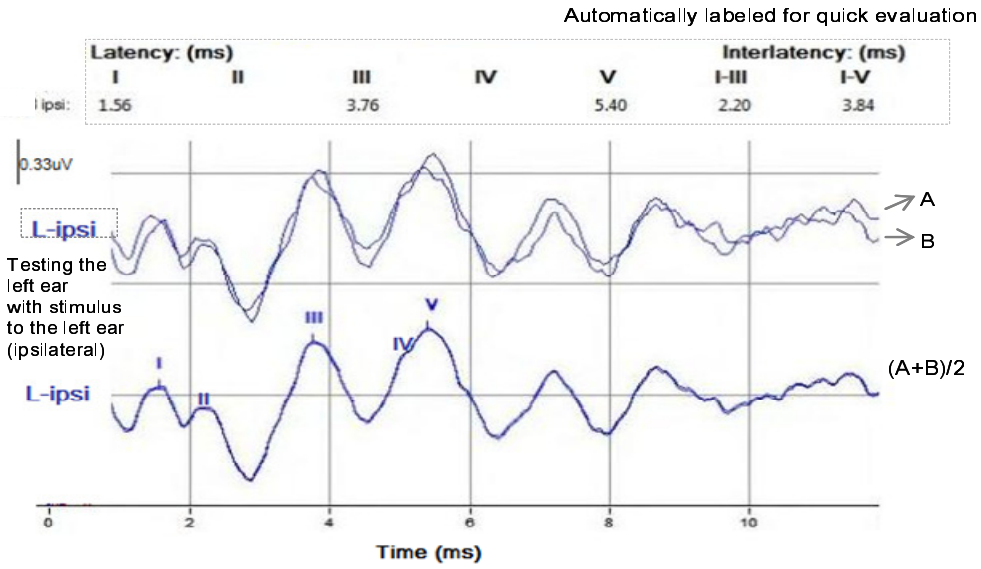

Figure 2.4. Typical ABRs recorded from a person with normal hearing showing the reproducible ABR with clear waveform morphology and response parameters within the normal limits.

noise ratio. As per Fig. 2.4, the upper curves represent two ABR signals each being a sum of 1,000 averaging responses alternately recorded in two independent memory storages A and B of the ABR-test equipment, which are used as a way to ensure the reliability and reproducibility of the recording procedures. The lower curve represents the stable ABR result with good morphology which is the average of the 2,000 averaging responses from the above two curves.

The normal ABR in Fig. 2.4 shows clear and good waveform morphology with absolute wave latencies (wave I, III, and V), inter-wave latencies (between waves I-III, III-V, and I-V), and amplitudes within the normal limits. Although, all waves I – V of the ABR can be identified in Fig. 2.4 and in most normal cases, the

prominent waves I, III, and V are typically used in diagnosis of the hearing impairment. For instances, the normative absolute wave latencies that are implemented at the Otolaryngology clinic of the King Chulalongkorn Memorial Hospital for quick evaluations are wave I at 1.64 (±2×0.12) ms, III at 3.51 (±2×0.11) ms, and V at 5.34 (±2×0.20) ms. The hearing loss and pathologies of the auditory organs are usually suspected if there is deviation from these desired ABR parameters. For example, in a typical case of conductive hearing loss, latencies of waves I, III, and V are usually beyond the normal limits, but the interwave latencies are within the normal ranges and the amplitudes and waveform morphology are also normal. For a case of sensorineural hearing loss that is of cochlear origin, the delayed latency, absent or reduced amplitude of wave I are usually expected, but the later components of ABR waves are unaffected. Poor waveform morphology might be seen. For a sensorineural loss that is of retrocochlear origin, the clear normal wave I and a prolonged or poor waveform of later wave components are typically present.

The conductive and sensorineural hearing loss effects on the ABRs are selected to present in Fig. 2.5 for illustrative purposes. Figure 2.5(a) shows the ABR measured from an ear with a typical case of conductive loss. Since the outer ear or middle ear is damaged, the sound intensity to the inner ear and the successive originating sites is reduced. The latencies of all waves are all delayed. The interwave latencies are generally within normal limits. The ABR typically shows good waveform morphology and normal amplitudes [47]-[48]. Figure 2.5(b) shows the ABR measured from an ear with sensorineural hearing loss that is due to a neural

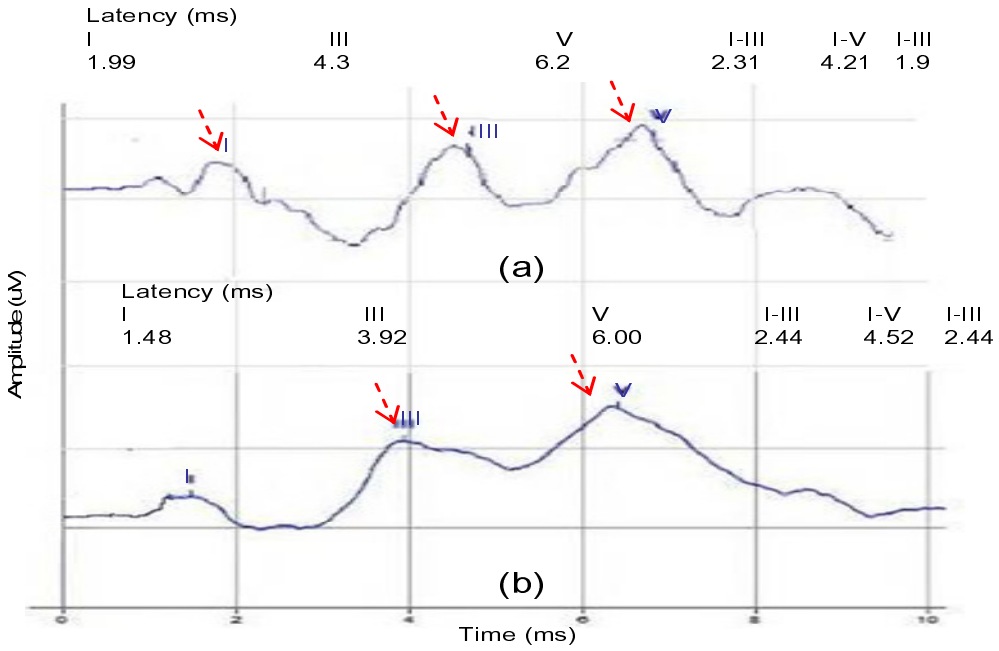

Figure 2.5. Two case examples of abnormal ABRs recorded from a patient with (a) a typical conductive hearing loss and (b) a mild sensorineural hearing loss. Dashed arrows indicate delayed latencies.

loss. The wave I is present within normal limits but wave III and V are slightly prolonged [48]. The ABR is certainly a useful tool to assess the hearing function and diagnose the hearing loss and disorder of the peripheral cochlea, auditory nerves, and brainstem auditory pathway.

2.3 Basics of a conventional hearing aid and reviews on relevant hearing aid researches

In order to compare with the proposed assistive device using technique investigated in the dissertation, in this section essential basics and information of

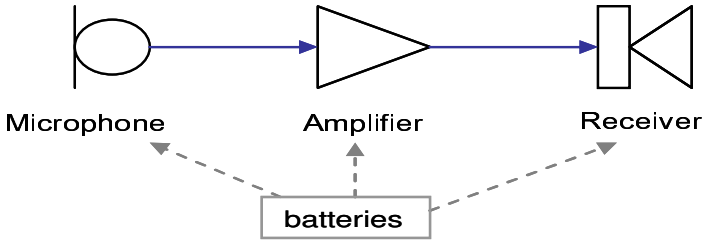

Figure 2.6. Simple diagram of hearing aid components

conventional hearing aids are introduced. A hearing aid is basically constructed from four main components which are (1) a microphone to transform audio signal into electrical signal, (2) an amplifier to raise the sound level, (3) a receiver to convert electrical signal back to sound, and (4) batteries to power all components as shown in Fig. 2.6. Its performance and capacity have been evolving and improving as changes in signal processing and technologies have become available. Smaller sizes and better designs have kept up with technology to satisfy the aid users with signal processing using analog, analog programmable, to digital programmable technologies. All these have the main common purpose of providing amplification of sound.

Hearing aid gains are set according to the degree of hearing loss typically measured by the pure tone audiogram as discussed in Section 2.1. An example of a threshold-frequency audiogram is given in Fig. 2.7(a) of which the gain-frequency settings of the hearing aid are then aimed to match these prescribed targets based on the results of the individual's audiogram. An audiogram in Fig. 2.7(a) shows the hearing levels tested by air conducted pure tone signals which shows normal threshold in the left ear and mild to moderate high frequency hearing loss in the right

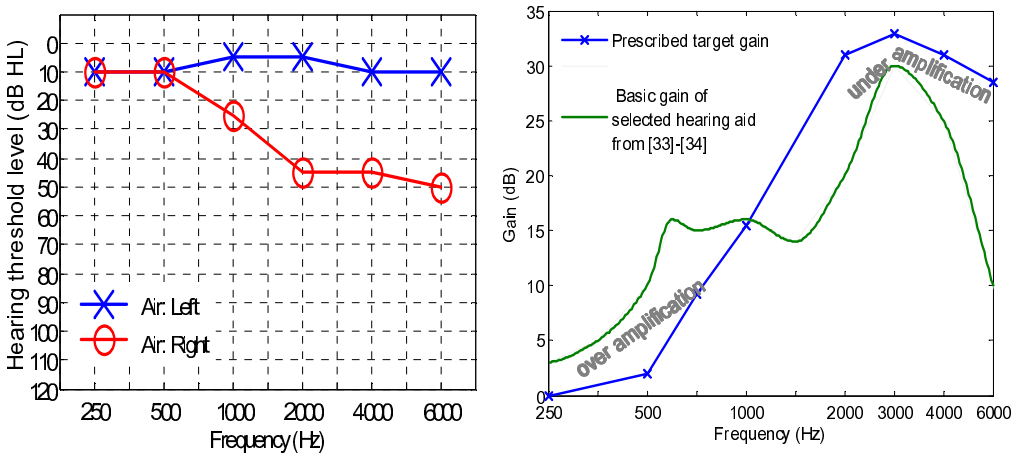

Figure 2.7. (a) A sample of audiogram of a unilateral hearing loss and (b) comparison of a target gain from (a) and a provided gain curve if fitted by analog hearing aid with a basic gain curve from [36]-[37] (for illustration)

ear. In Fig. 2.7(b), a result from an audiogram of a right ear in Fig. 2.7(a) is plotted as a prescribed gain target calculated by using the commonly used fitting formula from the National Acoustic Laboratories (NAL) [56]-[59] to find the real ear insertion gain. Basically the hearing levels at low, mid, and high frequencies are averaged and added to the hearing level at each audiometric frequency with some correction factors. Also shown is a gain curve if an analog hearing aid with a basic fixed gain curve adapted from [36]-[37] is selected for fitting. By comparing these two curves, the mismatches can be seen resulting as over- or under-amplifications which might discourage the users from wearing the hearing aids. More flexibility in the fitting procedure and added configurable filters for gain-frequency shaping might give a better fit.

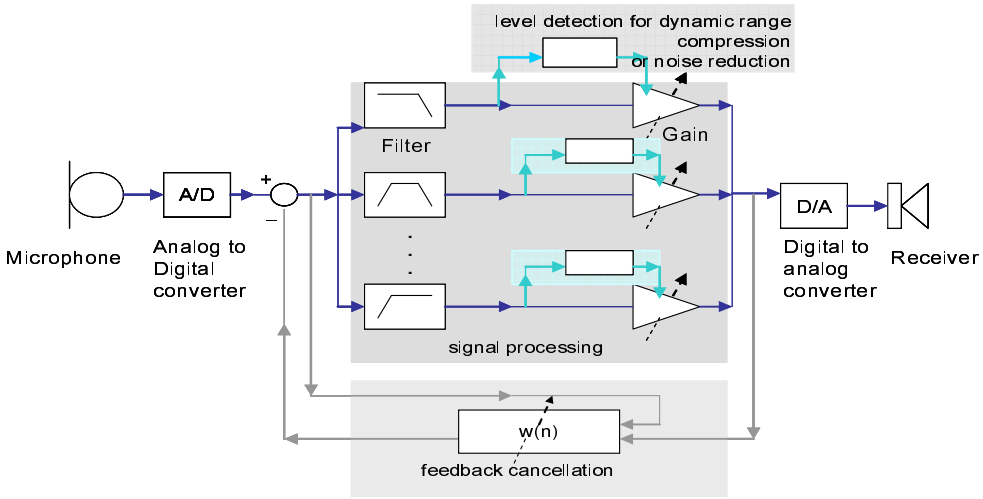

Figure 2.8. Diagram of a typical digital hearing aid (adapted from [36]-[37]).

A simplified block diagram of a more recent digital hearing aid is given in Fig. 2.8. An acoustic signal is transduced into an analog electrical signal by a microphone and is then converted into a digital signal so that the signal can be processed digitally and then is converted back into the analog signal from which it is sent to a receiver. This allows additional features such as, noise reduction circuits, feedback cancellation, or acoustic scene analysis [36]-[37], [49]-[51] to be employed for better quality of acoustic amplification.

As mentioned, the investigation of the noninvasive correction method in this dissertation is inspired by the concepts initiated in [1]-[2]. There have been a few other relevant researches exploring hearing aid techniques that are based on modeling of biological ears in addition to compensation of audibility loss based solely on the behavioral pure tone measurement in which they have attempted with different interesting approaches and results [52]-[55]. In [52], the mathematical building blocks of the peripheral ear ending at the inner hair cells were utilized with which the

mathematical inverse function of each block was then combined. Using simplified and approximated steps, the final compensator system resulted as a bank of bandpass filters followed by automatic gain control blocks which are similar to the technique used in conventional hearing aids. However, the gain control was implemented in multiplicative type manners instead of the typical feedback control; this yielded better performance than the selected conventional aids to which the authors compared the performances [53]. In [54], the authors made use of a model of a cat's cochlea to represent normal and impaired ears also ending at the hair cells. Electrocochleography was performed on the cats [54] with acoustically traumatized noise induced-hearing loss to record action potential firing rates and patterns of a single nerve cell inside the cochlea. The responses were then used to predict percentages of the frequency specific threshold losses between those resulting from damaged outer hair cells and damaged inner hair cells to be included into the models from which the compensating aid was then designed to compensate these ratios in terms of adjusting its weighted gain over frequencies. The ABRs have been measured in patients wearing conventional hearing aids [27]-[30], [97]-[99] which will be discussed in Section 4.5.1.

The conventional hearing aid is undeniably of value as an assistive device. However, the new approaches that look into the underlying auditory activities within the auditory system can potentially provide alternate techniques for improved assistive devices that have a potential to be able to restore the normal hearing functions providing extra valuable benefits for assisting the hearing impaired.

2.4 Summary

This chapter addresses first the anatomy and physiology of the peripheral and central auditory system and hearing impairments. Next, the nature and use of the auditory brainstem response in hearing diagnosis and general overviews of the responses are given. Lastly, basic amplification concepts of conventional hearing aids and literature surveys on related hearing aid researches are discussed. More knowledge on these topics can be found in textbooks [12]-[17], [36]-[37], [57]-[59]. Selected essential background information has been discussed preparing the readers for methods and results that are the main investigation of the dissertation in the following chapters.

In conclusion, the scope of the noninvasive correction method in the dissertation that utilizes signals from the ABR tests to assess the functions of the cochlea, auditory nerve, and brainstem auditory pathway is especially useful and purposefully aimed toward helping people with mild to moderate sensorineural hearing impairments. The ABR is able to identify for both conductive and sensorineural types but a conductive loss is often treatable medically. The extra advantages gained by using ABR are that the response characteristics can be used to diagnose the damages of the cochlea, nerve, and/or brainstem auditory nervous pathway while the pure tone audiogram simply accounts for a quantitative measure of audible sound. The ABR tests do not require subjective decision from patients. The analog circuits of the system for making a correction can be developed for use with air or bone conduction devices into an assistive device intended as an alternative to a conventional hearing

aid by implementing with the new proposed hearing assessment and correction technique of Chapter 4 and 5. The ideal case would be the new type of hearing aid for a patient with unilateral hearing loss whose clinical hearing evaluations and auditory brainstem responses are performed and data are kept on a regular basis such that any hearing deterioration and deviation from normal can be detected as soon as it happens. The normative parameters can also be implemented by using the patient's own records to reduce any variability for even more accurate outcomes.

Chapter 3

Modeling of the Auditory Brainstem Response

The method begins with the measurement and modeling of the auditory brainstem response (ABR) to develop an ear type system that can mimic the behaviors and capture the characteristics of the human hearing system. With its noninvasive properties and underlying nature reflecting the activities within the peripheral ear and section of the central auditory nervous system inside the brain, the ABR has been extensively used in clinics and academic researches. We utilize these properties and their response characteristics which are affected by the auditory loss and disorder and are associated with auditory signal processing mechanism from which the new concept of noninvasive correction and alternate hearing aid type device are proposed. The first part of the methodologies and results are discussed in this chapter which covers the following topics.

1. The ABR measurement set up for data recording,
2. The ear type system of ABR showing the mathematical representation using the modified nonlinear artificial neural network architecture and the methods for system identification,
3. The simulations and results of the developed ear type systems using data from a patient with a hearing impairment for a purpose of illustration to demonstrate the possible application of the developed system in the hearing

aid development and evaluate the results obtained from the proposed technique.

4. The extended ear type system for multielectrode recordings and/or binaural simultaneous stimuli.

3.1 The Auditory Brainstem Response Measurement

The data of auditory brainstem responses in the dissertation are obtained from the clinical hearing screenings at the Otolaryngology clinic of the King Chulalongkorn Memorial Hospital, Bangkok, Thailand as part of the clinical hearing screening and diagnosis and were supplied by Professor Permsarp Isipradit, M.D., at the department of Otolaryngology, Chulalongkorn University. As shown in Fig. 3.1, here the ABR is measured with three electrodes placed on the scalp at the hairline of the forehead, the mastoids, and the temples of the patient while staying still or asleep to reduce the muscle movement. Also, standard skin preparation is performed to reduce the skin-electrode resistance [60].

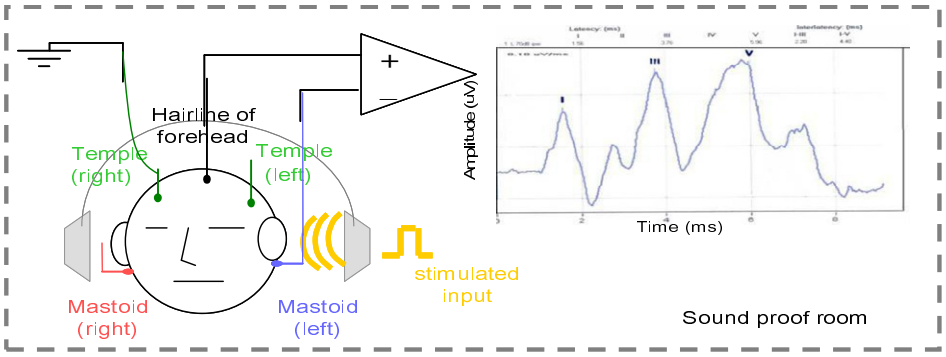

Figure 3.1. Diagram of the ABR measurement set up

For example, the left ear is being tested in Fig. 3.1, so the inverting electrode is at the left mastoid, the noninverting common electrode is at the hairline of the forehead and the ground electrode is at the right temple. The inverting electrode is switched to the right mastoid for testing the right ear. The measurement room is shielded from outside noise and strong electromagnetic fields. The stimulus used in the hearing evaluation is the click pulse presenting at the repeating stimulus rate, typically of 20/s, through the headphone which feeds the stimulus sound to the test ear as shown in Fig. 3.2. The electrical potentials of auditory system are picked up by the electrodes, filtered, and averaged inside the test equipment to reduce noise and artifacts. Various patients with different types of hearing losses and suspected hearing pathologies are tested for hearing evaluations.

3.2 The Ear Type System of Auditory Brainstem Response

3.2.1 The Modified Nonlinear Neural Network

The ear type system of measured auditory brainstem response (ABR) is developed using the data from the measurements. Identification of the human physiological systems using a modified artificial neural network is applied for deriving the mathematical representation of the ear type system. With its structure as a basic of other types of neural network architectures, the Hopfield neural network [61]-[64] has been widely studied and found useful in the application of system identification of the biological processes and physical systems [65]-[68]. The network structure is also suitable for hardware implementation [69]-[71].

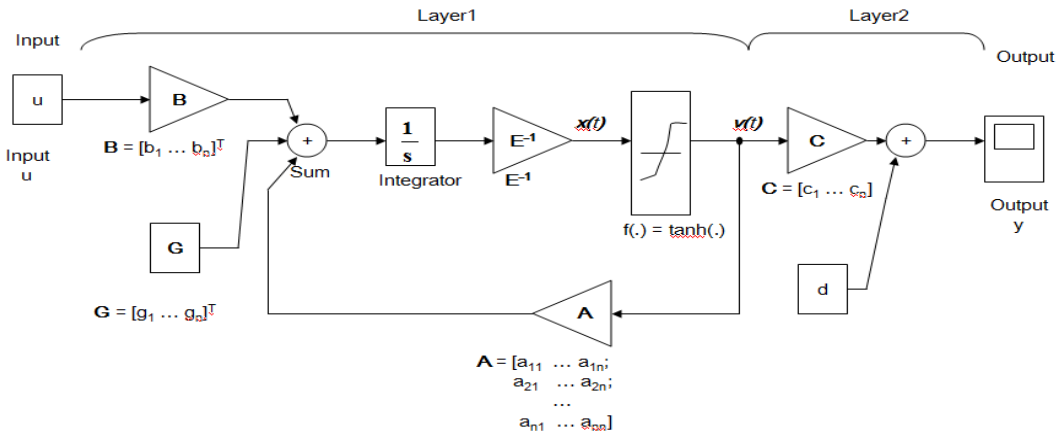

Figure 3.2. Schematic diagram of the modified artificial neural network

The classical structure of the Hopfield neural network [64] typically used for binary pattern classification problems is modified for the application to ear type system identification in which a second output layer and an external input are added, as shown in Fig. 3.2. This nonlinear ear type system with the basic structure adapted from the dynamical Hopfield neural network in a continuous time domain consists of n neurons in the first layer and one neuron in the second layer. The ABRs measured at the hospital used for illustration of the methods investigated in the dissertation are measured using three electrodes in a single channel recording meaning that the response ipsilateral (on the same side) to the test ear is recorded from one ear at a time. The mathematical representation of the ear type system modeling with the auditory brainstem response, measured in a described manner having a 1-vector input and 1-vector output, is defined in continuous time state space variable form

$$\mathbf{E}(d\mathbf{x}(t)/dt) = \mathbf{A}\mathbf{v}(t) + \mathbf{G} + \mathbf{B}u(t),\ \mathbf{x}(0) = \mathbf{x_0} \tag{3.1}$$

$$\mathbf{v}(t) = f(\mathbf{x}(t)) \tag{3.2}$$

$$y(t) = \mathbf{C}\mathbf{v}(t) + d \tag{3.3}$$

where u(t) is an input signal (1-vector)

y(t) is an output signal (1-vector)

x(t) is an internal state-type n×1 column vector with initial value $\mathbf{x}_0$

v(t) is a nonlinear n×1 column vector

E is a diagonal n×n matrix with diagonal entries equal to a constant e, = e×**I** (**I** = Identity matrix)

A is a constant n×n weight matrix

G is a constant n×1 column bias vector

B is a constant n×1 column vector

C is a constant 1×n row vector, and

d is a scalar output bias.

All quantities are assumed real. Since the activities within the human auditory system is highly nonlinear, the activation function, f(.) is selected to be a nonlinear n-vector function that is monotonically increasing and differentiable, such as a sigmoid function which is equal to 1/(1+exp(-x)) [64]. In the ear type system of ABR, a hyperbolic tangent, tanh(x) = (exp(x)-exp(-x))/(exp(x)+exp(-x)), shown in Fig. 3.3 is used, $v_i = f(x_i) = \tanh(x_i)$ (3.2), since it has a larger output range and resembles to a mechanical movement with saturation of hair cells in the cochlea. The hyperbolic tangent function is also convenient for implementation in hardware using the bipolar junction transistors (BJT). The BJT differential pair circuits with components for input voltage adjustment can be used to realize $\tanh(x_i)$ where x_i can be represented as the

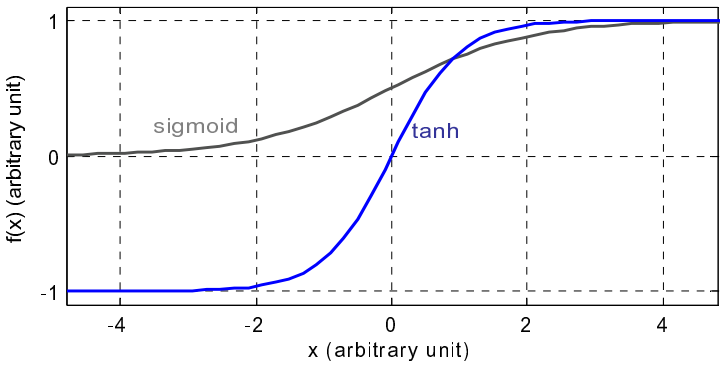

Figure 3.3. A hyperbolic tangent function, f(x) = tanh(x) compared to a sigmoid function, f(x) = 1/(1+exp(-x))

voltage in a circuit. The mathematical model of the ear type system is developed to mimic and capture the behaviors and characteristics of the individual auditory function via the measured ABR in which normal hearing function and effects of the hearing loss and disorder on the hearing function are characterized. These equations representative of the ear type system (3.1)-(3.3) can be extended applicable for multiple inputs and multiple outputs recorded in multichannel configurations and also for simultaneous stimulating both ears and recording auditory evoked brain activities from various locations on the scalp which will be further discussed in Section 3.4.

3.2.2 System Identification Methodologies

The system identification procedures for estimation of the coefficient vectors and matrices of the nonlinear ear type system in (3.1)-(3.3) are implemented using the modeling methods that combine the uses of the neural network modeling and the optimization algorithms together with the trial-and-error simulations. Given the

continuous time domain measurements of the input signal, u(t), and output signal, y(t), the parameters of the system coefficients in (3.1)-(3.3) are also estimated in the continuous time domain. Standard numerical optimization algorithms are applied to first find the dimension n of the internal neuron state and to second estimate the parameters of weight vectors and matrices and bias values: **A**, **B**, **C**, d, **E**, and **G**.

Estimating the dimension

The same as in most system identification problems, a dimension of the nonlinear dynamical system, that is, the number of the internal neuron states of the ear type system in (3.1)-(3.3), is typically chosen to be sufficiently small to construct the system with simple structure and minimum number of parameters that are capable of mimicking the physical system and capturing the system characteristics on which the developed system is based but flexible enough to give satisfying outputs with acceptable discrepancies between the real physical system and the simulated system responses. Increasing either the dimension and the number of parameters tends to generate a system with less mismatched signals and better fits but the system structure can become complicated requiring extra computational time and resources which might not be necessary [72]-[78]. The steps for finding the system dimension are improvised from the combination of different approaches including the model order selection techniques for a dynamical nonlinear system such as use the Lipschitz criterion [79] together with trial-and-error simulations to validate the results and choose the optimum numbers.

The Lipschitz criterion is a method to identify the optimal embedding orders based on the continuity property of the nonlinear function by calculating the Lipschitz quotients. It can be applied to an unknown nonlinear dynamical system typically of a general formulation

$$y(t) = f(y(t-1), y(t-2), \ldots, y(t-r), u(t), u(t-1), \ldots, u(t-s))$$
$$= f(\varphi(t)) \tag{3.4}$$

where y is a vector of outputs, u is a vector of inputs, and φ is called a regression vector consisting of *r* lagged outputs and *s* lagged inputs taken into account to construct the mathematically descriptive nonlinear system. To find the right order of the system that is the orders of regression vectors, *r* and *s*, to accurately simulate and map the nonlinear system from the input-output data $(u(t_i), y(t_i))$ where i = 1, 2, …, N and N is the data length, that is the number of equally sampled input and output signals analyzed, the Lipschitz quotients are calculated. The Lipschitz quotients, q_{t1t2}, are calculated directly using only the input and output data,

$$q_{t1t2} = \frac{|y(t_2) - y(t_1)|}{\|\varphi(t_2) - \varphi(t_1)\|}, (t_1 \neq t_2) \tag{3.5}$$

where $\|\varphi(t_2) - \varphi(t_1)\|$ is the Euclidean norm and $|y(t_2) - y(t_1)|$ is the difference of the scalar nonlinear outputs. The criterion is based on the bounded gradient which can be estimated from the largest quotient to decide on an optimum number, *r* and *s*, of the selected regressor vectors. The largest quotient for the system order occurs at the known sampled points calculated by

$$q_{t1t2}^{(r,s)} = \frac{|y(t_2) - y(t_1)\|}{\sqrt{\frac{1}{r}\sum_{k=1}^{r}\| y(t_2 - k) - y(t_1 - k)\|^2 + \frac{1}{(s+1)}\sum_{k=0}^{s}\| u(t_2 - k) - u(t_1 - k)\|^2}} \tag{3.6}.$$

where $|y(t_2)-y(t_1)|$ is the difference of the scalar nonlinear outputs and ||.|| is the Euclidean norm of regression variables (past inputs and past outputs) for determining the gradient . If the system order first selected is insufficient, meaning one or more of the past input-output variables needed to set up the nonlinear system are not included and are not completely independent of other included regression vectors, the Lipschitz quotient, $q^{(\hat{r},\hat{s})}$ of the insufficient orders where $\hat{r}<r$ and $\hat{s}<s$, can become unbounded and is very much larger than $q^{(r,s)}$ with the right selected numbers of past output, *r*, and past input, *s*, variables to completely map the nonlinear function. The more the necessary regression variables are not included, the much larger the quotients can become. On the other hand, if more variables of past inputs and past outputs are included than necessary, the Lipschitz quotient, $q^{(\hat{r},\ \hat{s})}$ of redundant orders where $\hat{r}>r$ and $\hat{s}>s$, is still bounded but has a value slightly smaller than $q^{(r,s)}$ with the right numbers of necessary variables. Increasing the numbers of regressor variables results in a smaller quotient values. Using these principles, the Lipschitz number, $q^{(r,s)}$, is calculated from

$$q^{(r,s)} = \left(\prod_{k=1}^{p} \sqrt{(r+s)} q^{(r,s)}(k) \right)^{1/p} \tag{3.7}$$

where $q^{(r,s)}(k)$ is the k-th largest quotient among all $q_{ij}^{(r,s)}$ and *p* is usually selected as one to two percent of the data length, N [79]-[80]. Using the above principles, if the optimum numbers of lagged input variables, *s*, and output variables, *r*, are included in the calculation of $q^{(r,s)}$, $q^{(r-1,s-1)}$ will be much larger than $q^{(r,s)}$ whereas $q^{(r+1,s+1)}$ is slightly smaller than $q^{(r,s)}$, so the optimum system order can be easily located at the

knee point of the curve between the Lipschitz numbers and the system orders [81]-[82].

The model order selection technique using the Lipschitz numbers has been successfully used in various system identifications [79]-[85]. The system order obtained from this technique can be used as a starting point from which the system structures can be defined and estimated.

Estimating the parameters

After the optimal order is selected, the nonlinear ear type system can be set up. Numerical optimization algorithms will be used based on the iterative prediction error minimization [74]-[76], [86]-[87] aiming to minimize the mean square error (mse) between the signals from measurements and simulations,

$$\text{mse} = (1/N)\sum_{i=1}^{N} (y_{\text{measured}}(t_i)-y_{\text{modeled}}(t_i))^2 \qquad (3.8)$$

can be applied to find the parameters of the individual ear type system. In (3.8), y_{measured} are signals from the measurements, y_{modeled} are signals from the models, and N is the number of measured and modeled output signal values in which the minimization becomes a nonlinear least square problem. The least square algorithms [86]-[87] including the Levenberg-Marquardt algorithm (LMA) [74] and the trust-region-reflective algorithm [88] are utilized in this dissertation. These are commonly used and effective approaches for nonlinear optimizations and are available in MATLAB toolboxes. Basically, the algorithms begin with an initial set of parameters from which the iterative trainings are applied so as to decrease the mean square error

in the search direction. At each training step, the algorithm is continued toward finding the optimum set of parameters until the criteria for stopping is met, such as the specified numbers of iterations are completed or the mean square error is within the given limit.

Validating the systems

After the system parameters are achieved, the final mean square error, (3.8), and the comparison of responses from measurements and MATLAB Simulink simulations are evaluated to analyze the quality of the identified system.

3.3 Simulations and Results

3.3.1 The ABR measurement

For consistency of the dissertation, the simulations and results are investigated by using the same sets of the auditory brainstem response data recorded from a patient who has a suspected hearing loss in the left ear. The click evoked ABR test was performed on both ears. The responses are shown in Fig. 3.4. Although the responses are present from both ears showing identifiable major waves with clear and repeatable waveforms, the responses are different. Compared against the normative criteria and standardized templates, the response of the right ear shows normal characteristics while that of the left ear shows some abnormal characteristics indicating a possible case of the sensorineural hearing loss. The absolute and interwave latencies of the left and right ABRs are listed along with the norms

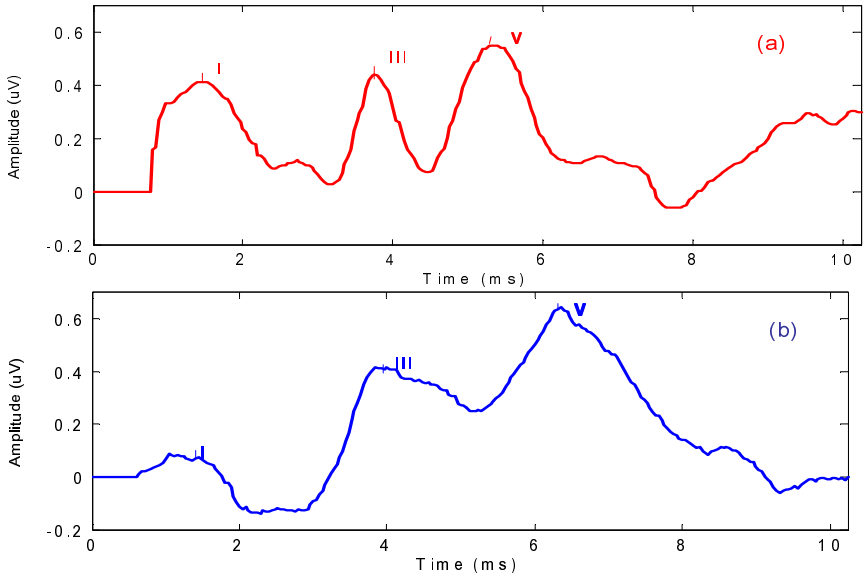

TABLE

Absolute and Interwave Latencies (millisec) of the ABR for a quick pass/fail criterion

Wave latency (ms)	I	III	V	I-III	III-V	I-V
Right	1.48	3.75	5.36	2.27	1.61	3.88
Left	1.48	3.92	6.44	2.44	2.52	4.96
Mean	1.64	3.51	5.34	1.88	1.83	3.71
S.D.	0.12	0.11	0.20	0.18	0.28	0.13
Comments:						

Figure 3.4. The ABRs from the measurements of (a) right and (b) left ears from the patient with sensorineural hearing loss in the left ear which are used for illustration of the investigation through out the dissertation

established at the clinic utilized in the dissertation. The absolute latencies of wave III and V and interwave latencies of wave I-III and I-V of the left ear responses are out of normal limits (= mean values ± 2.5×Standard deviation (S.D.)) which suggest a case of sensorineural hearing loss.

3.3.2 Systems simulated results

Two ear type systems with mathematical expressions in (3.1)-(3.3) mimicking the characteristics of the left and right ears measured through the auditory brainstem

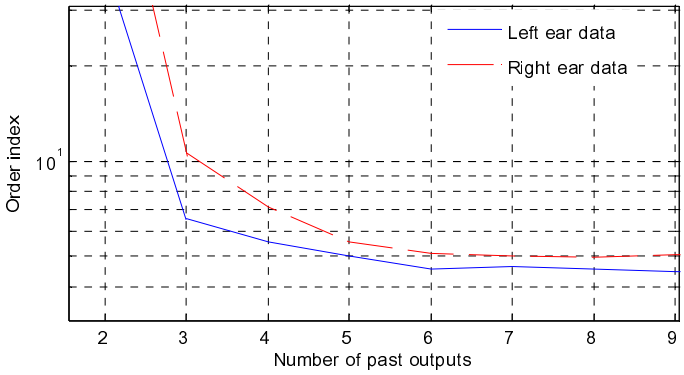

Figure 3.5. Lipschitz numbers using input and output data for system order selection guideline of the two ear type systems of the patient with ABR in Fig. 3.4

responses are developed. The number n of the internal states, x(t) in (3.1)-(3.3), is defined first in order to set up the system for training by inferring from the Lipschitz numbers. The Lipschitz numbers (3.7) are plotted in Fig. 3.5. The curves of both left and right ear data show a rapid drop at 3 and continues to decrease until 6 after which the curve does not significantly decreased. Using the analysis described earlier, the optimum system order obtained from the Lipschitz number is likely to be 6. The orders obtained from the technique can be used as a guideline for setting up the systems. Trial and error runs can be simulated using a range of possible numbers obtained from the Lipschitz numbers, in this case from 3 to 6 as discussed below.

Using the measured auditory brainstem responses, the ear type systems of the patient are constructed and trained to estimate the parameters of the systems for various n from 3 to 6. The iterative network training is carried on until reasonable simulated responses are achieved and no further significant reduction of the mean

square error (3.8) is expected. Using six internal states inferred from the model order selection technique, satisfying simulated signals are achieved from the developed ear type systems of both ears. Additional trial and error simulations and extensive comparisons of the results are performed using a range of possible orders with lower numbers from three to five but simulated responses and systems with reasonable fits cannot be achieved. The simulation results for n = 6 from the left and right ears are compared with the measured ones in Fig. 3.6 showing good agreements. The final mean square error is equal to 1.1e-3 on the left ear system and 3.2e-4 on the right ear system. The ear type systems representing the normal hearing function of the patient's right ear and the impaired hearing function of the patient's left ear diagnosed and measured through the auditory brainstem responses are set up in Simulink models as shown in Fig. 3.7.

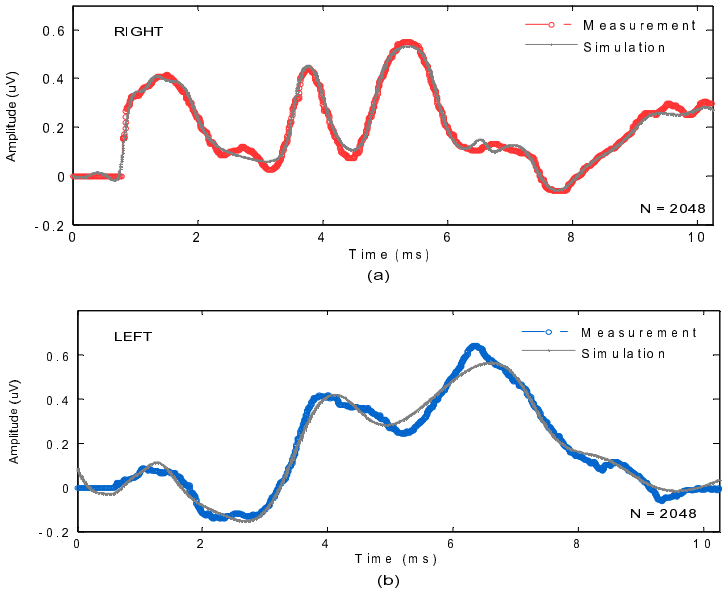

Figure 3.6. Measured and Simulink modeled auditory brainstem responses testing (a) the right ear and (b) the left ear.

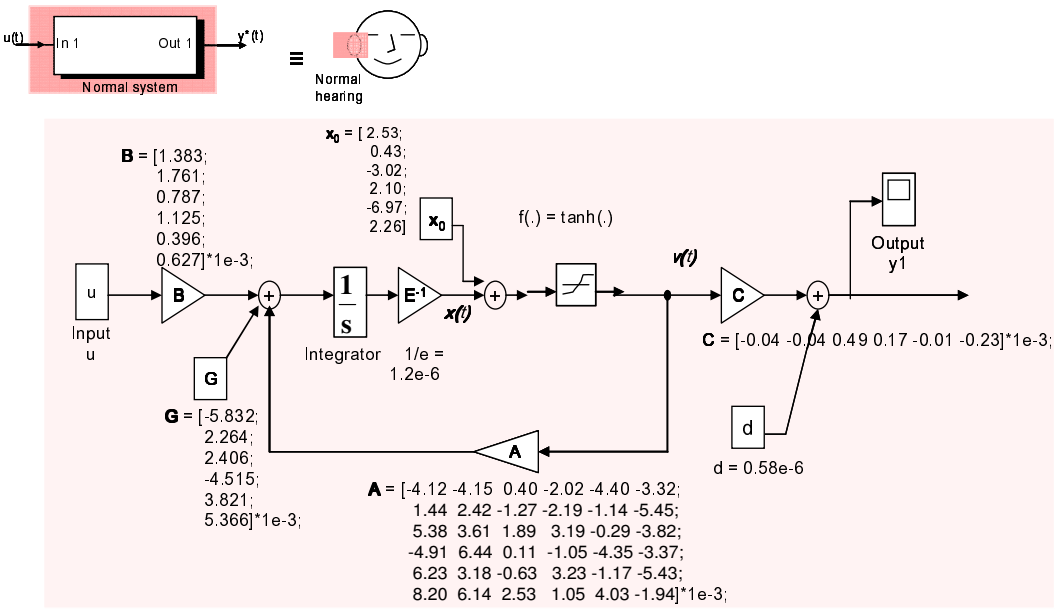

(a)

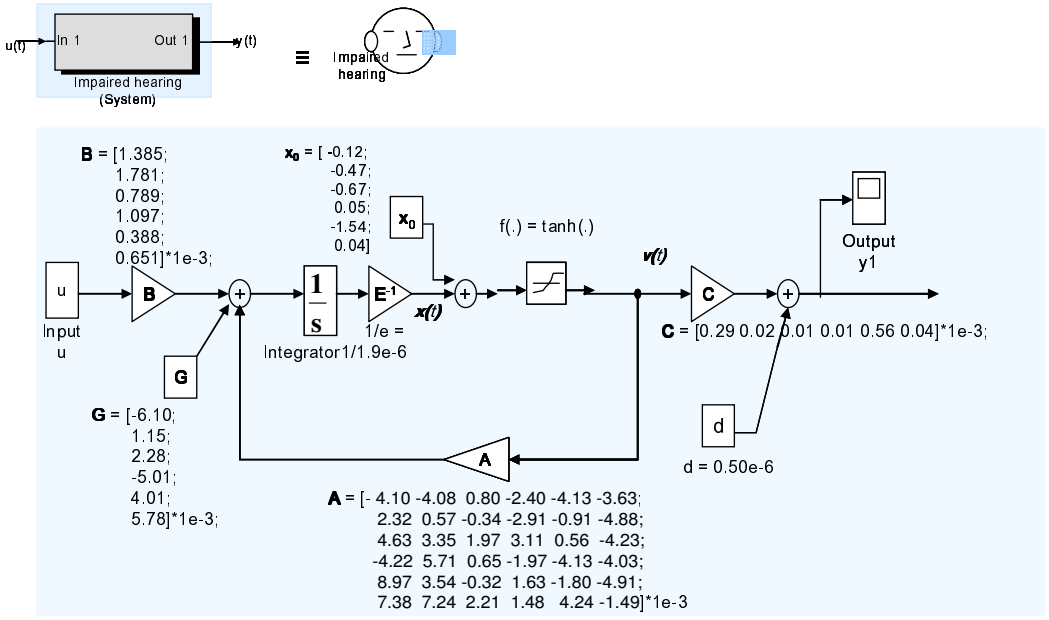

(b)

Figure 3.7. Simplified Simulink diagrams of ear type systems (a) normal hearing of the right sided measurement and (b) abnormal hearing with sensorineural hearing loss of the left sided measurement

The ear type system for characterization of the individual auditory system and hearing function are achieved with satisfying results. The system is able to simulate the auditory brainstem responses with characteristics representing the normal hearing function and the effects from the hearing loss and disorder in order to be further used in the design of new correction scheme and assistive device.

3.4 The ear type system of the auditory brainstem response extendable for possible applications of multiple inputs and/or outputs of the ABRs and other pertinent auditory evoked potentials

3.4.1. The extended ear type system

In addition to the ear type system developed from the auditory brainstem response measured using three electrodes placed on the scalp at the typically chosen locations using a single channel recording as shown in Fig. 3.1 and also performed at the Chulalongkorn hospital, the recordings of the ABR are possible to be performed using different recording configurations. For example, it is possible to measure only one sided ABR with simultaneous stimuli in both ears, both ipsilateral (on the same side) and contralateral (on the different side) ABRs with acoustic stimulus in one ear, and both sided ABRs with simultaneous stimuli in both ears. The latter two, usually referred to as two channel recordings, also require test equipment with two channel capabilities. Simultaneous stimulating both ears is not typically performed, the recording of contralateral (to the stimulus ear) ABR can be clinically useful [13],

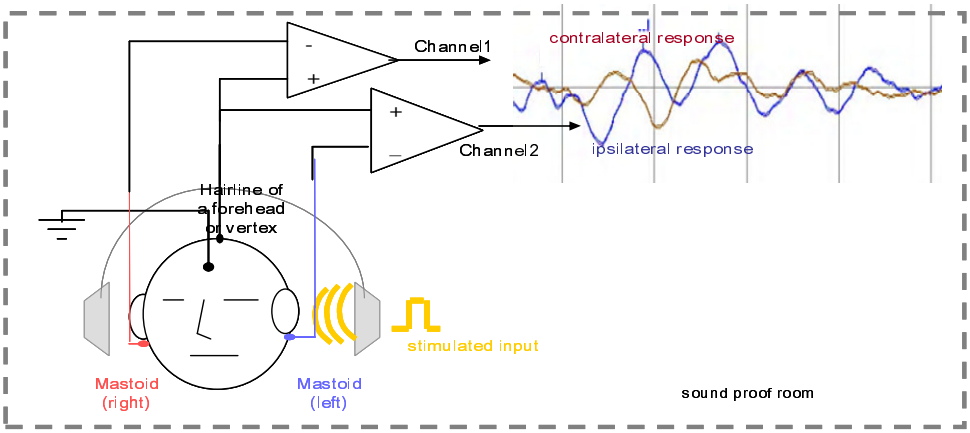

Figure 3.8. Two channel recordings of the ABRs

[116]-[117]. The diagram of the two channel recordings of both sided ABRs is illustrated in Fig. 3.8.

Beside these two channel recordings, the assessment of hearing function and diagnosis can also be performed utilizing the measurement using multiple electrodes typically referred to as the multichannel recordings. The ABR is a far field differential recording of the electrical potentials reflecting activities of the human auditory system. It is typically measured between two exact points on the scalp. The sites of the three electrodes used in Fig. 3.1, where the inverting electrode is at the mastoid same side of the ear being stimulated, the noninverting electrode is at the hairline of the forehead, and the ground electrode is at the temple on the opposite side of the ear being stimulated, are suggested since they sufficiently ensure the identifications of all wave components and reliable outcomes [60].

The measurements of other auditory event-related electrical activities inside the brain referred to as the auditory evoked potentials (AEPs) in additional to the auditory brainstem response (ABR, short latency about 10 ms after stimulus) including the auditory middle latency response (MLR, latency about 10-50 ms after stimulus), the auditory late latency response (LLR, latency about 50-300 ms after stimulus), and other event-related potentials of the brain such as P300 cognitive auditory evoked potential (CAEP, positive peaks at about 300 ms after stimulus) have been of interest in both clinical diagnostic and academic researches [46], [96]-[100], [105]-[106]. Although all are very useful, the measurements require different settings and environments from those used in obtaining the ABR, which is the most commonly and routinely used in most hospitals.

For example, the wave characteristics of MLR are affected by the patient's responsive state and more variable within and between patients [20]-[21], [97]. The LLR is also affected by the patient's attentive state but with less variability within and

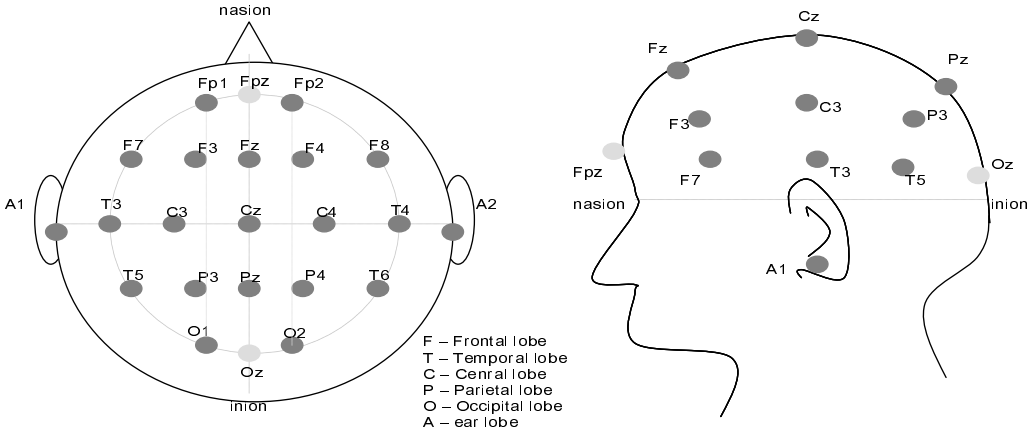

Figure 3.9. The electrode placements of the international 10-20 system [103]

between the patients; there has been an increased interest in the LLR [96]-[98],[100] since the response is believed to be generated from a deeper level within the brain that is highly linked to the cognitive function and speech perception ability. The measurements hence require very experienced audiologists, longer analysis time, and cooperation with the patients. The recordings of the responses especially for those with late latencies are performed using multiple electrodes typically following the electrode placements of the international 10 to 20 system [103], [12]-[14] as shown in Fig. 3.9 of which the locations of electrodes are marked referenced to the underlying cerebral cortex. For this electrode caps have been invented for a robust and quick measurement from which measurement with a more number of electrodes such as 32, 64, or 128 have also been utilized whose electrode placements are modified from the extension of the 10-20 system [104]-[105].

The two channel recordings of the ABR and the auditory evoked potentials mentioned above are certainly useful for additional detailed diagnosis and for study of the underlying mechanism and activities inside the brain in a noninvasive way for which an extension of the ear type system is investigated here. The ear type system of auditory brainstem response described earlier in the chapter can be extended and modified for the simultaneous two channel recordings of the ABRs and the multiple electrodes recordings of auditory evoked potentials of the brain. The mathematically representative neural type system modified from the ear type system of ABR in (3.1)-(3.3) to multiple signals can be represented as

$$\mathbf{E}(d\mathbf{x}(t)/dt) = \mathbf{A}\mathbf{v}(t) + \mathbf{G} + \mathbf{B}[u_1(t)\ u_2(t)]^T \quad (3.9)$$

$$\mathbf{v}(t) = f(\mathbf{x}(t)) \quad (3.10)$$

$$\mathbf{y}(t) = [y_1(t)\ y_2(t)\ \ldots\ y_m(t)]^T = \mathbf{C}\mathbf{v}(t) + \mathbf{d} \quad (3.11)$$

where $\mathbf{u}(t)$ are the inputs consisting of appropriate input signals such as $u_1(t)$ is a 1-vector stimulus to a right ear and $u_2(t)$ is a 1-vector stimulus to a left ear and $\mathbf{y}(t) = [y_1(t)\ y_2(t)\ \ldots\ y_m(t)]^T$ are the outputs from each of m electrodes and channels analyzed. In (3.10) $\mathbf{x}(t)$ is an internal state-type n×1 column vector. The appropriate sizes of parameter vectors and matrices are adjusted accordingly: $\mathbf{E}$ is a diagonal n×n matrix with diagonal entries equal to a constant e, = e×$\mathbf{I}$ ($\mathbf{I}$ = Identity matrix), $\mathbf{A}$ is a constant n×n weight matrix, $\mathbf{G}$ is a constant n×1 column bias vector, $\mathbf{B}$ is a constant n×2 matrix, $\mathbf{C}$ is a constant m×n matrix, and $\mathbf{d}$ are the output bias values.

3.4.2. Example of the Extended Ear Type System

In this section, the extended ear type system mathematically represented in (3.9)-(3.11) developed through the ABRs measured in a two channel recording per

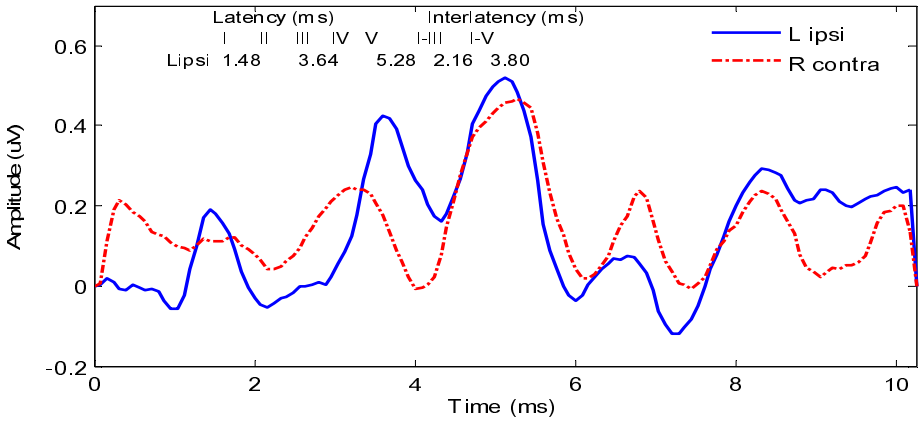

Figure 3.10. The ABRs from two channel recordings

Fig. 3.8 is investigated. The ipsilateral (same sided) and contralateral (opposite sided) ABRs are both recorded with the stimulus in one ear. As shown in Fig. 3.10, the ipsilateral (left) ABR is plotted as a solid line and the contralateral (right) ABR is plotted in a dash line with the stimulus sound being in the left ear. The responses show normal characteristics and wave latencies within normal limits. The extended ear type system is set up through the ABRs using (3.9)-(3.11) in which the input u(t) = u(t) and the output y(t) = [y_1(t) y_2(t)] are applied. Following the similar steps for

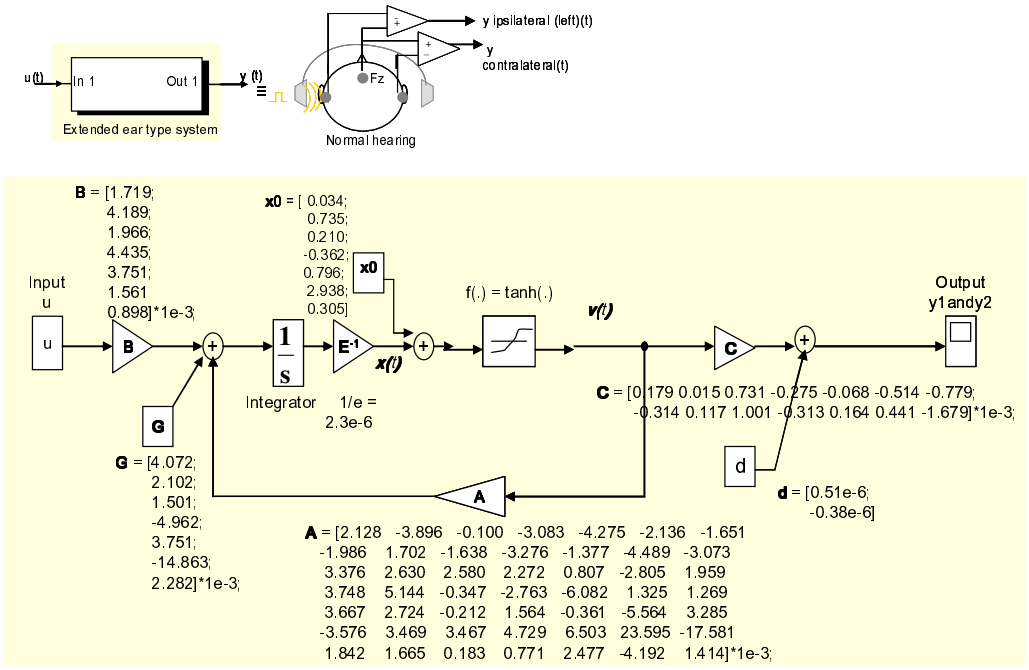

Figure 3.11. Simulink model of the extended ear type system illustrative case of the two channel recording of ABRs

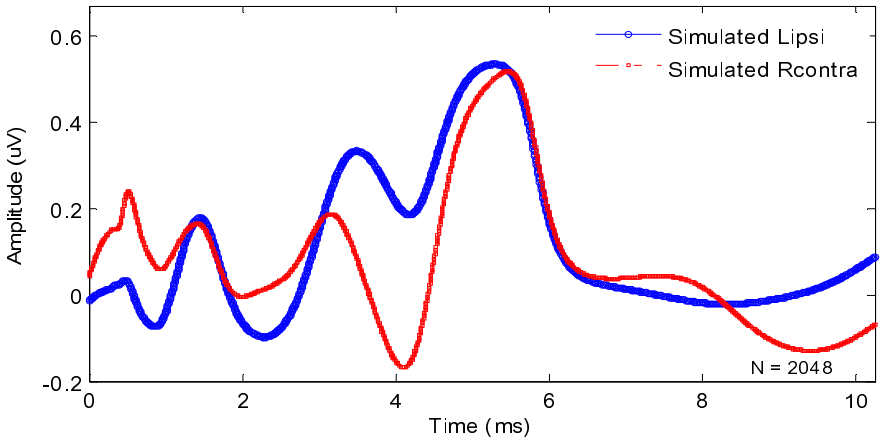

Figure 3.12. The two sided ABRs in the two channel recording with the stimulus in one ear simulated from the model of extended ear type system in Fig. 3.11

system identification of the auditory brainstem responses using the modified neural network and nonlinear least square search algorithms, the simplified diagram of the extended ear type system with the parameters is shown in Fig. 3.11. The responses simulated from the model are shown in Fig. 3.12 yielding signals comparable to the ABRs in Fig. 3.10. The system is able to capture the overall waveform and important waves of the ABRs showing a possibility of the extended ear type system using multiple electrodes for identification of the neural activities inside the auditory system. The application of the extended ear type system can be also found useful in a similar way where the inverse term used for cancellation of any undesired response can be incorporated and implemented for alleviating the effects from hearing loss and other pertinent auditory dysfunctions as well.

3.5 Summary

Modeling methods to develop the mathematical descriptions representative of the ear type systems are discussed. The auditory brainstem responses that reflect activities within the human auditory system differentiating between normal and abnormal hearing functions are measured and utilized to assess and characterize the individual ear type system. The modification of the nonlinear Hopfield type neural network purposefully for modeling of the measured ABRs is implemented. Methods and results are given using the data measured from a patient having a unilateral sensorineural hearing loss. The ear type systems are set up and trained for estimating the system orders and parameters to identify for the optimal ones. The results show the simulated responses in good agreement with the measured ones. The investigation of the ear type system using an artificial neural network can reasonably simulate the human auditory system. The selection of the system with nonlinear dynamical neural network structure is probably more appropriate than other system structures, such as a linear ARMA filter, since the underlying anatomical organs and their mechanisms giving rise to the auditory brainstem response are beyond those of the inner ear. The responses reflect the activities within the peripheral auditory system and central nervous system inside the brain where there are many complex networks of auditory neurons, nerves, and fibers connecting together to send and receive the signals for sound perception and interpretation. The developed system is able to capture the changes in hearing function of normal and impaired characteristics through the measured auditory brainstem responses. The noninvasive characterizations of the individual auditory functions reflecting the characteristics and effects from the

hearing loss and disorder have been achieved in this chapter from which noninvasive correction of the undesired effects are made possible and investigated in the next chapter.

Chapter 4

Noninvasive Correction of Auditory Disorders

Modeling of the auditory brainstem response is investigated in Chapter 3 from which a new noninvasive correction method is proposed and investigated in this chapter. The detailed discussions on the following topics are presented.

1. A scheme for a new noninvasive method for correction of the auditory loss and disorder
2. Methods for developing a system for making the correction by utilizing the inverse artificial neural network
3. An application of the proposed correction method and the derived inverse artificial neural network to a simple problem for illustration of the use of the inverse neural network.
4. The simulations and results of the method by simulating on the model of the same patient with a unilateral hearing loss.
5. Discussion on result evaluation, potential benefits and performance analysis of the proposed noninvasive correction method to be implemented as an assistive device alternate to a conventional hearing aid.

4.1 Concept of the New Noninvasive Assistive Device

A new noninvasive scheme for correction of auditory loss and disorder is investigated from the valuable usefulness of the auditory brainstem response (ABR) as assessment and diagnostic tools in clinical evaluation of hearing function and hearing disorder as well as in ear and hearing researches. The many advantages of the ABR include the following examples. It can be used to assess and gain insights into the functions and characteristics of the central auditory nervous system in addition to those of the cochlea typically tested in other hearing diagnostics. Its objective way of performing and making the hearing evaluation is especially useful for testing hearing of children. Its waveforms and characteristics are highly stable regardless of the patient responsive states and also are less variable within and between the patients. The ABRs are therefore easy to be identified and the normative criteria of their wave characteristics can be set up and compared against the individual measured responses for hearing evaluation and hearing loss and disorder diagnosis. Its noninvasive way of recording the evoked potential reflecting the activities of auditory neurons within the human auditory system that is more likely to be related to the underlying speech perception and interpretation processes inside the brain such that the correction technique investigated in the dissertation possibly results as an improved way of correcting and compensating for the auditory loss and disorder yielding a better hearing aid.

The technique for noninvasive correction of the auditory loss and disorder is realized using the developed ear type systems given in Chapter 3 which can lead to an

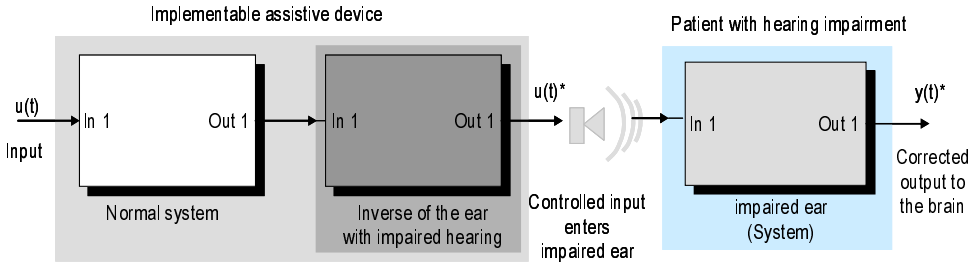

Figure 4.1. The noninvasive correction concept

implementation of a system for making a correction as a new type of hearing aid. Differentiation between normal and impaired ears and their hearing functions and characterization of the effects from the hearing loss and disorder have been made possible through the use of the ABRs which allow for evaluation of the hearing loss and disorder and determination of the internal pathology of the human auditory system. The ear type systems representing these normal and impaired characteristics were realized using the modified artificial neural network in system identification step showing the satisfying results as per Fig. 3.6 from which the correction technique is investigated. The technique utilizes the ear type system of the patient with a hearing impairment from which another system inverse to it can be developed by deriving the inverse of the nonlinear neural network representative ear type system. Therefore cascading the inverse and original neural networks yields the identity output in theoretic and possibly with some delay in practical application. To form the corrector system for making a noninvasive correction of the undesired effects, the inverse system is proposed to be used in combination with the ear type system of normal hearing function of which can be defined based on the established normative

criteria or the characteristics of the opposite ear in a case of the unilateral (single-sided) hearing loss. The diagram of the noninvasive correction concept is shown in Fig. 4.1.

4.2 Methodologies

4.2.1 Neural network and its inverse system

The modification of the nonlinear neural network adapted for system identification of the ear type system of the auditory brainstem response measured in a single channel recording provided in the dissertation. The ABR on the same side of the ear being stimulated is measured one at a time discussed in Section 3.1 for which the ear type system is developed as present in (3.1)-(3.3) is reprinted in (4.1)-(4.3).

$$\mathbf{E}(d\mathbf{x}(t)/dt) = \mathbf{A}\mathbf{v}(t) + \mathbf{G} + \mathbf{B}u(t), \mathbf{x}(0) = x_0 \tag{4.1}$$

$$\mathbf{v}(t) = \mathbf{f}(\mathbf{x}(t)) \tag{4.2}$$

$$y(t) = \mathbf{C}\mathbf{v}(t) + d \tag{4.3}$$

where u(t) is an input signal, y(t) is an output signal, $\mathbf{x}(t)$ is a vector of *n* internal neurons, and $\mathbf{A}_{[n\times n]}$, $\mathbf{B}_{[n\times 1]}$, $\mathbf{C}_{[1\times n]}$, $d_{[1\times 1]}$, $\mathbf{E} = [e\times\mathbf{I}]_{[n\times n]}$, and $\mathbf{G}_{[n\times 1]}$ are vectors and matrices of parameters that are characterized for the individual system by using the ABRs measured from the individual patient. The nonlinear activation function f(.) is a hyperbolic tangent and **E** is a diagonal matrix with entries equal to a nonzero constant e, $\mathbf{E} = e\times\mathbf{I}$ where **I** is an identity matrix. All parameter values are real. The inverse of the original modified Hopfield type neural network is to be derived whose output is equivalent to the input of the original network. The way to inverse the Hopfield

network was motivated by the simple and useful techniques in [89]-[90]. However, higher dimensional networks with interdependent internal neurons and different arrangement of the inverse and original networks are needed for the ear type systems making the inverse problem more complicated. To find the inverse of the original nonlinear neural network with mathematical expressions in (4.1)-(4.3), the concepts of the inverse and converse systems from the linear system theory - state space approach [91] are utilized. The concepts for finding the inverse by using the equivalence of the input and output pairs of the original and inverse systems [91] and the approach to avoid the need for vector and matrix inversions are applied by using the differentiation of the output from the original system [92] as the input to the inverse system in the nonlinear case. Using the theoretical analysis of the inverse and converse concepts, the inverse of the state space system, F,

$$y = F(x; u) \tag{4.4}$$

exists when for every state of the original system there exists a state of the inverse system such that

$$F_{inv}(x_{inv}, F(x; u)) = u \tag{4.5}.$$

F_{inv} is an inverse of F where u is the input of the original system and y is the output of the original system. The original and inverse systems exhibit the equivalency of the input and output. The input to the original system is equivalent to the output from the inverse system in theoretical result.

The applied techniques utilizing the converse concept and the differential output allow the inverse system to be derived which does not require the reciprocal of

a transfer function and the invertibility of parameter vectors and matrices. This is especially useful in the case of a system of neural network architecture with multiple layers. It is also applicable to a system identification using an artificial neural network whose numbers of output signals, $[\mathbf{y}(t)]_{m\times n}$, are less than numbers of internal neurons, $[\mathbf{x}(t)]_{n\times 1}$. For example, as in (4.3) for a single output, **C** is a vector of dimension 1×n where 1<n which has only one sided inverse if its inverse exists [93]. From the developed nonlinear ear type system with the modified neural network structure mathematically represented in (4.1)-(4.3), the inverse of the ear type system can be derived by differentiating the output from (4.3),

$$\begin{aligned} y'(t) &= dy(t)/dt \\ &= \mathbf{C}[d\mathbf{v}(t)/dt] \\ &= \mathbf{C}[(\partial f_x)\mathbf{I}][d\mathbf{x}(t)/\,dt] \end{aligned} \qquad (4.7)$$

where ∂f_x stands for $\partial f(.)/\partial x$, **C** is a 1×n vector, $[(\partial f_x)\mathbf{I}]$ is written as a n×n diagonal matrix, and $[d\mathbf{x}(t)/dt] = [dx_1(t)/dt \ \ldots \ dx_n(t)/dt]^T$. Substitute $d\mathbf{x}(t)/dt$ from (4.1) in (4.7) and rearrange to get u(t),

$$u(t) = (\mathbf{C}[\partial f_x\mathbf{I}]\mathbf{B}/e)^{-1}\left\{ (y'(t)) - (\mathbf{C}[\partial f_x\mathbf{I}]/e)(\mathbf{A}\mathbf{v}(t) + \mathbf{G}) \right\} \qquad (4.8)$$

where **B** is a n×1 vector and e is a constant entry of a diagonal matrix **E** so a term $(\mathbf{C}[\partial f_x\mathbf{I}]\mathbf{B}/e)^{-1}$ is hence a scalar value. The term **A** is a constant n×n matrix, **G** is a constant n×1 vector and $\mathbf{v}_i(t)$ is a nonlinear function of $\mathbf{x}_i(t)$. Hence, (4.8) returns a scalar signal. Substituting (4.8) in (4.1) yields (4.9) and the inverse of the original nonlinear neural network in (4.1) - (4.3) can be written as (4.9) – (4.11),

$$\mathbf{E}d\mathbf{x}_{inv}(t)/dt = \{\mathbf{A} - \mathbf{B}\,(\mathbf{C}[\partial f_x\mathbf{I}]\,\mathbf{B}/e)^{-1}(\mathbf{C}[\partial f_x\mathbf{I}]\mathbf{A}/e)\}\,\mathbf{v}_{inv}(t)$$
$$+ \mathbf{G} - \mathbf{B}(\mathbf{C}[\partial f_x\mathbf{I}]\,\mathbf{B}/e)^{-1}(\mathbf{C}[\partial f_x\mathbf{I}]/e)\,\mathbf{G}$$
$$+ \mathbf{B}(\mathbf{C}[\partial f_x\mathbf{I}]\,\mathbf{B}/e)^{-1}\,u_{inv}(t),$$
$$\mathbf{x}_{inv}(0) = \mathbf{x}_0 \qquad (4.9)$$

$$\mathbf{v}_{inv}(t) = f(\mathbf{x}_{inv}(t)) \qquad (4.10)$$

$$y_{inv}(t) = -(\mathbf{C}[\partial f_x\mathbf{I}]\mathbf{B}/e)^{-1}(\mathbf{C}[\partial f_x\mathbf{I}]\mathbf{A}/e)\,\mathbf{v}_{inv}(t)$$
$$-(\mathbf{C}[\partial f_x\mathbf{I}]\,\mathbf{B}/e)^{-1}(\mathbf{C}[\partial f_x\mathbf{I}]/e)\,\mathbf{G}$$
$$+(\mathbf{C}[\partial f_x\mathbf{I}]\,\mathbf{B}/e)^{-1}\,u_{inv}(t) \qquad (4.11)$$

where $(\mathbf{C}(\partial f_x\mathbf{I})\mathbf{B}/e)^{-1} \neq 0$ to avoid divided by zero terms, $\mathbf{x}_{inv}(t)$ is an internal state of the inverse network, $u_{inv}(t)$ is an input to the inverse network, $y_{inv}(t)$ is an output of the inverse network, and the parameter vectors and matrices: $\mathbf{A}_{[n\times n]}$, $\mathbf{B}_{[n\times 1]}$, $\mathbf{C}_{[1\times n]}$, $d_{[1\times 1]}$, $\mathbf{E} = [e\times\mathbf{I}]_{[n\times n]}$, and $\mathbf{G}_{[n\times 1]}$ are of the original network. Given the input u(t) to the original network, we can achieve the output from the inverse network, $y_{inv}(t)$, which returns u(t) as well, $y_{inv}(t) = u(t)$, so the inverse is completed. Cascading the inverse and original networks gives the identity result.

4.2.2 The system for noninvasive correction

The system for noninvasive correction of the unwanted effects from the auditory loss and disorder can be constructed by using the inverse system mathematically represented in (4.9) – (4.11) which is derived from the ear type system of the patient with hearing impairment developed earlier in Chapter 3 and the normal ear type system which can be parameterized using the normative criteria of the desired auditory brainstem responses or identified from the measurement from the

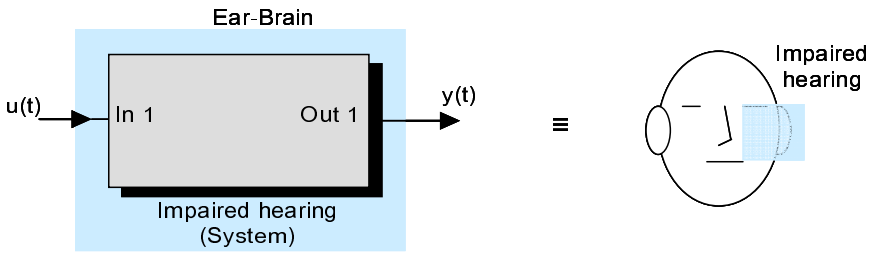

(a) The ear type system of the impaired hearing

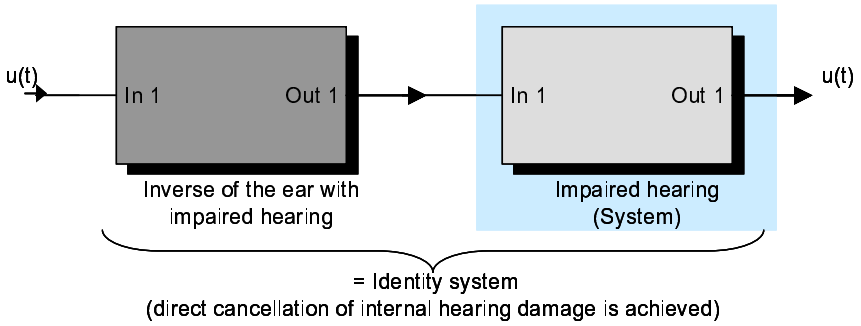

(b) The inverse and original systems

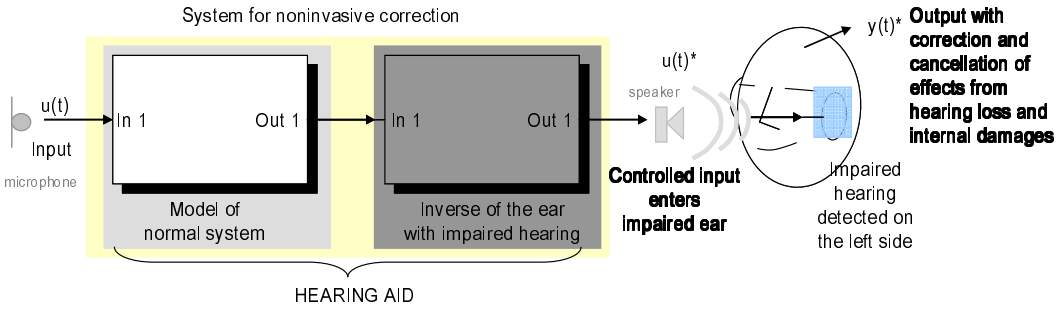

(c) The system for noninvasive correction

Figure 4.2. Simplified diagrams of the methods and systems

normal side in a case of the one sided hearing loss. The simplified diagrams of the methods are shown in Fig. 4.2.

The proposed noninvasive technique is aimed to correct the unwanted effects from the auditory loss and disorder. It should be able to adjust and modify the input sound to the ear such that the characteristics of the auditory brainstem response can be transformed into the normal ones. The corrector system using the proposed noninvasive way of correction can then be developed into an alternative hearing aid.

4.3 Application to a Simple Example

In this section a simple example is given for illustrative purpose. An original neural network and its derived inverse neural network given as an example in this section are of the same structure as the ear type system proposed in the dissertation and developed in Chapter 3 but with smaller network dimension for simplified analysis and calculation. The simplified original artificial neural network has two network layers, two internal neurons in the first layer with the hyperbolic tangent activation functions, and one neuron in the second layer with a linear activation function. The simplified original network is shown in Fig. 4.3(a) with mathematical representatives described by (4.12) – (4.14). The inverse of these representatives of the original neural network is derived following the methods given in Section 4.2. The mathematically representative inverse network is presented in (4.15)-(4.17) and shown in Fig. 4.3(b).

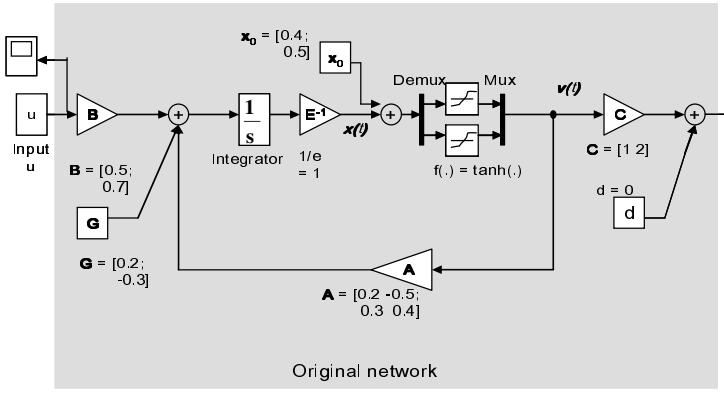

$$\mathbf{E}(d\mathbf{x}(t)/dt) = \mathbf{A}\mathbf{v}(t) + \mathbf{G} + \mathbf{B}\mathbf{u}(t), \longrightarrow \begin{bmatrix} 1 & 0 \\ 0 & 1 \end{bmatrix}\begin{bmatrix} dx_1/dt \\ dx_2/dt \end{bmatrix} = \begin{bmatrix} 0.2 & -0.5 \\ 0.3 & 0.4 \end{bmatrix}\begin{bmatrix} v1 \\ v2 \end{bmatrix} + \begin{bmatrix} 0.2 \\ -0.3 \end{bmatrix} + \begin{bmatrix} 0.5 \\ 0.7 \end{bmatrix}u(t) \quad (4.12)$$

$$\mathbf{v}(t) = \mathbf{f}(\mathbf{x}(t)) \longrightarrow \begin{bmatrix} v_1 \\ v_2 \end{bmatrix} = \begin{bmatrix} \tanh(x_1) \\ \tanh(x_2) \end{bmatrix} \quad (4.13)$$

$$y(t) = \mathbf{C}\mathbf{v}(t) + d \longrightarrow y(t) = \begin{bmatrix} 1 & 2 \end{bmatrix}\begin{bmatrix} v_1 \\ v_2 \end{bmatrix} + 0 \quad (4.14)$$

(a)

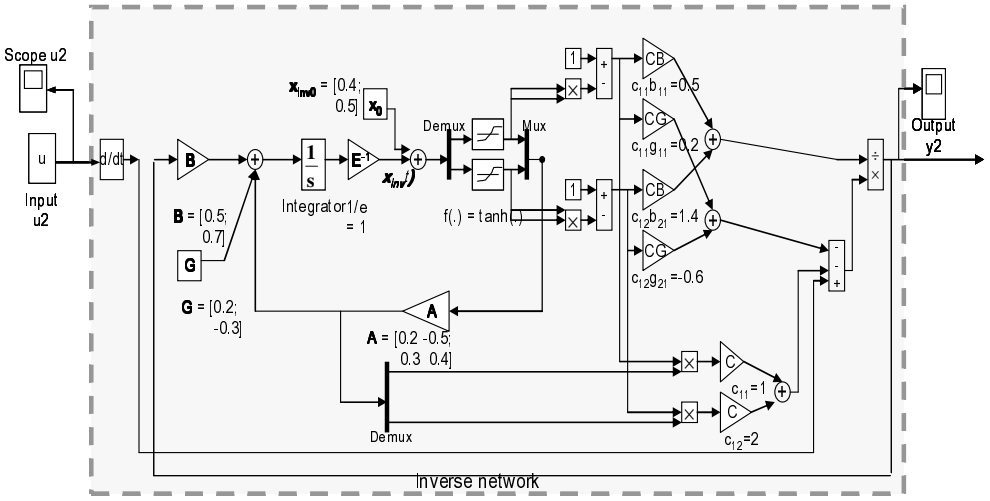

$$\mathbf{E}d\mathbf{x}_{inv}(t)/dt = \{\mathbf{A} - \mathbf{B}(\mathbf{C}[\partial f_x \mathbf{I}]\mathbf{B}/e)^{-1}(\mathbf{C}[\partial f_x \mathbf{I}]\mathbf{A}/e)\}\mathbf{v}_{inv}(t) + \mathbf{G} - \mathbf{B}(\mathbf{C}[\partial f_x \mathbf{I}]\mathbf{B}/e)^{-1}(\mathbf{C}[\partial f_x \mathbf{I}]/e)\,\mathbf{G} + \mathbf{B}(\mathbf{C}[\partial df_x \mathbf{I}]\mathbf{B}/e)^{-1}u_{inv}(t),$$

$$\longrightarrow \begin{bmatrix} e & 0 \\ 0 & e \end{bmatrix}\begin{bmatrix} dx_{inv1}/dt \\ dx_{inv2}/dt \end{bmatrix} = \left\{\begin{bmatrix} a_{11} & a_{12} \\ a_{21} & a_{22} \end{bmatrix} - \begin{bmatrix} b_{11} \\ b_{21} \end{bmatrix}(C[\partial f_x \mathbf{I}]B/e)^{-1}\begin{bmatrix} c_{11} & c_{12} \end{bmatrix}\begin{bmatrix} \partial f/\partial x_1 & 0 \\ 0 & \partial f/\partial x_2 \end{bmatrix}\begin{bmatrix} a_{11} & a_{12} \\ a_{21} & a_{22} \end{bmatrix}/e\right\}\begin{bmatrix} v_{inv1} \\ v_{inv2} \end{bmatrix}$$

$$+ \begin{bmatrix} g_{11} \\ g_{21} \end{bmatrix} - \begin{bmatrix} b_{11} \\ b_{21} \end{bmatrix}(C[\partial f_x \mathbf{I}]B/e)^{-1}\begin{bmatrix} c_{11} & c_{12} \end{bmatrix}\begin{bmatrix} \partial f/\partial x_1 & 0 \\ 0 & \partial f/\partial x_2 \end{bmatrix}/e\begin{bmatrix} g_{11} \\ g_{21} \end{bmatrix}$$

$$+ \begin{bmatrix} b_{11} \\ b_{21} \end{bmatrix}(C[\partial f_x \mathbf{I}]B/e)^{-1}\begin{bmatrix} b_{11} \\ b_{21} \end{bmatrix}/e\,u_{inv}(t) \quad (4.15)$$

$$\mathbf{v}_{inv}(t) = f(x_{inv}(t)) \longrightarrow \begin{bmatrix} v_{inv1} \\ v_{inv2} \end{bmatrix} = \begin{bmatrix} \tanh(x_{inv1}) \\ \tanh(x_{inv2}) \end{bmatrix} \quad (4.16)$$

$$y_{inv}(t) = -(\mathbf{C}[\partial f_x \mathbf{I}]\mathbf{B}/e)^{-1}(\mathbf{C}[\partial f_x \mathbf{I}]\mathbf{A}/e)\,\mathbf{v}_{inv}(t) - (\mathbf{C}[\partial f_x \mathbf{I}]\,\mathbf{B}/e)^{-1}(\mathbf{C}[\partial f_x \mathbf{I}]/e)\,\mathbf{G} + (\mathbf{C}[\partial f_x \mathbf{I}]\,\mathbf{B}/e)^{-1}\,u_{inv}(t)$$

$$\longrightarrow y_{inv}(t) = (\mathbf{C}[\partial f_x \mathbf{I}]\mathbf{B}/e)^{-1}\begin{bmatrix} c_{11} & c_{12} \end{bmatrix}\begin{bmatrix} \partial f/\partial x_1 & 0 \\ 0 & \partial f/\partial x_2 \end{bmatrix}\begin{bmatrix} a_{11} & a_{12} \\ a_{21} & a_{22} \end{bmatrix}/e\begin{bmatrix} v_{inv1} \\ v_{inv2} \end{bmatrix}$$

$$-(\mathbf{C}[\partial f_x \mathbf{I}]\mathbf{B}/e)^{-1}\begin{bmatrix} c_{11} & c_{12} \end{bmatrix}\begin{bmatrix} \partial f/\partial x_1 & 0 \\ 0 & \partial f/\partial x_2 \end{bmatrix}/e\begin{bmatrix} g_{11} \\ g_{21} \end{bmatrix}$$

$$-(\mathbf{C}[\partial f_x \mathbf{I}]\mathbf{B}/e)^{-1}u_{inv}(t) \quad (4.17)$$

where $(\mathbf{C}[\partial f_x \mathbf{I}]\mathbf{B}/e) = (c_{11}b_{11}(1-\tanh^2(x_{inv1})) + c_{12}b_{21}(1-\tanh^2(x_{inv2})))/e$

(b)

Figure 4.3. A simple example of (a) original and (b) inverse neural networks

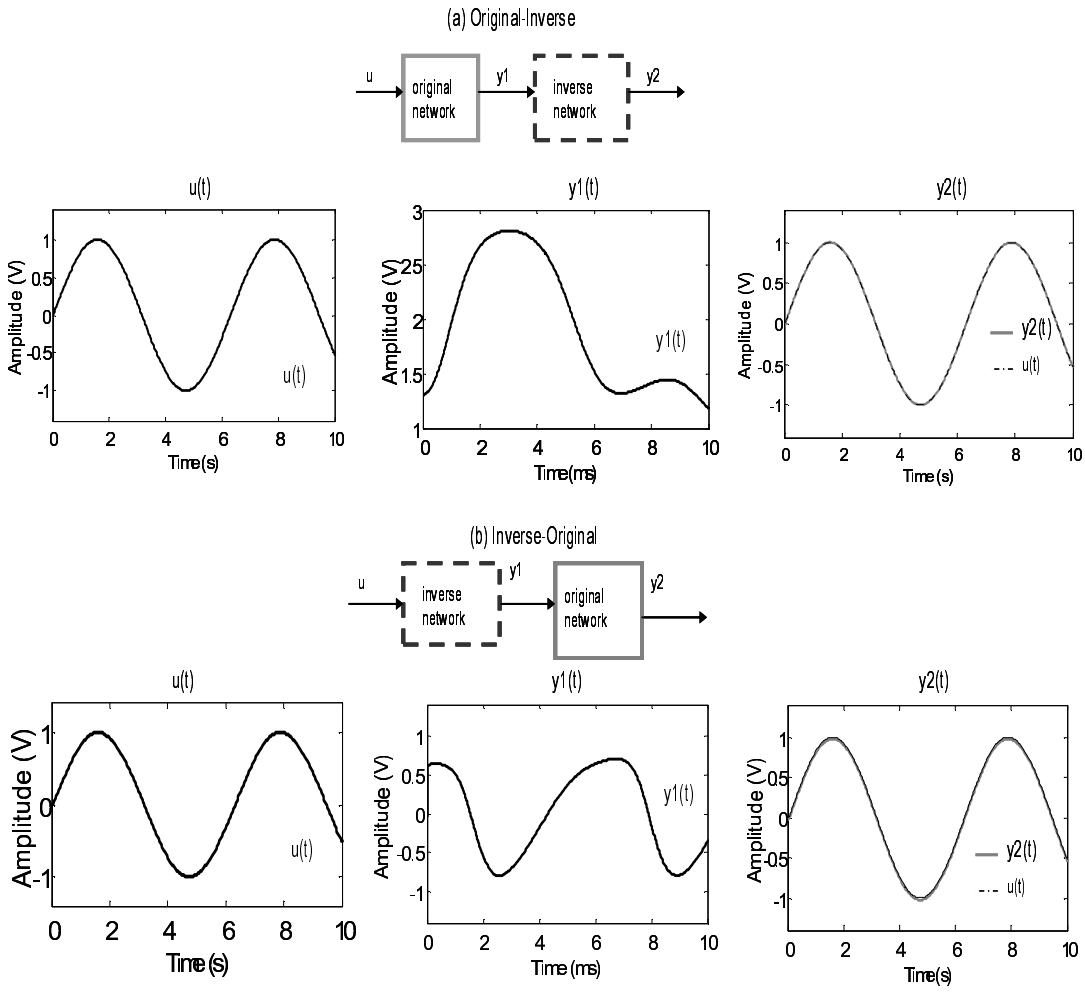

Figure 4.4. Results from the original and inverse networks of Fig. 4.3 for two different orders of cascade

The simulations are performed on the two networks set up in Simulink. The original network is fed with a input signal, u(t), which is a sine wave of amplitude 1 and frequency 1 rad/s. Cascading the original and the inverse networks, an output, $y_1(t)$, from the original network is taken to be an input, $u_{inv}(t)$, to the inverse network. The final output from the inverse network, $y_2(t)$, is obtained which shows the signal to

be equivalent to the input of the original network, $y_2(t) = u(t)$, as present in Fig 4.4(a). By switching the order of the two neural networks, the equivalency of the input and output is also obtained as shown in Fig 4.4(b). The derived inverse network is able to act as both left and right inverses of the original one which is especially useful for the implementation of a noninvasive assistive device.

4.4 Simulation Results on the System of Impaired ABR

The ABRs of the same patient with a sensorineural hearing loss in his left ear measured at the hospital discussed in Section 3.3.1 is used through out the dissertation for consistency as previously utilized in Chapter 3. The ear type systems characterizing the normal and impaired behaviors are developed. From the system of the impaired characteristics, the proposed correction method is applied. The system that is inverse to the impaired left ear system as presented in equations (4.9) – (4.11) is set up and used with the system of normal characteristics of which can be implemented using the measured data and characteristics of his right ear as the desired normative criteria for normal working ear and undamaged auditory system. The proposed system for making a noninvasive correction of effects from the hearing loss is present in Simulink diagram as shown in Fig 4.5.

The Matlab simulation is done on the Simulink model of the impaired ear. The response after the aided impaired ear is shown in Fig. 4.6 where the correction is applied. The desired normal type response as the one measured from his right ear with normal hearing is achieved satisfying the validity of the method. The corrector

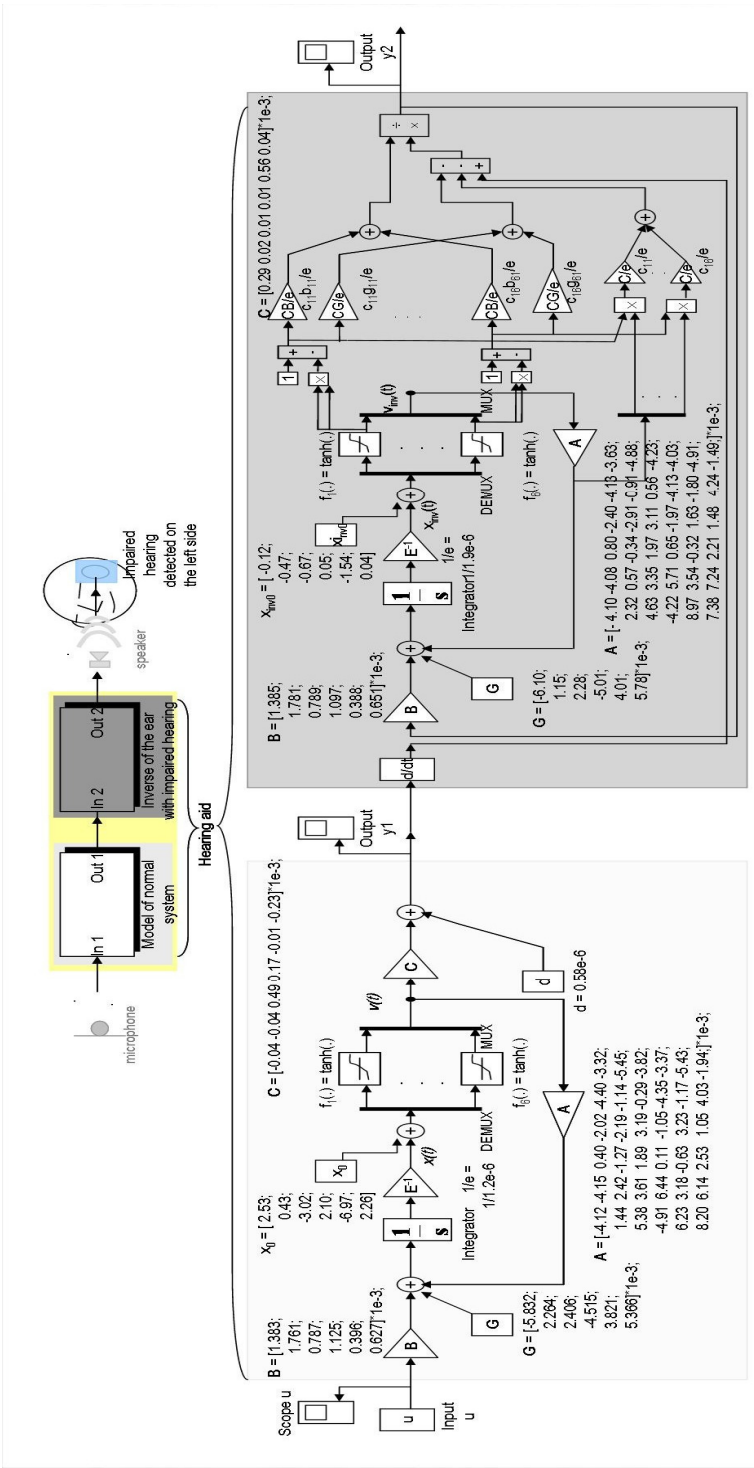

Figure 4.5. Simulink diagrams of the corrector system based on the proposed noninvasive correction technique

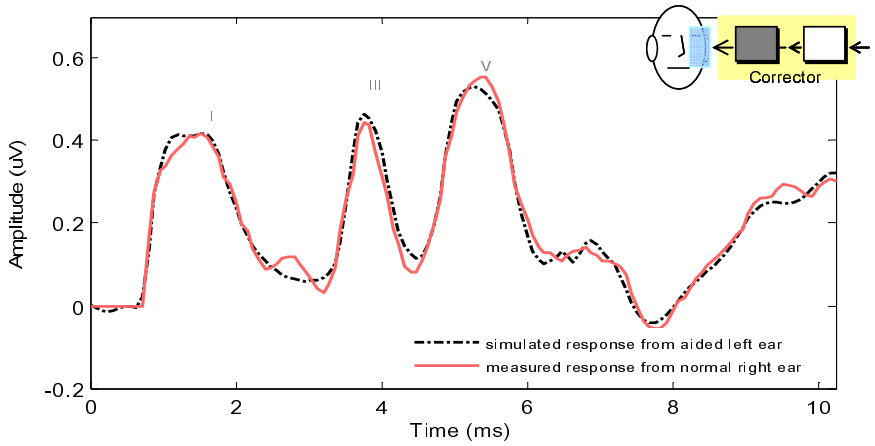

Figure 4.6. The response from simulation on the impaired ear type system with the proposed corrector system

system as per Fig. 4.5 can be developed into the new type of assistive device alternate to the conventional hearing aid that can produce the auditory brainstem response with desired characteristics within normal limits potentially correcting the unwanted effects from auditory loss and disorder and resulting in improved hearing and better speech perception.

4.5 Result Analysis and Evaluation on Potential Benefits and Performances

The noninvasive correction method of auditory loss and disorder effects is proposed and the system for making a correction is developed earlier in the chapter. Promising simulation results on the system of the impaired ear show auditory brainstem responses with improved characteristics to normal types as shown in Fig. 4.6. An analog circuit realization of the corrector system will be presented and

discussed in Chapter 5 leading to a possible implementation of a new type of hearing aid hardware based on the proposed method. To evaluate the performance of the proposed correction method and the potential effectiveness as an actual hearing aid, additional simulations and results are discussed and some aspects are compared with the signal processing techniques used in the conventional analog and digital hearing aids.

4.5.1 Comparison of the ABRs from the conventional and proposed hearing aids

The ABR has been clinically used and well established as a reliable tool for auditory function assessment and diagnosis by evaluating its temporal waveform characteristics. The response measured from the patient is compared against the established normative values and standardized templates. The particular advantages of the ABR include the nature of the response that reflects the neural signal processing of sound inside the human auditory system and the objective way of the measurement that can be used in infants, young children, and difficult-to-test patients. It is also useful as a tool for monitoring the human auditory system integrity during surgical procedures [25]-[26]. Currently, the measurement of the electrical nerve and neuron responses such as the auditory brainstem response or other electrophysiologic signals have not been widely utilized and incorporated into the development of new signal processing schemes for hearing aids. The evoked responses are, however, found helpful in the fitting process of the conventional hearing aids for very young infants to estimate the hearing threshold audiograms or validate the capabilities of the

conventional hearing aids [27]-[30], [94]-[100]. By comparing the evoked responses recorded from a patient without and with an aid on, the hearing aid gain is consequently set based on the presence, absence, or improvement of the measured ABR wave characteristics.

In fact our proposed correction technique is supported by the findings from these fitting approaches which share the common underlying principle of the correlation between the measured auditory evoked responses and the auditory perception. Normal type responses are indicators of normal working hearing function and normal speech perception. The use of ABR is incorporated into the signal processing of our proposed hearing aid whose section for making a correction and cancellation of the unwanted effects from the auditory loss and disorder is designed to modify the input sound to the ear which in turn yields the auditory evoked response with normal characteristics. By utilizing our proposed method that allows direct cancellation of the unwanted effect as part of the signal processing scheme of the proposed hearing aid, the simulated ABRs on the model of impaired ear with the proposed hearing aid thus show clearer correction of the waveform. The ABR characteristics obtained from our results are closer to normal which generally agree with the past findings of the ABRs recorded from the patients while wearing the conventional hearing aid [29]-[30]. However, the response from our proposed hearing aid of which the use of ABR is incorporated into the signal processing schemes shows better and clear waveforms as shown in Fig. 4.8 when compared to the ABRs

obtained from the hearing impaired subjects while wearing the conventional hearing aid as shown in Fig. 4.7 from [30].

Although, the appearance of ABR and improved waveform morphology can be detected by increasing the amplification of the conventional hearing aid, despite the unreliable or no responses at all in the unaided conditions, the estimated hearing threshold obtained from the aided and unaided measurements require specific correction factors at each of the test frequencies which can result in under or over amplifications. Also, there can be an interaction between the hearing aid equipment circuitry and the input sound and interference from outside noise and

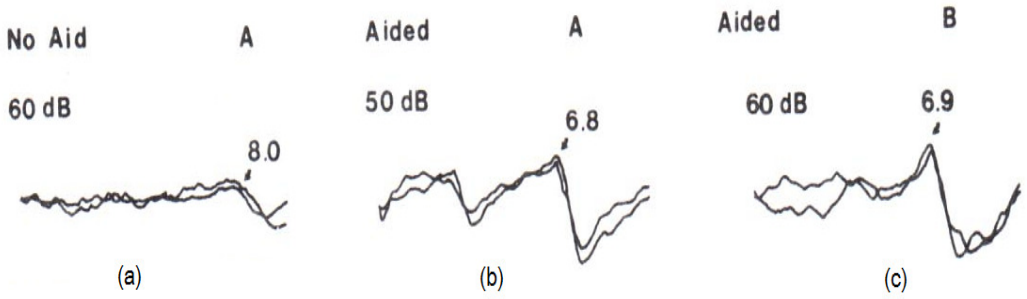

Figure 4.7. The ABRs recorded from (a) patient A in the unaided condition, (b) patient A in the aided condition showing the improvement of responses after the amplification, and (c) patient B, whose ABR in the unaided condition cannot be detected, showing responses in the aided condition (selected figures with comparable dB from [30, p.52] with permission from Wolters Kluwer Health)

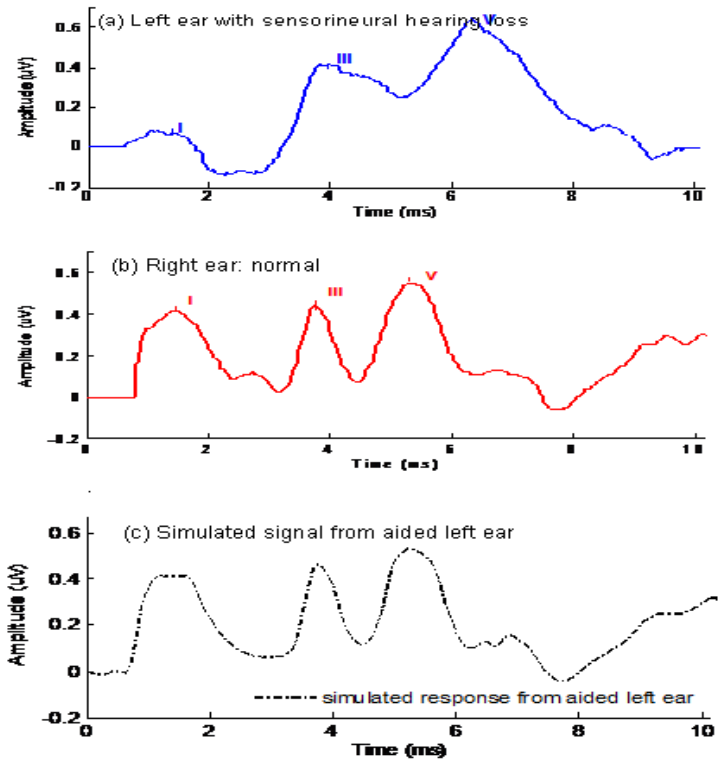

Figure 4.8. The ABR data from a patient with suspected hearing loss in the left ear: (a) the ABR of the left ear with delayed latency and waveform morphology confirming the hearing loss (from measurement), (b) the ABR of the normal working right ear with characteristics within normative references (from measurement), and (c) the ABR of the left ear after the proposed hearing aid system (from simulation).

other artifacts that give rise to the inaccuracy limiting the application of these aided and unaided approaches for conventional hearing aid settings [96]-[98]. Nonetheless the conventional hearing aids are all based on the increase of the sound volume at each of a limited number of audiometric frequencies. Although some of the newer

models may include added-on features such as directional microphones for better one to one conversation [37], the ability of our proposed hearing aid introduced in this dissertation to make a correction in a noninvasive way is worth further investigation.

The proposed hearing aid system can be implemented utilizing signals from other electrophysiologic measures as well, for example, the late latency response (LLR), also known as the auditory cortical responses, which reflects the auditory activities deeper along the auditory pathway inside the brain. However, the steps required for measuring the LLR are more complicated and difficult. The increasing interest in these electrophysiologic signals such as the ABR or the LLR arises from their clinical usefulness assisting in the evaluation of the hearing aids for infants [96]-[97], [100]. In a way it is possible to infer that the correction made at the signals obtained from deeper level along the auditory pathway including the central nervous system inside the brain has potentially taken into account the underlying sound perception mechanism which might provide extra advantages and more benefits for the patients.

4.5.2 Comparison of signal processing by the conventional and proposed hearing aids

To compare other aspects and learn more about what modifications of sounds and signals are implemented by a new hearing aid based on the proposed correction technique, additional simulations are presented and compared with those based on the

available data of the conventional hearing aids. The results from the ear type systems and corrector system of the same patient with unilateral hearing loss are analyzed for consistent comparisons. The patient has a sensorineural hearing loss in his left ear whose ABRs have been measured from which the systems proposed for making a correction of these detected effects from the hearing impairment have been developed and discussed earlier in the chapter.

First, the signals are analyzed at the input and output of the proposed aid system to see the effects of the method on the signals and calculate the gain curve of the new hearing aid. The block diagram of the noninvasive correction is shown again in Fig. 4.9(a). The auditory input used in the dissertation for measuring the evoked potentials of the auditory brainstem is the click stimulus whose theoretical frequency spectrum is broad, ideally stimulating the whole working region of the cochlea. Also the abrupt onset of the click temporal waveform can evoke synchronous activities and firings of more auditory neurons than an input with less abrupt onset, such as frequency specific tones [12]-[14]. The frequency spectrum of the acoustic click input obtained by using the Fast Fourier Transform (FFT) is presented in Fig. 4.9(b). By monitoring the signals at the output of the proposed aid system, the properties of the hearing aid can be analyzed. The frequency spectrum at the output of the corrector system is presented in Fig. 4.9(c). Following the results of this patient, the simulated gain curve of the hearing aid can be achieved as shown in Fig. 4.9(d).

The full-on (maximum volume setting [36]) gain curves from the commercially available hearing aids are presented for illustrative purposes in Fig. 4.10 [101]-[102]. The figures show that the proposed corrector system for this patient with his hearing loss is also capable of providing comparable amplification as those from the commercial aids. Moreover the results from these simulations show that the

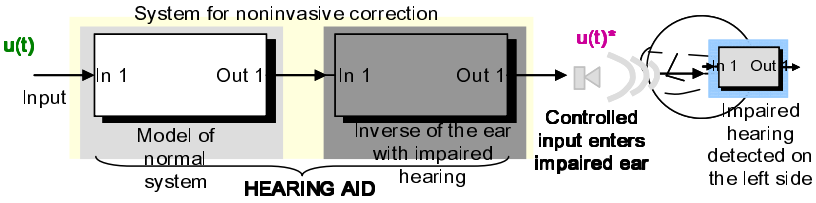

(a) The system for noninvasive correction

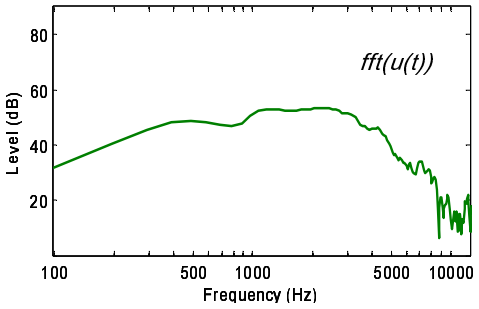

(b) Click stimuli input : Acoustical signal ≡ u(t)

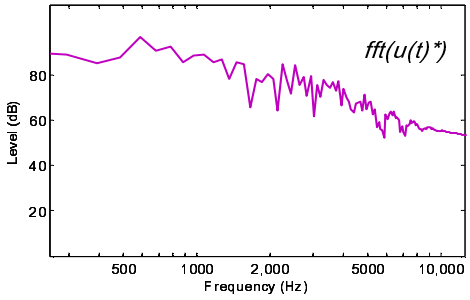

(c) Input to the impaired ear (system) ≡ u*(t) (from simulation)

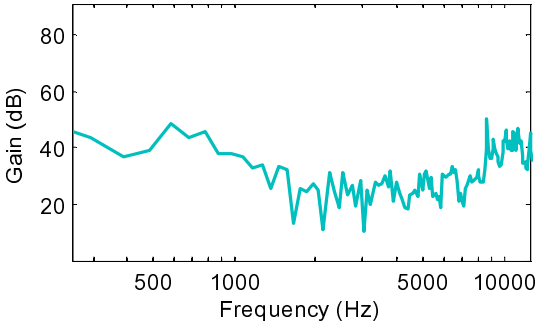

(d) Gain curve of the proposed hearing aid ≡ fft(u*(t)/u(t)) (from simulation)

Figure 4.9. Analysis of the signals in frequency domain

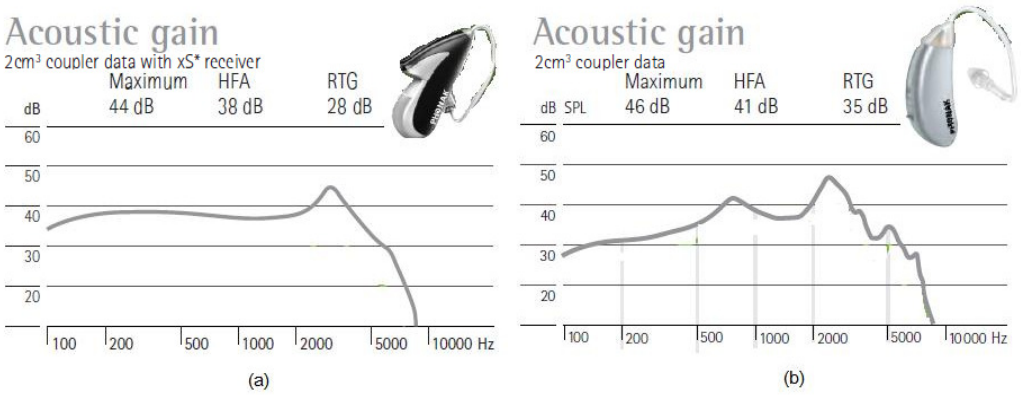

Figure 4.10. Samples of the gain curves of two different commercial digital behind-the-ear hearing aids: (a) standard model from [101] and (b) more advanced model from [102] (with permission from Phonak, Inc., USA.)

input gets amplified evaluated in the frequency domain which give rise to an application of the proposed correction method to be used assisting in the prescription and fitting processes instead of adjusting the gain per a limited number of frequency bands tested with the pure tone audiogram currently utilized in the conventional hearing aid prescriptions and distributions which can result in over- or under-amplification of the aid, also discussed earlier in Section 2.3 Fig. 2.4. The proposed hearing aid developed based on the correction technique can serve as the desired settings and characteristics of the hearing aid that potentially stimulate the auditory system yielding the auditory brainstem response with normal characteristics. The idea to use the ABR as the main criteria to set the gain of conventional hearing aids was also mentioned in [22] but no further literatures on the topic were found. The uses of the late latency responses for evaluation of hearing aid benefits in infants in recent

researches [96]-[98],[100] have shown successful results on these electrical signals measured from the brain to determine the hearing improvement on the patients.

From Fig. 4.10, we can see that the gains of conventional hearing aids are typically cut off around 8000Hz which corresponds to the maximum frequency used in standard pure tone measurement and typically presented in speech spectrum. The high frequency pure tone audiometry can also be useful for testing the hearing loss primarily of high frequencies typically found in the hearing loss due to aging and ototoxic medications. The increase of high frequency gain also means the amplification of both speech and noise which can limit the hearing aid benefit. The problems concerning the internal feedback and distortion at high frequency have been resolved by using digital feedback reduction and by using the special ear-mold that allows better ventilation [57, pp. 176-201]. To evaluate the effects of this limitation on our proposed hearing aid, the data of the signal curves of Fig. 4.9 at frequency above 5 kHz are filtered out with a reduction in magnitude of about 40dB to reduce high frequency components and mimic those curves of commercially available hearing aids of Fig. 4.10. The new filtered gain curve of the proposed aid is shown in Fig. 4.11(a). The filtered signals are then simulated on the model of the impaired hearing. The ABR output from the model is shown in Fig. 4.11(b) which shows the desired signal with normal characteristics similar to the signal previously achieved from the simulation of Fig. 4.8(c). This shows that the amplification in the high frequency region as previously presented in Fig. 4.9(d) does not make any effect on the ABR output the reason for which could be due to the magnitudes of high

frequency components of the signal to get the ABR are actually very low compared to the low frequency components which can be seen in Fig. 4.11(c). The figure is plotted using the magnitude of the fast Fourier transform in a linear scale. The other reason could be due to the frequency components of ABRs are primarily in the low frequency region [127]. Hence the hearing aid gain can be cut off in the high frequency region which resolves a concern about high frequency noise of the hearing aid.

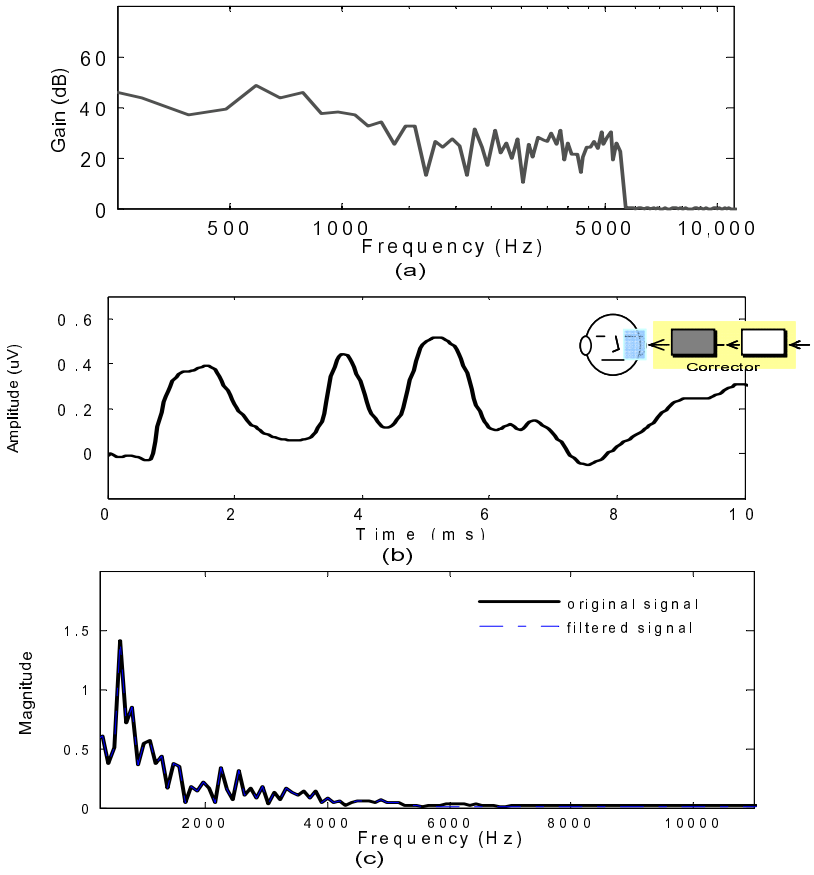

Figure 4.11. (a) new filtered gain curve of the proposed hearing aid, (b) the ABR of the model of impaired left sided-hearing using the filtered signal (from simulation), and (c) magnitude of the signal of Fig. 4.9(c) in a linear scale

4.5.3 Analysis of the developed neural network representative of the ear type systems with speech signal input

To further analyze and learn more about the developed neural network of the ear type system through the ABR and the proposed system for making a correction based on the technique to be implemented as the real hearing aid, the developed neural network systems are simulated with speech signal as the input. For this illustrative example, the input signal is a segment of an utterance of vowel sound /a/ with its temporal waveform as shown in Fig. 4.12(a) and its spectral waveform as shown in Fig. 4.12(b). The waveforms show a characteristic of the voiced sounds which usually exhibit regular and periodic waves [37, pp.1-17]. The temporal waveform has the periodic pattern with a period about 1ms corresponding to the peaks at a fundamental frequency of 100Hz and at the successive harmonic

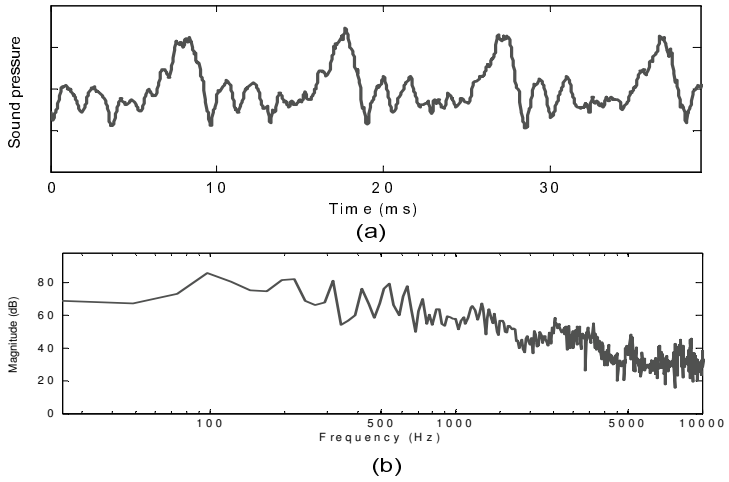

Figure 4.12. A waveform of a segment of the utterance of sound /a/ in (a) a time domain, and (b) in a frequency domain

(data provided by Professor Carol Espy-Wilson)

frequencies presented dominantly in the low frequency region as shown in Fig. 4.12(b). An onset click stimulus followed by a 20ms delay of this speech signal is used as the input of which the total time lasts about 60ms. The input is then given to our neural networks of the ear type systems set up via the ABRs measured from normal right sided-hearing and hearing loss affected-left sided hearing of the patient as previously developed and presented as the Simulink diagrams in Fig. 3.7(a) and (b). The outputs from the simulation are shown in Fig. 4.13(b) and (c) showing the ABR wave outputs with some patterned components resembled to those of the speech stimulus used to stimulate the systems. Our results from simulations are in agreement with the measurements of ABR to some specific speech syllables recorded from normal hearing people in the literatures [14, p. 614], [128]-[130] from which they stated that the measured ABRs are composed of the transient component and periodic frequency following component of which its periodicity follows the temporal envelopes of the speech stimulus. The speech stimulus typically used in the measurement is the consonant followed by the vowel sound, such as /ba/, /da/, or /ga/. The consonant sound with its short duration stimulates auditory neurons with a rapid temporal onset reflected in the transient components and the vowel sound with its periodic structure is reflected in the steady state components [128]. However the periodic frequency following portions of the ABRs from the measurements have exhibited time lagged following the stimulation quite longer than in our simulations.

The ABR output to the speech stimulus from the system of normal hearing type is shown in Fig. 4.13(b) which has higher magnitude compared to the output from the system of hearing loss type shown in Fig. 4.13(c).

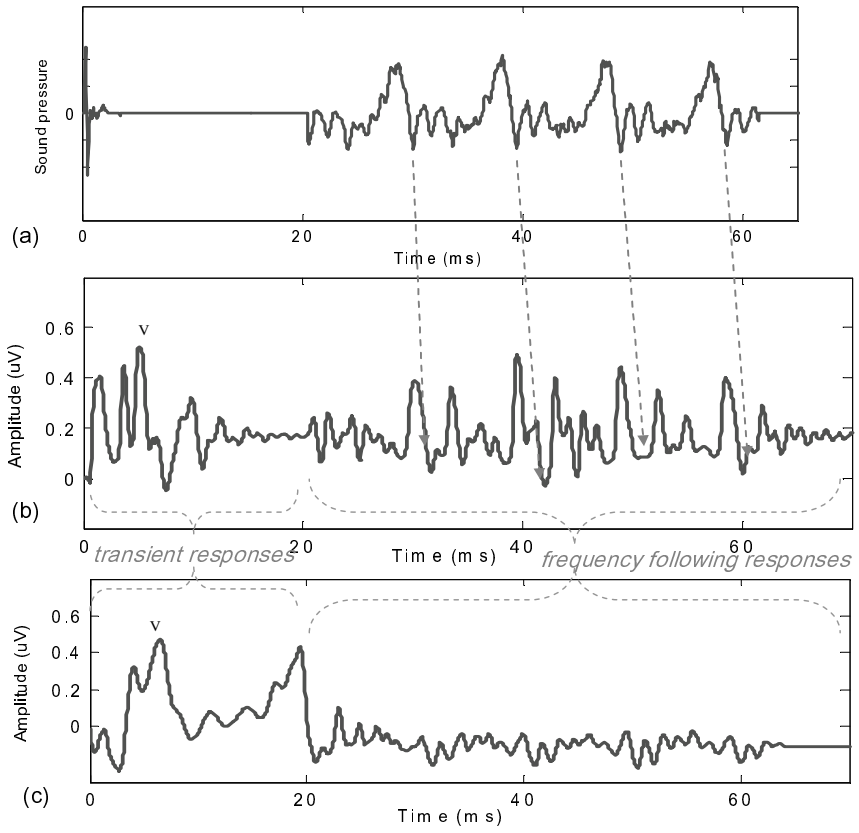

Figure 4.13. Additional analysis using speech stimulus: (a) a speech stimulus of Fig. 4.12a used as the simulation for easy comparison, (b) the ABR output from the neural network of normal ear type system, and (c) the ABR output from the neural network of ear type system with hearing loss

4.6 Summary

The proposed noninvasive correction method is discussed in this chapter. Since we are able to develop an individual ear type system that can characterize the normal and hearing loss-affected functions of the human auditory system through the measured auditory brainstem responses, the system developed for canceling and correcting these hearing loss effects is investigated. The resulted corrector system can be developed in to a new noninvasive assistive device alternate to a conventional hearing aid. The noninvasive correction concept is given as well as the technique for deriving the corrector system using the inverse artificial neural network. The technique for finding the inverse of the ear type system can also be applied to other systems with multilayer neural network architectures used in other applications as well. For example, this method can be used in a control design where the correction technique can be applied to achieve a certain signal or in a speech signal application where it is possible to retrieve back a certain input from a known output.

A simple example is given in Section 4.4 for a network with two internal neurons for illustration of the method. The simulations on the model of the patient with unilateral sensorineural hearing impairment are presented giving satisfying results. The chapter ends with discussion on potential benefits and performances of the proposed technique when being used as a hearing aid and additional analysis on the proposed hearing aid in time and frequency domains and to the speech signal. A hearing aid based on the proposed correction technique can potentially provide an improved means for assisting hearing impaired patients.

Chapter 5

Circuits for the Proposed Hearing Aid

Characterizations between normal and impaired hearing functions have been made possible through the auditory brainstem responses based on which the individual ear type system is developed in Chapter 3. A noninvasive way to correct these detected effects of the hearing loss and impairment was introduced in Chapter 4 where the new technique that implements the system inverse to the ear type system of impaired hearing function was given. The system for making a correction has been simulated showing satisfying corrected responses (see Fig. 4.8). A possible hardware design of a new assistive device based on the noninvasive correction technique can be developed of which circuit design and realization are investigated in this chapter including the following topics.

1. A framework for designing the circuit from the hearing aid system. The design and parameter scaling of the corrector system suitable for circuit implementation are given as the basis steps for implementing the circuits.
2. A set of transistorized circuits required to complete the system of which the bipolar junction transistors (BJT) and complementary metal oxide semiconductor field effect transistors (CMOS) are utilized. The basic transistorized circuit components constituting the proposed corrector system together with options for circuits with variable weight setting capability for possible external tuning and faster adjustment are given.

The design and realization of the corrector system as the electrical circuits serve to show that the investigation of the new assistive device developed based on the proposed noninvasive correction technique to be implemented as a real hearing aid can be further made possible.

5.1 Overview of Circuit Realization

From the corrector system developed in Chapter 4, the circuits for the assistive device are first designed for the schematic and parameters used. The mathematically representative system for making a noninvasive correction, as shown in Fig. 4.5 in a Simulink diagram, is first transformed into its representative circuits. The parameter scaling of the corrector system is then designed to be suitable for appropriate working ranges of the transistors from which the circuits can be built. For illustration of the methods and results, the circuits and their parameter values investigated in this chapter are based on the data of the patient who has a sensorineural hearing loss in the left ear from which two ear type systems differentiating between the loss-affected and normal hearing functions have been developed through the use of auditory brainstem responses in Chapter 3 (Fig. 3.6 and Fig. 3.7); the corrector system based on the proposed noninvasive correction technique has been investigated in Chapter 4 (Fig. 4.5 and Fig. 4.6).

5.1.1 Circuit Representatives of the Corrector System

As discussed in Chapter 4, the corrector system based on the proposed

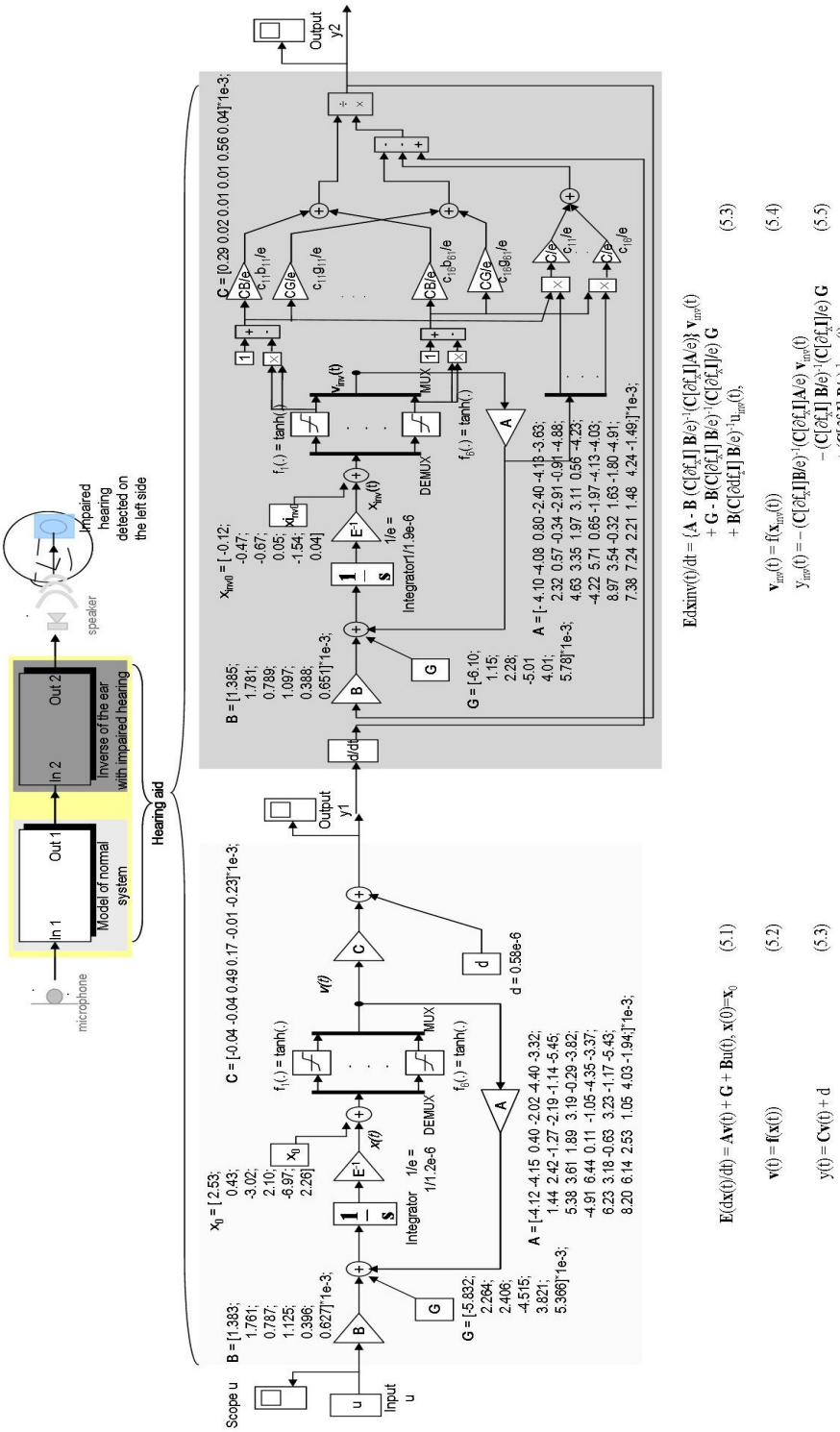

Figure 5.1. The Simulink diagram of the proposed assistive device

technique is composed of the ear type system of normal hearing function and the inverse system that is derived from the ear type system of abnormal hearing function measured and developed through the auditory brainstem responses (ABRs) of the patients. The corrector system based on the proposed noninvasive correction technique is to be used as a new type of hearing aid whose circuits are investigated in this chapter to show that the application of the corrector system as a real hearing aid is possible. The corrector system for making a noninvasive correction of the auditory loss and disorder of the patient as shown in the Simulink diagram of Fig. 4.4 is redrawn in Fig. 5.1 with its respective parameters. The mathematically descriptive equations of the corrector system given in Chapter 4 are also presented in Fig. 5.1.

The corrector system is constructed from the ear type system of normal hearing function and characteristics and the system inverse to the patient's impaired hearing function. In the case of the patient with a one-sided sensorineural hearing loss used for illustrative purpose in this dissertation, the ear type system of normal type can be set up through the evoked ABR measured with the stimulus to his normal working right ear for which the mathematical representatives are expressed in (4.1)-(4.3) and are reprinted as

$$\mathbf{E}_R(d\mathbf{x}_R(t)/dt) = \mathbf{A}_R\mathbf{v}_R(t) + \mathbf{G}_R + \mathbf{B}_R u_R(t),\ \mathbf{x}_R(0) = x_{R0} \quad (5.1)$$

$$\mathbf{v}_R(t) = \mathbf{f}(\mathbf{x}_R(t)) \quad (5.2)$$

$$y_R(t) = \mathbf{C}_R\mathbf{v}_R(t) + d_R \quad (5.3)$$

where $u_R(t)$ is a stimulus input signal to the test ear, $y_R(t)$ is an output signal, $\mathbf{x}_R(t)$ is a vector of *n* internal neurons, and $\mathbf{A}_{R[n\times n]}$, $\mathbf{B}_{R[n\times 1]}$, $\mathbf{C}_{R[1\times n]}$, $d_{R[1\times 1]}$, $\mathbf{E}_R = [e_R\times\mathbf{I}]_{[n\times n]}$,

$e_{R[1\times1]}$, and $\mathbf{G}_{R[n\times1]}$ are scalar, vectors and matrices of real parameter values identified according to the right sided ABR. For the system that is inverse to the hearing loss-affected auditory system measured through the ABR, this inverse system can be derived from the ear type system set up through the measured responses with stimulus to the left ear. The mathematically representative inverse system are presented in (4.9) – (4.11) and reprinted as

$$\begin{aligned}\mathbf{E}_L d\mathbf{x}_{Linv}(t)/dt = \{&\mathbf{A}_L - \mathbf{B}_L (\mathbf{C}_L[\partial f_{xL}\mathbf{I}]\, \mathbf{B}_L/e_L)^{-1}(\mathbf{C}_L[\partial f_{xL}\mathbf{I}]\mathbf{A}_L/e_L)\}\mathbf{v}_{Linv}(t)\\ &+ \mathbf{G}_L - \mathbf{B}_L (\mathbf{C}_L[\partial f_{xL}\mathbf{I}]\, \mathbf{B}_L/e_L)^{-1}(\mathbf{C}_L[\partial f_{xL}\mathbf{I}]/e_L)\, \mathbf{G}_L\\ &+ \mathbf{B}_L (\mathbf{C}_L[\partial f_{xL}\mathbf{I}]\, \mathbf{B}_L/e_L)^{-1}\, u_{Linv}(t),\end{aligned}$$

$$\mathbf{x}_{Linv}(0) = \mathbf{x}_{L0} \qquad (5.4)$$

$$\mathbf{v}_{Linv}(t) = f(\mathbf{x}_{Linv}(t)) \qquad (5.5)$$

$$\begin{aligned}y_{Linv}(t) = &- (\mathbf{C}_L[\partial f_{xL}\mathbf{I}]\mathbf{B}_L/e_L)^{-1}(\mathbf{C}_L[\partial f_{xL}\mathbf{I}]\mathbf{A}_L/e_L)\, \mathbf{v}_{Linv}(t)\\ &- (\mathbf{C}_L[\partial f_{xL}\mathbf{I}]\, \mathbf{B}_L/e_L)^{-1}(\mathbf{C}_L[\partial f_{xL}\mathbf{I}]/e_L)\, \mathbf{G}_L\\ &+ (\mathbf{C}_L[\partial f_{xL}\mathbf{I}]\, \mathbf{B}_L/e_L)^{-1}\, u_{Linv}(t)\end{aligned} \qquad (5.6)$$

where $(\mathbf{C}_L(\partial f_{xL}\mathbf{I})\mathbf{B}_L/e_L)^{-1} \neq 0$ to avoid a divided by zero term, $\mathbf{x}_{Linv}(t)$ is an internal neuron of the inverse system, $u_{Linv}(t)$ is an input to the inverse system which is equivalent to the differential of $y_R(t)$, $u_{Linv}(t) = dy_R(t)/dt$, $y_{Linv}(t)$ is an output of the inverse system, and the coefficients: $\mathbf{A}_{L[n\times n]}$, $\mathbf{B}_{L[n\times1]}$, $\mathbf{C}_{L[1\times n]}$, $d_{L[1\times1]}$, $\mathbf{E}_L = [e_L\times\mathbf{I}]_{[n\times n]}$, e_L and $\mathbf{G}_{L[n\times1]}$ are scalar biases, vectors, and matrices of real values of the original ear type system whose parameters are identified according to the left sided ABR signals. The corrector system based on the correction technique to be developed into a hearing aid with its respective variables and parameters are shown in Fig. 5.1.

To model the corrector system in circuits, the variables of the corrector system (5.1) – (5.6) are realized as the voltages and currents in electrical circuits. The circuit design is presented to show a possibility of implementing the correction system as hardware. The selection of system variables as voltages or currents does not necessary mean the physical relationship of the system variables and the electrical signals. For example, an appropriate selection of the representative circuit signal for the internal neuron, $x_i(t)$, can be the voltage since its differential product can be represented as the current signal proceeding from which the remaining representatives of the system variables and parameters can be subsequently selected.

In (5.1), the internal neurons, $\mathbf{x}_R(t)$, are the voltage signals on capacitors with values equal to e_R. Equation (5.1) can be implemented as a summation of the current signals following Kirchhoff's current law [118]. So all $\mathbf{A}_R\mathbf{v}_R$ (t), $\mathbf{G}_R$, and $\mathbf{B}_R u_R$ (t) terms are equivalent to currents. The variable $\mathbf{v}_R$ (t) is selected to be a current signal, so the term $\mathbf{A}_R\mathbf{v}_R$ (t) can be implemented using current mirrors. The bias vector $\mathbf{G}_R$ can be implemented using current sources. The input variable u_R (t) is selected to be a voltage signal, so the term $\mathbf{B}_R u_R(t)$ can be implemented using CMOS differential pairs.

In (5.2), with the internal neurons, $\mathbf{x}_R(t)$, chosen as the voltage signals and $\mathbf{v}_R(t)$ as the current signals, a hyperbolic tangent term, f(.) = tanh(.), can then be implemented using a BJT differential pair.

In (5.3) a term $\mathbf{C}_R\mathbf{v}_R$ (t) can be represented as a summation of the current signals which is conveniently implemented by connecting the wires to the same node following Kirchhoff's current law from which $v_{Ri}(t)$ is the current signal and $\mathbf{Cv}(t)$ can be implemented using current mirrors. A scalar output bias d_R can be realized by a current source. All currents are then summed and connected to the resistor yielding the final output. The output $y_R(t)$ is selected to be a voltage signal the same as the input $u_R(t)$ which also corresponds to the electrical potentials recorded on the scalp through the ABR measurement.

Since the mathematically representative inverse system of (5.4)-(5.6) are derived from the original system of (5.1)-(5.3), the same representatives of the same variables in circuits are applied. The subscript $_L$ is referred to the original system set up through the measured left sided ABR that exhibits the auditory loss and disorder effects for which the noninvasive correction technique will be applied. The variable $x_{Linv}(t)$ as the voltage signal, v_{Linv} (t) ($v_{Linv}(t) = f(x_{Linv}) = \tanh(x_{Linv}(t))$) as the current signal, u_{Linv} (t) as the voltage signal, and y_{Linv} (t) as the voltage signal. The additional terms required for the inverse system seem complicated however they are designed to be the scalar gain values when calculated from their matrix elements. The gradient of the hyperbolic tangent function requires the multiplier circuits, as shown in Fig. 5.1.

In (5.4), a term ∂f_{xL} is equal to $(1-\tanh^2(x_{iL}))$ which needs a multiplier to implement the square product of the current signals. The entries of term $(\mathbf{C}_L[\partial f_{xL}\mathbf{I}]\mathbf{B}_L/e_L)^{-1}$ are equal to scalars which can be implemented using current mirrors. The

terms $(\mathbf{C}_L[\partial f_{xL}\mathbf{I}]\mathbf{A}_L/e_L)\mathbf{v}_{Linv}(t)$ and $(\mathbf{C}_L[\partial f_{xL}\mathbf{I}]\mathbf{A}_L/e_L)\mathbf{G}_L$ are also implemented in a similar way as the current signals with their respective gains which again can be implemented using current mirrors. The internal neuron variables in $\mathbf{x}_{Linv}(t)$ are represented by the voltage signals on the capacitor with capacitance values e_L.

In (5.5) using $\mathbf{x}_{Li}(t)$ as voltage signals and $\mathbf{v}_{Li}(t)$ as current signals, a hyperbolic tangent term, f(.) = tanh(.), can then be implemented with a BJT differential pairs.

In (5.6) the entries in $(\mathbf{C}_L[\partial f_{xL}\mathbf{I}]\mathbf{B}_L/e_L)^{-1}$ are equal to scalar values for which $[\partial f_{xL}\mathbf{I}]$ is represented as current signals multiplied by their respective gains which can be implemented using current mirrors in the same way as the implementations of $(\mathbf{C}_L[\partial f_{xL}\mathbf{I}]\mathbf{A}_L/e_L)\mathbf{v}_{Linv}(t)$ and $(\mathbf{C}_L[\partial f_{xL}\mathbf{I}]\mathbf{A}_L/e_L)\mathbf{G}_L$. The final output $y_{Linv}(t)$ to be fed into the transducer as part of the hearing aid can then be implemented as a summation of all current signals connected to a resistor to simulate the corresponding voltage output $y_{Linv}(t)$.

Sections of the circuits of the corrector system to be used as the hearing aid, as shown in Fig. 5.1, are given in Fig. 5.2 showing various basic circuit components, the outline of the schematic and the circuit representatives of the system variables described earlier. For easier comparison, Fig. 5.2 is divided into Fig.5.2a of the normal system and Fig. 5.2b of the inverse system making up the hearing aid.

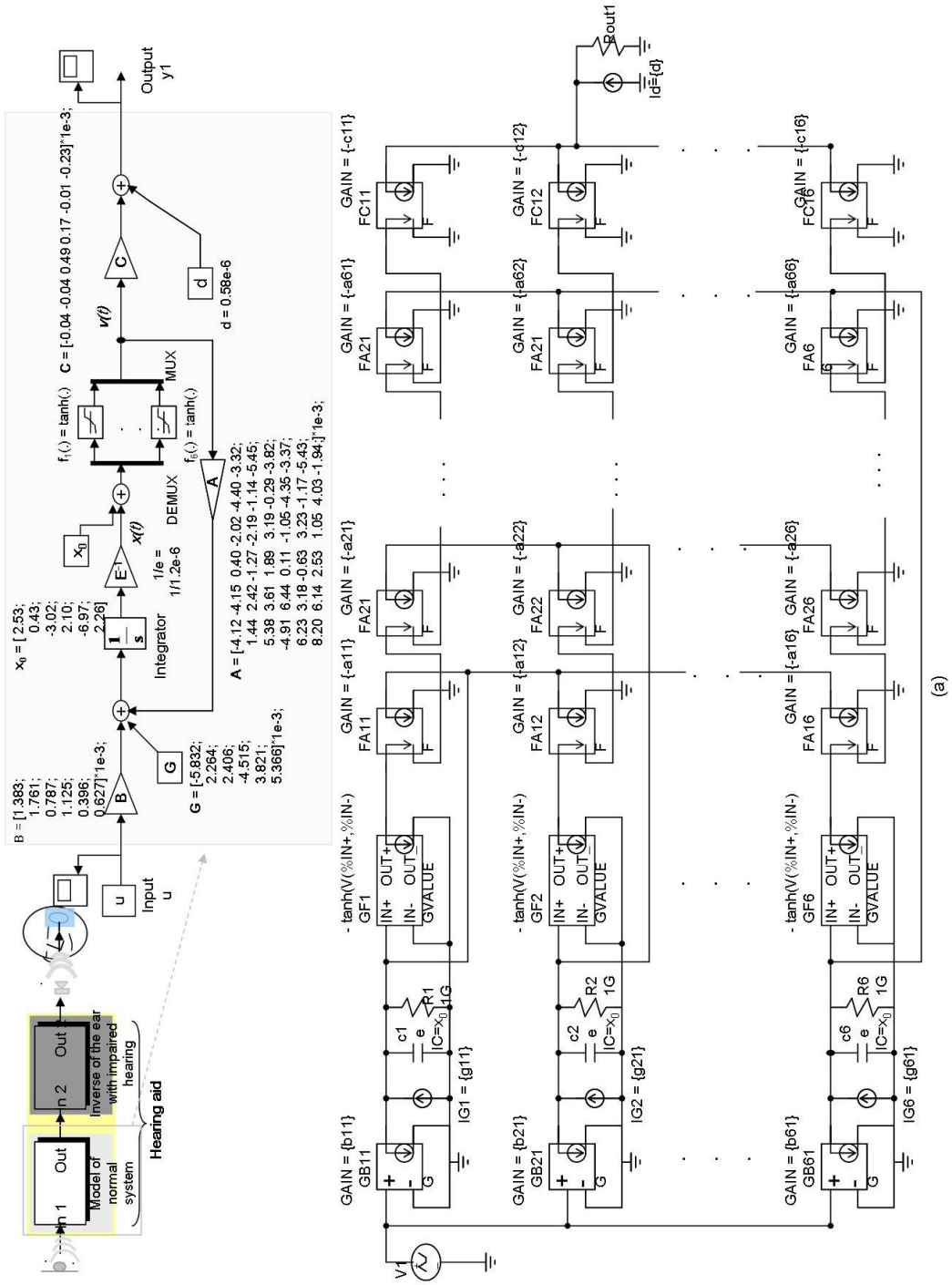

Figure 5.2.(Part 1) Schematics for the corrector system of Fig.5.1 consisting of a) the model of normal system and b) the inverse of the system with hearing loss

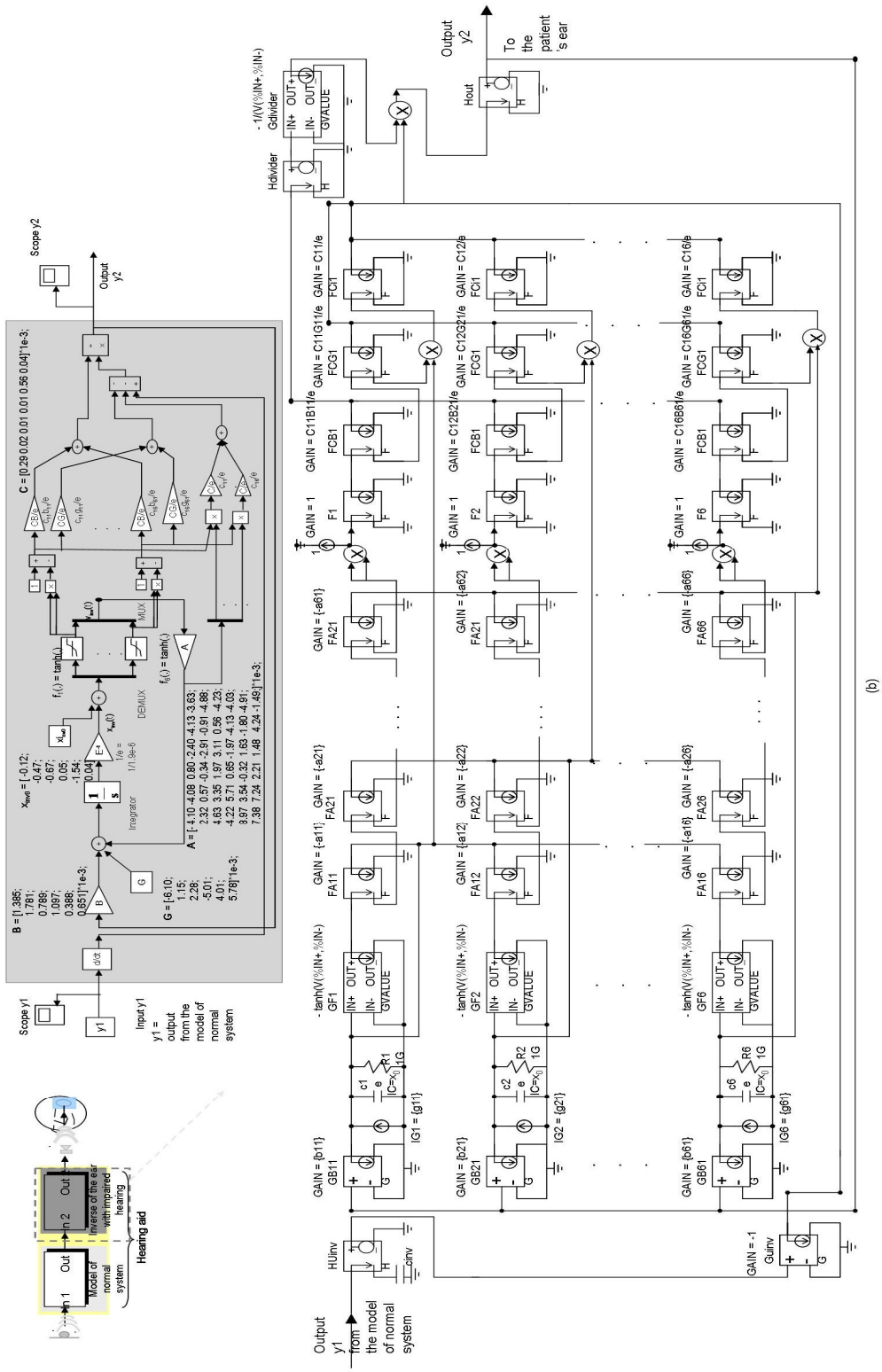

Figure 5.2.(Part 2) Schematics for the corrector system of Fig.5.1 consisting of a) the normal system and b) the inverse of the system with hearing loss

5.1.2 Basic Circuit Components for the Corrector System

The Simulink model for the proposed hearing aid is shown in Fig. 5.1 with the schematic in Fig. 5.2. The parameters of the system are to be scaled suitable for circuit implementation in Section 5.1.3. Here, the basic overviews of the circuit components utilized in the design are given. The simulations are presented using AMI 1.5um CMOS process technology to realize the corrector system. Vdd is +5V and Vss is -5V.

5.1.2.1 Current Mirror for Coefficient Gain Parameters

The coefficient vectors and matrices required for the corrector system are designed to be implemented using current mirrors and as part of current mirror loads of the differential pairs, so the parameters of the corrector system for hearing aid hardware can be adjusted by varying the gains of the current mirrors. The basic CMOS current mirror circuits are shown in Fig. 5.3. Two PMOS or NMOS transistors are connected together at the gate and operating in the saturation region. The

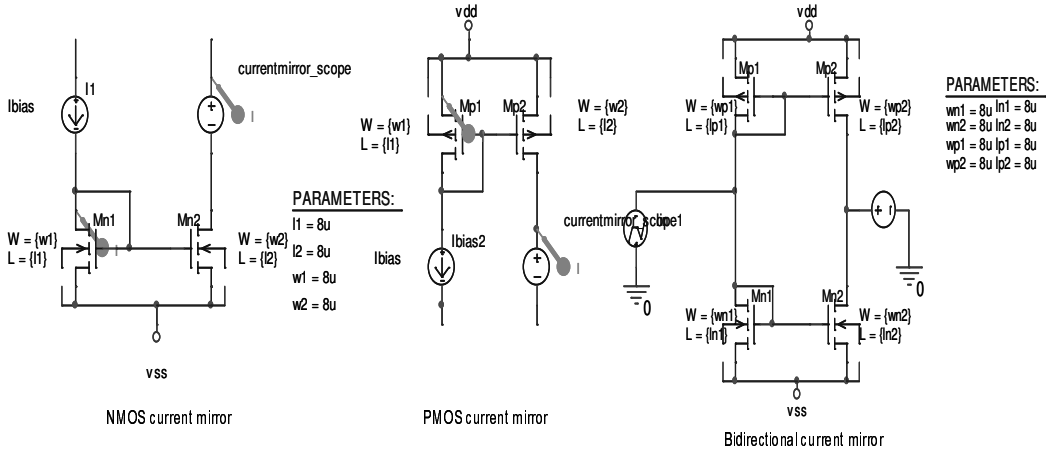

Figure 5.3. Simple CMOS current mirrors

equations of the drain currents of the transistors operating in the saturation region can be expressed as [122, p.371]

$$I_{M1} = \beta_{M1}(V_{GS1} - V_{TH1})^2(1+\lambda V_{DS}) \quad (5.7)$$

$$I_{M2} = \beta_{M2}(V_{GS2} - V_{TH2})^2(1+\lambda V_{DS}) \quad (5.8)$$

where V_{GS} is the gate-source voltage of the transistor, V_{TH} is the threshold voltage of the transistor, $\beta_{Mni,Mpi} = (K_{n,p}/2)(W_i/L_i)$ and λ is the term accounting for the channel modulation effect. The transconductance parameter $K_{n,p}$ is equal to $\mu_{n,p}C_{ox}$ where $\mu_{n,p}$ is a mobility coefficient of electron or hole and C_{ox} is the gate oxide capacitance per unit area. The aspect ratio of the transistor is W_i/L_i where W_i is the channel width and L_i is the channel length. According to (5.7) and (5.8), since $V_{GS1} = V_{GS2}$, the relationship between I_{M1} and I_{M2} is equal to

$$I_{M2}/ I_{M1} = (W_2/L_2) / (W_1/L_1) \quad (5.9)$$

where the channel length modulation is neglected. The same relationship also applies to the PMOS current mirror. By adjusting the aspect ratios (W_i/L_i) of the transistors, the desired current gains can be achieved. The current mirrors can also be used for carrying the currents to various points of the circuits. Since some of the variables in the developed corrector system for hearing aid have both positive and negative values, the bidirectional current mirror is required which can be implemented by using both PMOS and NMOS current mirrors to carry the bidirectional signals.

5.1.2.2 CMOS Differential Pairs for Signal Type Conversion

The linear function of a voltage to current converter can be realized using the

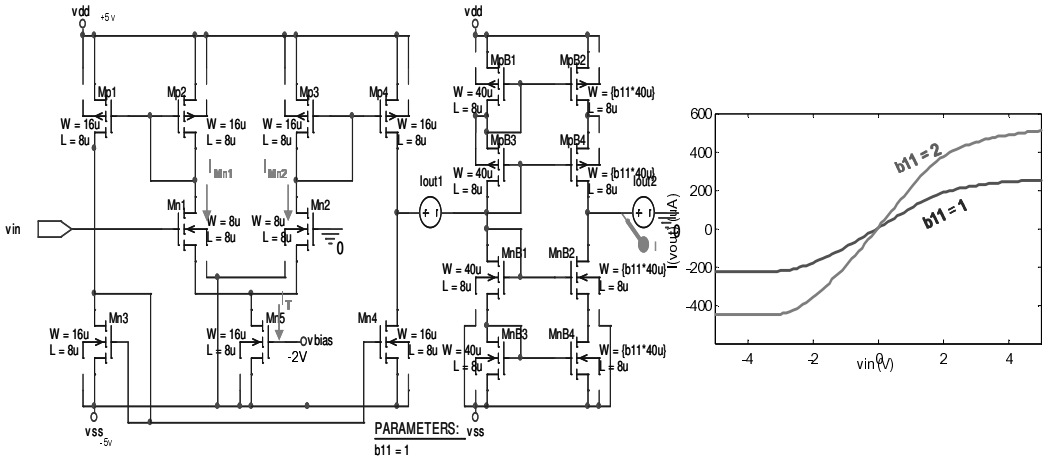

Figure 5.4. Basic CMOS Differential pairs

CMOS differential pairs as shown in Fig. 5.4 [120]-[121]. The currents of transistors operating in the saturation region neglecting the channel length modulation are

$$I_{Mn1} = \beta(V_{GS1} - V_{TH1})^2 \tag{5.10}$$

$$I_{Mn2} = \beta(V_{GS2} - V_{TH2})^2 \tag{5.11}$$

The summation of these two currents is equal to the tail current I_T of the transistor Mn5,

$$I_T = I_{Mn1} + I_{Mn2} \tag{5.12}$$

By connecting the current mirrors, the output from the differential pairs is taken to be $I_{out} = I_{Mn2} - I_{Mn1}$ which is a function of the voltage difference $V_{id} = V_{In+} - V_{In-}$,

$$I_{out} = \beta V_{id}\sqrt{\frac{2I_T}{\beta} - (V_{id})^2} \tag{5.13}.$$

The differential pairs with current mirror loads can be used to represent a linear voltage to current converter for small differential input signals, $(V_{id})^2 << 2I_T/\beta$. The additional current mirrors are added at the output of the differential pair in order to vary the gain according to each system variable, for example, to realize the $\mathbf{B}_R u_R(t)$

term for the corrector system where the equivalent input signal $u_R(t)$ is taken to be the voltage and $\mathbf{B}_R = [b_{R11}\ b_{R21}\ \ldots b_{R61}]$, the current mirrors with the gains b_{R11}, b_{R21}, …, b_{R61} are utilized so the same setting of the differential pair can be used and the parameter values can be set through current mirrors. An example of the current output, I_{out}, from the voltage input, $V_{id} = V_{In+} - V_{In-}$, is shown in Fig. 5.4.

5.1.2.2 BJT Differential Pairs for Hyperbolic Tangent Function

The hyperbolic tangent function, tanh(x), of the system is realized with the differential pairs using the BJT transistors Q_1 and Q_2 in place of the transistors Mn1 and Mn2 in Fig. 5.5, as shown in Fig. 5.4. We take advantage of an exponential relationship between a current and a voltage of the BJT to implement the function tanh(.). The emitter currents of the two matched transistors Q1 and Q2 are

$$i_{E1} = \frac{I_S}{\alpha} e^{(V_{B1} - V_E)/V_T} \tag{5.14}$$

$$i_{E2} = \frac{I_S}{\alpha} e^{(V_{B2} - V_E)/V_T} \tag{5.15}$$

where I_S is a saturation current of the transistor, α is a constant value of the transistor which is close to 1, V_B is the voltage at the base, V_E is the voltage at the emitter, and V_T is the thermal voltage which is approximately equal to 25mV at room temperature. The summation of these two currents is equal to the tail current of the transistor Mn5,

$$I_T = i_{E1} + i_{E2} \tag{5.16}.$$

By connecting the current mirror loads, the output from the differential pairs is taken to be $i_{out} = i_{E2} - i_{E1}$ which is a function of the voltage difference $V_{id} = V_{In+} - V_{In-}$,

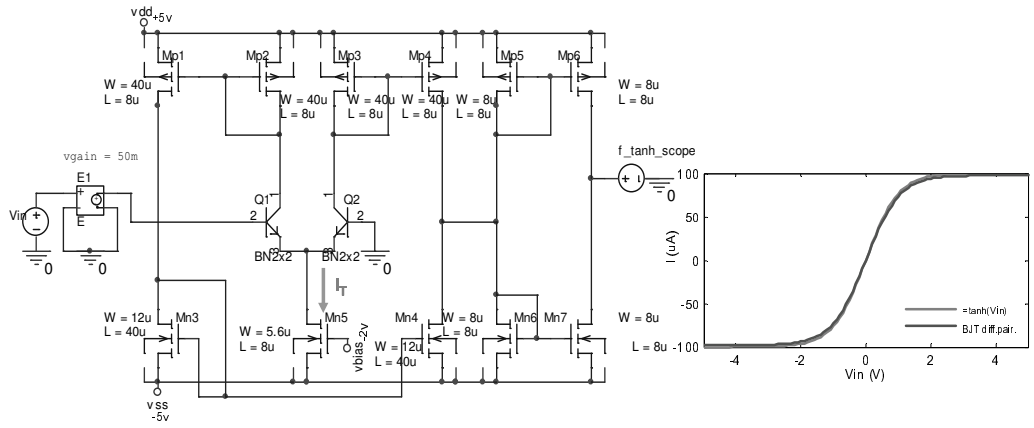

Figure 5.5. Basic BJT Differential pairs

$$i_{out} = I_T \frac{(-1+e^{-V_{id}/V_T})}{(1+e^{-V_{id}/V_T})} \tag{5.17}$$

which is also equal to $I_T\tanh(-V_{id}/2V_T)$. The BJT differential pairs with the current mirror loads and the respective input voltage to voltage gain block can be used to represent a hyperbolic tangent function, f(.) = tanh(.) needed for the corrector system. An example of the output current from BJT differential pairs is shown in Fig. 5.5. Beside BJT differential pair, the hyperbolic tangent function can also be realized using the CMOS differential pair of Fig. 5.4 working in a sub-threshold region ($V_{GS}<V_{TH}$) in which the current expresses a similar exponential function of the voltage [126, p.172] as

$$I_{DS} = I_0 e^{KV_{GB}/V_T}(e^{-V_{SB}/V_T} - e^{-V_{DB}/V_T}) \tag{5.18}.$$

I_0 is the sub-threshold current factor, K is the sub-threshold factor and V_T is the thermal voltage.

5.1.2.4 Current to Voltage Converter for Signal Type Conversion

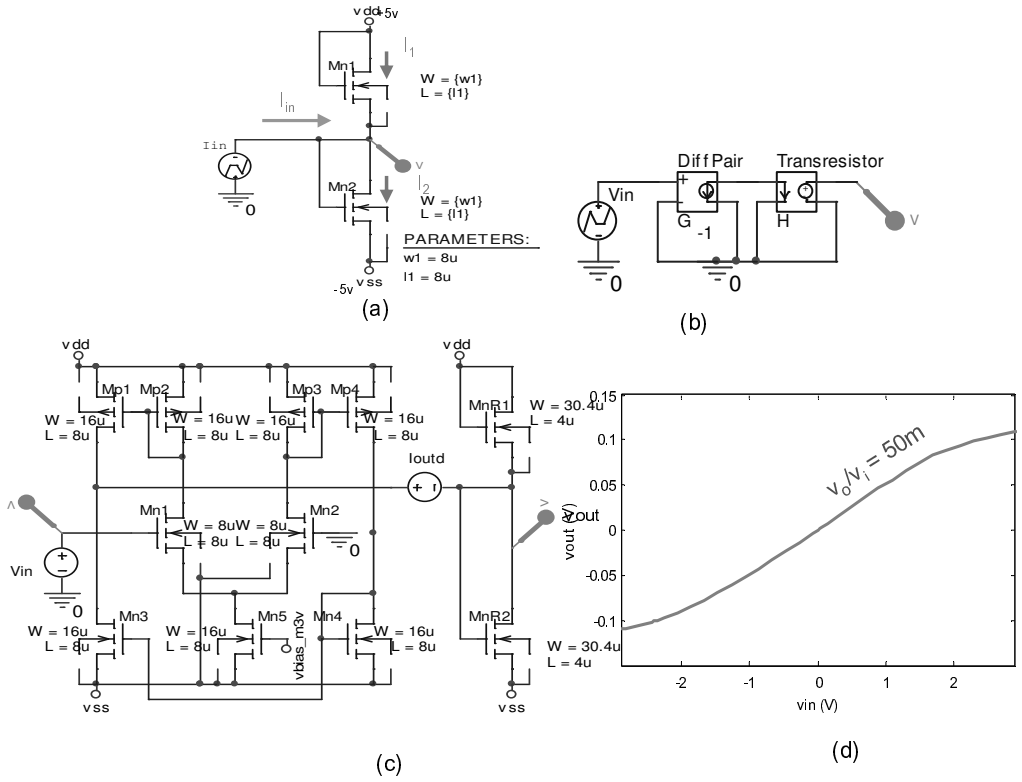

Figure 5.6. (a) The transresistor circuit consisting of two transistors in [123], (b) the voltage to voltage component circuit, (c) transistor circuit, and (d) simulated voltage to voltage gain output

The circuit for current to voltage converter is utilized for conversion of the signal types for example the input voltage gain block of the BJT differential pair can be realized from the combination of the voltage to current converter using differential pair and the current to voltage converter or the current to voltage converter at the output of the system. For the current to voltage circuit, two MOS transistors designed for the transresistor circuit in [123] as shown in Fig. 5.6(a) can be used. The transresitor consisting of two transistors operating in the saturation region can be utilized giving the output resistance R. From Fig. 5.6(a),

$$I_{in} = I_2 - I_1 = (1/2)K_n(W/L)_n(V_o - Vss - V_{TH})^2 - (1/2)K_n(W/L)_n(V_{dd} - V_o - V_{TH})^2 \quad (5.19)$$

$$R = V_o/I_{in} = V_o/(I_2-I_1) = 1/(2(K_n)(W/L)_n(V_{DD} - V_{TH})) \qquad (5.20).$$

An example of the voltage gain block using the differential pair and the transresistor circuit that can be used as the input voltage to voltage gain block with a gain value of ($1/2V_T \approx 0.05$) to be used with BJT differential pair for realizing a tanh function is shown in Fig. 5.6(c) and (d).

5.1.2.5 Current Multiplier Circuit for Signal Multiplier and Divider

The current multiplier circuits are based on the four quadrant current multiplier of [124] implementing from the current squaring circuit as shown in Fig. 5.7(a). The transistors are connected in the translinear loop. Using Kirchhoff's voltage law,

$$V_{GS1} + V_{GS2} = V_{GS3} + V_{GS4} \qquad (5.21)$$

All transistors are assumed identical and operating in saturation region, hence (5.21) equal to

$$V_{TH1} + \sqrt{I_1/\beta} + V_{TH2} + \sqrt{I_2/\beta} = V_{TH3} + \sqrt{I_3/\beta} + V_{TH4} + \sqrt{I_4/\beta} \qquad (5.22)$$

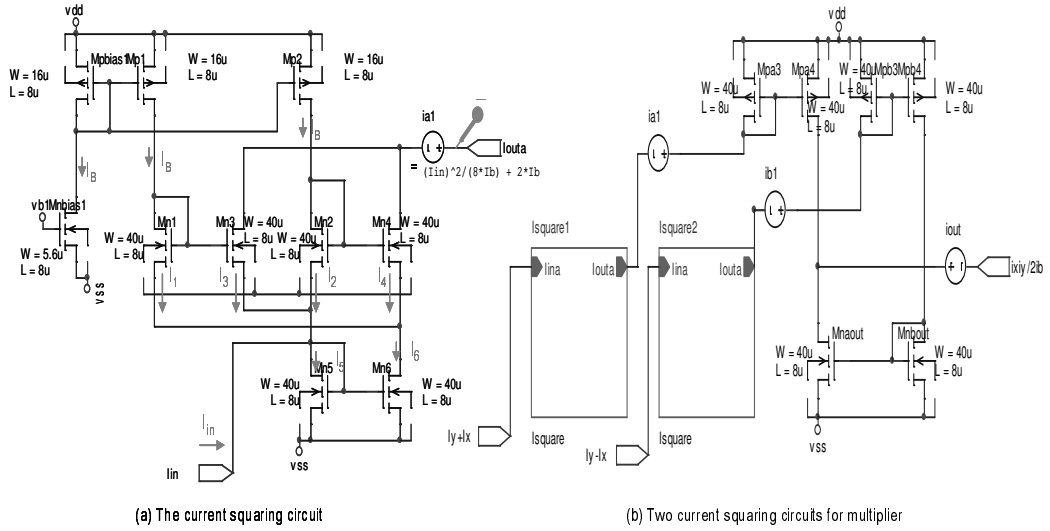

(a) The current squaring circuit (b) Two current squaring circuits for multiplier

Figure 5.7. (a) Current squaring circuit and (b) current multiplier circuit

$$\sqrt{I_1} + \sqrt{I_2} = \sqrt{I_3} + \sqrt{I_4} \tag{5.23}$$

The currents I_1 and I_2 are each equal to I_B, hence,

$$\sqrt{I_3} + \sqrt{I_4} = \sqrt{4I_B} \tag{5.24}$$

$$I_3 + I_4 = 2I_B + (I_3\text{-}I_4)^2/8I_B \tag{5.25}$$

The current mirror composed of Mn5 and Mn6 yields $I_{in} + I_2 + I_3 = I_1 + I_4$ where I_1 and I_2 are equal to I_B, so the output of the squaring circuit is equal to

$$I_{out} = 2I_B + I^2_{in}/8I_B \tag{5.26}$$

To implement the current multiplier, two current squaring circuits are connected as shown in Fig. 5.7(b). The output of the multiplier is therefore equal to

$$I_{out} = I_{out1} - I_{out2} \tag{5.27}$$

$$= 2I_B + (I_y+I_x)^2/8I_B - 2I_B - (I_y-I_x)^2/8I_B \tag{5.28}$$

$$= I_xI_y/2I_B \tag{5.29}$$

which yields the multiplication of the currents I_x and I_y. The simulated output current from the current multiplier circuit is shown in Fig. 5.8(a) as an example where the x axis is the sweep of current I_y and the y axis is the output current I_{out} with I_x as the secondary sweep. The current divider can also be implemented using the multiplier circuit by selecting the currents I_y and I_B as the variables and using I_x as the bias current as shown in Fig. 5.8(b).

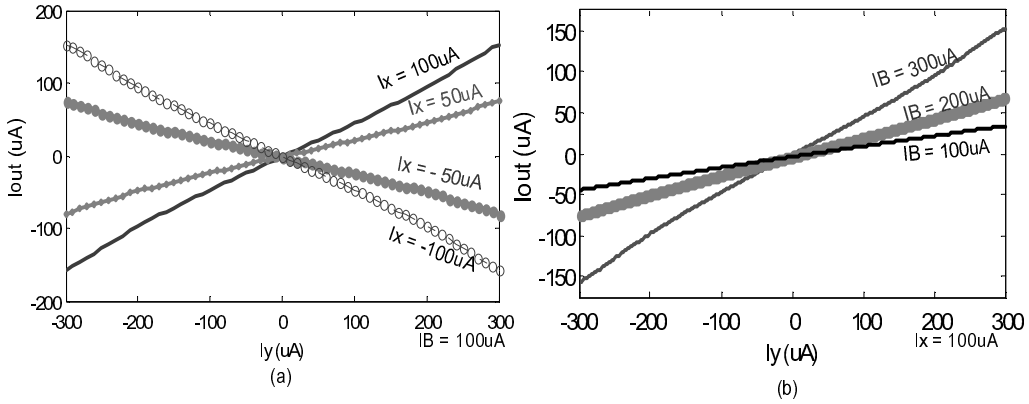

Figure 5.8. Simulated signals from the current multiplier circuit used (a) as the multiplier (I_B =100uA) and (b) as the divider (Ix=100uA)

5.1.2.6 Current Sources for Constant Biases

The current sources needed for the constant biases of the corrector system can also be implemented using the transistors. By connecting the voltage at the terminals of the transistor to operate in the saturation region, it can be used to realize the constant current bias where the channel modulation effect is neglected. An example of a transistor circuit for current source and simulated output are shown in Fig. 5.9.

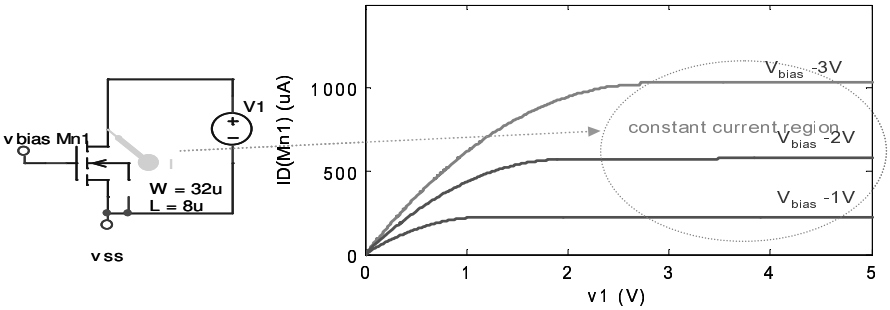

Figure 5.9. Constant current source for constant bias

5.1.2.7 CMOS Gyrator-C circuits for Derivative of Input Signal for the Inverse System

In order to derive the system that is inverse to the ear type system of impaired hearing function, the need for a differentiation of the output from the original ear type system is required as illustrated in (4.1)-(4.11). This way allows the direct inverse of the system with a single output and more than one internal neurons, y = **Cx** where **C** is a row vector of 1×n dimension, 1<n, y is the output and **x** are n-internal neurons. Also, it allows for the inverse for both different orders of cascade. Therefore the synthesis of the derivative of the input for the inverse system can be achieved through the transistorized circuits using a gyrator with the capacitance load [120]. The gyrator consists of a parallel connection of two voltage controlled current sources which can be implemented using two CMOS differential pairs. The circuits as shown in Fig. 5.10 result as the two port network of which

$$\begin{bmatrix} I_1 \\ I_2 \end{bmatrix} = \begin{bmatrix} 0 & -g_m \\ g_m & 0 \end{bmatrix} \begin{bmatrix} V_1 \\ V_2 \end{bmatrix} \tag{5.30}.$$

By connecting the capacitor, C, at the second port as shown in Fig. 5.10(b), it can be

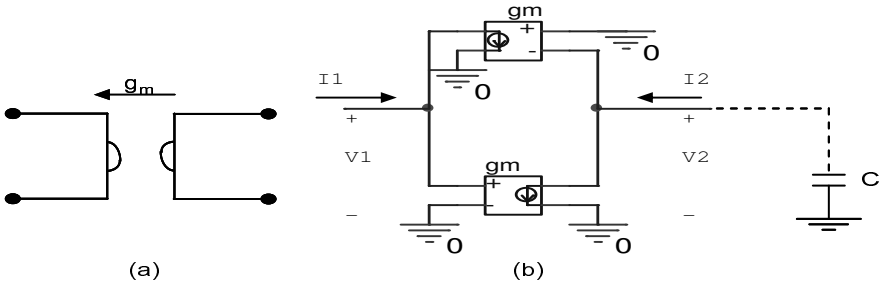

Figure 5.10. A gyrator (a) symbol and (b) inductor circuit [120]

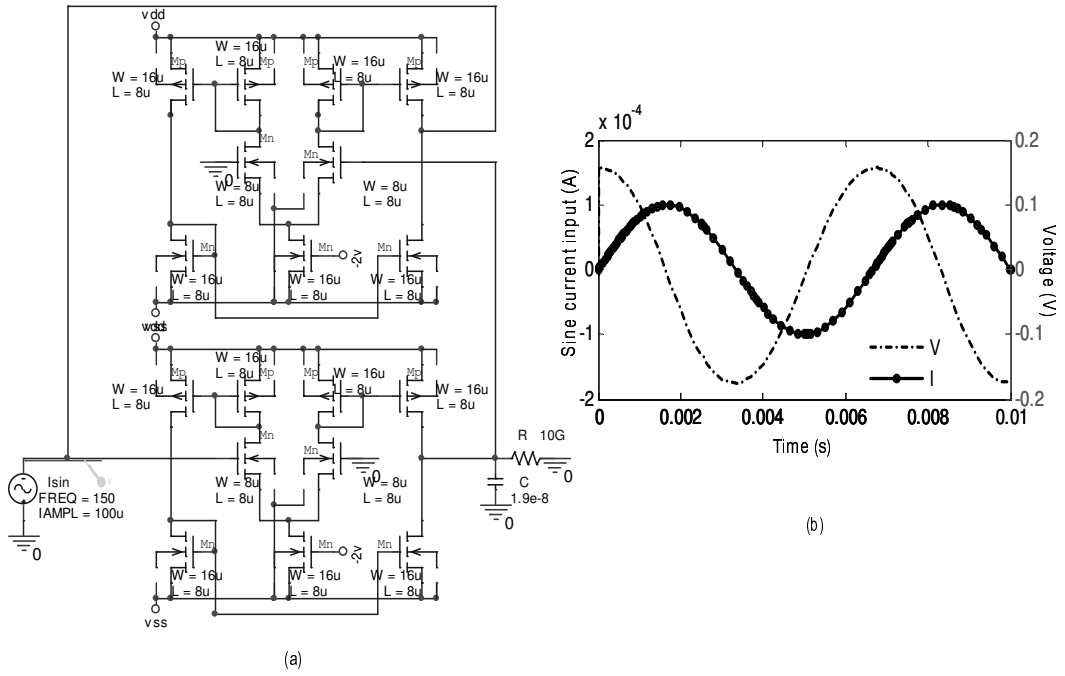

Figure 5.11. The gyrator-C circuits for the differentiation of the signal

used to equivalently realize the inductor where

$$V_1 = (C/(g_m)^2)\, dI_1/dt \qquad (5.31).$$

The circuits and simulated results are shown as an example in Fig. 5.11 using the sine current input. The voltage is successfully achieved as the derivative of the input signal. The gyrator with C load can then be used at the input of the inverse system for which the realization of the differentiation is implemented.

5.1.3 Parameter Scaling of the Corrector System for Circuits

The scaling of parameter values of the system for making a noninvasive correction of auditory loss and disorder effects is investigated in order to implement the system using transistors. From the mathematically representative corrector system

in (5.1)-(5.6), the scaling of their parameter values can be performed without affecting the important input and output signals by determining the dependence of each variable and equation from which the appropriate scaling factors for the parameters can be applied. For example, from (5.1)-(5.3), the mathematically representative ear type system can also be written as

$$\tilde{\mathbf{E}}_R\,(d\mathbf{x}_R\,(t)/dt) = \tilde{\mathbf{A}}_R\,\tilde{\mathbf{v}}_R\,(t) + \tilde{\mathbf{G}}_R + \tilde{\mathbf{B}}_R\,u_R\,(t),\;\; \mathbf{x}_R\,(0) = x_{R0} \qquad (5.32)$$

$$\tilde{\mathbf{v}}_R(t) = k_{R3}\times f(\mathbf{x}_R(t)) \qquad (5.33)$$

$$y_R\,(t) = \tilde{\mathbf{C}}_R\,\tilde{\mathbf{v}}_R\,(t) + d_R \qquad (5.34)$$

where $\tilde{\mathbf{E}}_R = k_{R1}\times\mathbf{E}_R = [k_{R1}\times e_R\times\mathbf{I}]$, $\tilde{e}_R = k_{R1}\times e_R$, $\tilde{\mathbf{G}}_R = k_{R1}\times\mathbf{G}_R$, $\tilde{\mathbf{B}}_R = k_{R1}\times\mathbf{B}_R$. The variable $\mathbf{v}(t)$, which is a hyperbolic tangent of the neurons $\mathbf{x}(t)$, can also be scaled where $\tilde{\mathbf{v}}_R(t) = k_{R3}\times \mathbf{v}_R(t) = k_{R3}\times\tanh(\mathbf{x}_R(t))$ by using $\tilde{\mathbf{A}}_R = k_{R2}\times\mathbf{A}_R$ with $k_{R2}\times k_{R3} = k_{R1}$ and $\tilde{\mathbf{C}}_R = \mathbf{C}_R/\,k_{R3}$. The scaling factors are k_{R1}, k_{R2}, and k_{R3}. The method allows the scaling of the parameter values into the desired ranges without the changes in the desired output signal.

The mathematical representatives of the inverse system, (5.4)-(5.6), are derived from those of the original ear type system of (5.1)-(5.3) therefore the parameter scaling is also applied in a similar way to the inverse system. From the inverse system of (5.4)-(5.6), the scaled system of the inverse system that is derived from the original ear type system of the left sided ABR with the hearing loss affected characteristics can be represented as

$$\tilde{\mathbf{E}}_L(d\mathbf{x}_{Linv}(t)/dt) = \{\tilde{\mathbf{A}}_L - \tilde{\mathbf{B}}_L(\tilde{\mathbf{C}}_L[\partial f_{xL}\,\mathbf{I}]\tilde{\mathbf{B}}_L/\tilde{e}_L)^{-1}(\tilde{\mathbf{C}}_L[\partial f_{xL}\,\mathbf{I}]\tilde{\mathbf{A}}_L/\tilde{e}_L)\}\tilde{\mathbf{v}}_{Linv}(t) + \tilde{\mathbf{G}}_L - \tilde{\mathbf{B}}_L(\tilde{\mathbf{C}}_L[\partial f_{xL}\,\mathbf{I}]\tilde{\mathbf{B}}_L/\tilde{e}_L)^{-1}(\tilde{\mathbf{C}}_L[\partial f_{xL}\,\mathbf{I}]/\tilde{e}_L)\tilde{\mathbf{G}}_L + \tilde{\mathbf{B}}_L(\tilde{\mathbf{C}}_L[\partial f_{xL}\,\mathbf{I}]\tilde{\mathbf{B}}_L/\tilde{e}_L)^{-1}u_{Linv}(t)$$

$$, \mathbf{x}_{Linv}(0) = \mathbf{x}_{L0} \qquad (5.35)$$

$$\tilde{\mathbf{v}}_{Linv}(t) = k_{L3} \times f(\mathbf{x}_{Linv}(t)) \qquad (5.36)$$

$$\mathbf{y}_{Linv}(t) = -(\tilde{\mathbf{C}}_L[\partial f_{xL}\,\mathbf{I}]\tilde{\mathbf{B}}_L/\tilde{e}_L)^{-1}(\tilde{\mathbf{C}}_L[\partial f_{xL}\,\mathbf{I}]\tilde{\mathbf{A}}_L/\tilde{e}_L)\}\tilde{\mathbf{v}}_{Linv}(t) - (\tilde{\mathbf{C}}_L[\partial f_{xL}\,\mathbf{I}]\tilde{\mathbf{B}}_L/\tilde{e}_L)^{-1}(\tilde{\mathbf{C}}_L[\partial f_{xL}\,\mathbf{I}]/\tilde{e}_L)\tilde{\mathbf{G}}_L + (\tilde{\mathbf{C}}_L[\partial f_{xL}\,\mathbf{I}]\tilde{\mathbf{B}}_L/\tilde{e}_L)^{-1}u_{Linv}(t) \qquad (5.37)$$

where $\tilde{\mathbf{E}}_L = k_{L1} \times \mathbf{E}_L = [k_{L1} \times e_L \times \mathbf{I}]$, $\tilde{e}_L = k_{L1} \times e_L$, $\tilde{\mathbf{G}}_L = k_{L1} \times \mathbf{G}_L$, $\tilde{\mathbf{B}}_L = k_{L1} \times \mathbf{B}_L$. The hyperbolic tangent of the neuron $\mathbf{x}_{inv}(t)$ can be scaled as $\tilde{\mathbf{v}}_{Linv}(t) = k_{L3} \times \mathbf{v}_{Linv}(t) = k_{L3} \times \tanh(\mathbf{x}_{Linv}(t))$ as such $\tilde{\mathbf{A}}_L = k_{L2} \times \mathbf{A}_L$ with $k_{L2} \times k_{L3} = k_{L1}$ and $\tilde{\mathbf{C}}_L = \mathbf{C}_L / k_{L3}$. The scaling factors are k_{L1}, k_{L2}, and k_{L3}. The desired output signal from the corrector system to the hearing aid's user does not change as a result of the parameter scaling methods therefore the correction technique and the results investigated earlier in the dissertation are kept unchanged. The scaling of the corrector system allows the shifting of the parameter values suitable for the circuit realization of the system mainly using transistors.

5.2 Designed Circuits of the Corrector System

A possible circuit for the system for making a noninvasive correction of the auditory loss and disorder is designed and realized in this chapter showing the possibility of developing the hearing aid from the proposed method. The proposed hearing aid is constructed from various basic circuit components as outlined in the diagrams in Fig. 5.2. Various basic circuit components designed to make up the proposed hearing aid are discussed earlier. The top level of the whole hearing aid circuit is shown in Fig. 5.12 of which the sub-circuits with respective scaled parameters are presented in Fig.A1-30 in the Appendix section of this chapter. The schematics are shown using the hierarchical blocks [119] to make it easy to follow. Their respective sub-circuits are subsequently provided which are referenced as the names under the hierarchical blocks.

5.2.1 Circuits and Results

The designed circuits are then simulated with the ear type model of the

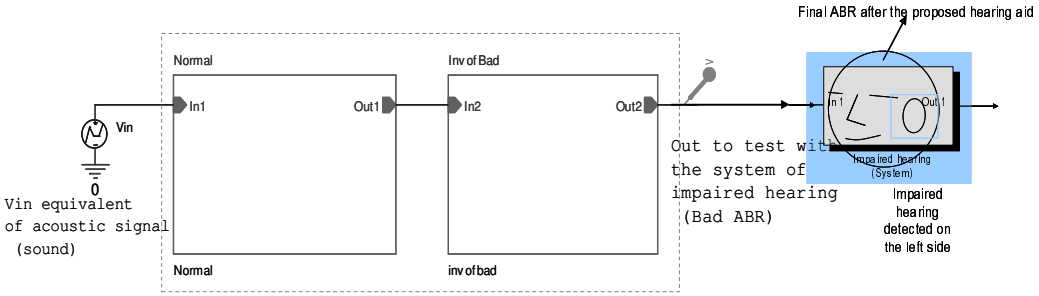

Figure 5.12. The top level circuit for the proposed hearing aid to be used with the patient

impaired hearing function to see the result. The corrected ABR simulated from the model of the patient with left sided sensorineural hearing loss together with the designed hearing aid circuit are shown in Fig. 5.13b. The simulated signal shows the ABR whose wave characteristics and morphology are transformed toward the normal types. The measured normal right sided response is also depicted in Fig. 5.13c which is utilized as the desired response in the proposed correction method. There is some difference between the ideal desired response and response achieved with the hearing aid circuit using mainly transistors as shown in Fig. 5.14 which is due to the offset from the biases and some parameter mismatches between the designed system and circuits. However the improvement of the ABR toward the desired normal type response obtained from the hearing aid circuit gives a satisfying result. The aid circuit is able to correct the overall waveform morphology and main waves of ABR as intended to by the use of the investigated noninvasive correction method.

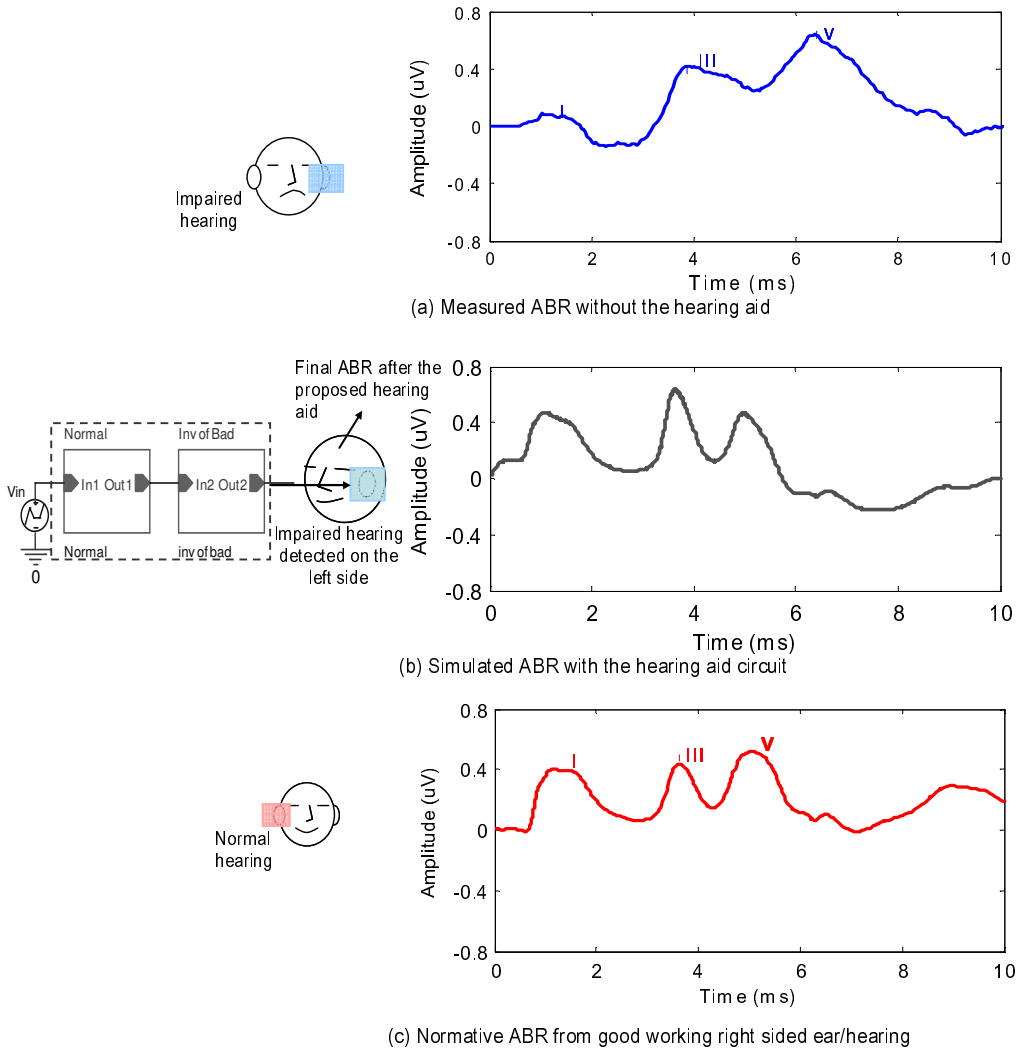

Figure 5.13. The simulated ABR with the hearing aid circuit from the model of the patient with hearing loss detected on the left sided measurement

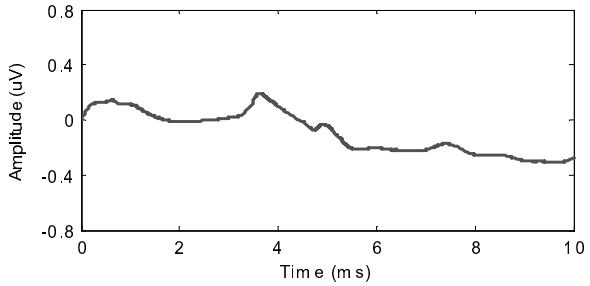

Figure 5.14. Differences between the ideal desired and simulated responses

5.2.2 Possible Circuits for Alternate Adjustment

Most of the parameters required for the proposed hearing aid system are designed to be implemented as part of the current mirror circuits as shown in Fig.A1-A31. As a result the parameters of the system for making a noninvasive correction of auditory impairment can be adjusted by simply changing the widths and lengths of current mirrors according to their respective parameters for which they represent in the circuits. This allows the circuits to be easily pre-adjusted and assigned with the new parameter values. Possible alternate circuits with variable gains can also be utilized for a more flexible implementation. Current mirrors with variable gain set by external voltage or current sources can be utilized. For example, the tunable current mirror in [125] can be used as shown in Fig. 5.15a. The transistors M3 and M4 are operating in the triode region so by varying the $V_{bias} \pm V_{tune}$, the output current can be set accordingly. An example of the output is given in Fig. 5.15b.

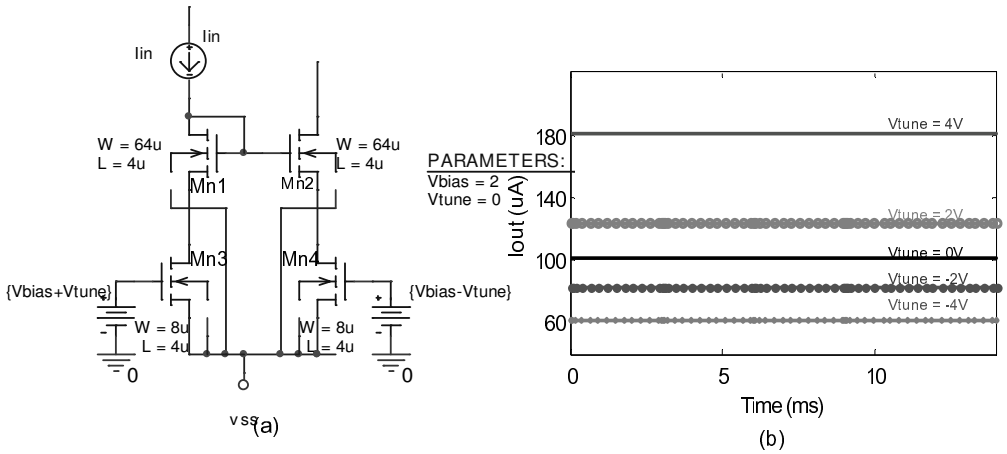

Figure 5.15. Current mirror circuit with variable gain from [125].

5.3 Summary

The preliminary circuits of the hearing aid based on the noninvasive correction method proposed in this dissertation have been designed and realized in this chapter. From the mathematical representation of the proposed hearing aid, the variables are taken to be the equivalent voltage or current signals for which the counterpart circuit can then be synthesized. The parameters of the hearing aid are scaled suitable for circuit implementation using mainly transistors. The designed circuit of the proposed hearing aid is able to yield the ABR with improved characteristics as the result of the noninvasive correction method. As discussed in the previous chapters, the ABR is a reliable technique utilized for gaining access into the status of the human auditory system and identifying for the auditory loss and disorder. Recent researches on the incorporation of the ABRs and other auditory related electrical signals measured from the brain in the hearing aid evaluation [96]-[100], the applications of ABRs in the operative procedure to monitor and make sure the preservation of the patient's hearing [25]-[26], the applications of ABRs in cochlear implantations [131]-[132], and the worldwide acceptable uses of ABRs as the standard for testing the hearing function [12]-[17]. They infer the association between the characteristics of the ABR and human's sound perception and understanding. The ABR with normal characteristics generally indicate the healthy auditory organs and normal hearing ability. The preliminary circuit given in this chapter shows the possibility of developing the system into the hearing aid alternate to the conventional hearing aid. This hearing aid developing from the proposed noninvasive correction

method utilizing the ABR is therefore potentially able to correct the effects from hearing loss and disorder and improve the patient's hearing.

Chapter 6

Summary and Open Problems

6.1 Summary

An investigation of a new assistive device for helping people with hearing impairment is presented. The assistive device is developed based on the proposed noninvasive means to correct and cancel the effects from the auditory loss and disorder. The investigation has made use of the auditory brainstem response (ABR) which is the electrical potentials measured by using electrodes placed on the human scalp in response to an acoustical stimulus in the ear to characterize the developed ear type system. The literature review on the ABR and its clinical usefulness is given in chapter 2 pointing out the reasons behind the proposed investigated approach and the possible validation of the method. In chapter 3, the mathematically representative ear type system developed through the measured ABR is introduced utilizing the modified nonlinear neural network architecture. Modeling approaches and steps are given using the combination of the model order selection, the nonlinear least square algorithms, and trial and error simulations. The application of the developed ear type system extendable for the multichannel recording of the neural activities of the auditory nervous system inside the brain is also explored. The developed ear type systems give satisfying results for which the individual hearing function can be characterized through the measured ABRs both from normal and impaired hearing

functions. The ear type system is then applied with the proposed alternate technique to correct the effects from auditory loss and disorder in a noninvasive way in chapter 4. The technique utilizes the ability of the ear type system to capture the effects from the auditory loss and disorder for which the cancellation of these effects can be set up utilizing the newly derived neural network of the ear type system. The system for making a correction is developed and simulated on models of a patient with hearing impairment showing the results as an example of the investigation. The system is able to transform the characteristics of an ABR from the hearing loss affected to the normal desired one. This gives a promising result of the system as the new assistive device alternate to the conventional hearing aids to which the potential benefits and pertinent aspects are compared at the end of the chapter. A preliminary set of circuits for implementing the proposed method into a hearing aid are designed and given in the chapter 5. In that chapter are shown satisfying results with Spice simulations of the new assistive device.

The investigation gives the new assistive device which can provide the alternate noninvasive way to correct and cancel the effects from the hearing loss and disorder. By utilizing the auditory brainstem response whose characteristics and signals objectively reflecting the auditory activities within the human auditory system and incorporating its clinical use in developing the assistive device, these can result in an improved means which can greatly benefit to the hearing impaired. It can also be used in cases where the patient cannot give rational responsive indications, as in the case for young children and babies.

6.2 Open Problems

The open problems and further applications from this investigation can bring more useful researches and interesting results. Some examples are suggested in these following areas.

- The preliminary analog circuit of the proposed assistive device is presented from which further improvement on the circuit and implementation of the device into the hearing aid can be further investigated. For example, the CMOS transistors working in subthreshold region can also be used to realize the nonlinear hyperbolic tangent function as already mentioned in Section 5.1.2.2. Also for a more simple way of fitting the device for each user or readjusting the hearing aid characteristics over time, some sorts of easily adjustable and adaptive circuits such as the current mirrors with variable gains adjusted by external voltages in Section 5.2.2 can be incorporated into. The proposed assistive device can be developed for use with the transducer devices such as microphones and air conduction devices for further subjective evaluation of the proposed aid.

- The further investigation on the temporal delay of the signals simulated in the developed neural network of the ear type systems can be further addressed. In practical implementation there could be some delays exhibited in the system which does not show up in the theoretical set up of our systems which can be due to the simulation settings such as a very small sampling time.

- The simulations of the speech signal as the input to the developed systems have been shown in Section 4.5.3, p. 81 which show the results in agreement with the results obtained from the measurement in the references. Further investigation on

these findings can be done to incorporate its findings and usages into the proposed hearing aids For example, establishing some similar characteristics of ABRs with speech stimulus with a group of people with normal hearing and hearing impairment has to be first researched. The results can be very useful since they can be used to learn more and simulate the potential benefits of the proposed aid used with speech as in everyday conversation and listening environment.

- The ear type system extendable to the multiple electrodes recording of the auditory activities inside the brain. As mentioned in section 3.4, the recordings of the electrophysiological signals from deeper along the auditory nervous pathways inside the brain, such as the auditory evoked cortical response, require multiple electrodes placed on various locations on the scalp. The application of the extended ear type system designed can be found useful in a development of a hearing aid where the inverse term used for correction and cancellation of any detected responses with abnormal characteristics can possibly be implemented. The representative ear type system can then set up as a planar mapping of the underlying brain regions giving rise to the recorded signals. Any deviation from normal activities and possible disorders of the auditory system can be identified from which the noninvasive system to control these unwanted effects is possibly set up and applied. This can be useful for developing the alternate noninvasive treatment and studying the complex hearing function of human. Also it can be useful assisting in the alleviations and treatments of some other pertinent disorders and impairments as well. For example, the tinnitus also known as the ringing of sound in the ear has been an incurable problem. The research investigations to locate the generating sites of these ringing sound show that the

tinnitus is believed to be likely generated from mechanisms of the auditory nervous system inside the brain rather than from those of the inner ear [107]-[110]. The measurements involved include the measurement of magnetic fields such as in the Magnetoencephalography (MEG) [31], [111] and the measurement of electric signals such as in the Electroencephalography (EEG) [110]-[112]. The signals from various points on the scalp can be averaged to pinpoint the exact location of internal damage that gives rise to the abnormal behaviors. Also using multiple electrodes, the representative system planar mapping of the underlying brain regions could also be developed from which the noninvasive system to control the generation of tinnitus is possibly realized to cancel and correct the abnormal activities in a somewhat similar way to a current treatment utilizing the masking sound and the electrical or magnetic brain stimulations to reduce and suppress the tinnitus sound [113]-[115].

- It is also interesting to apply the investigated method with other electrophysiological signals such as the middle latency response and the auditory evoked cortical response. Beside the ABR, the use of other signals such as the auditory cortical response for young children and babies [96]-[98] are also proved to be valuable. Since the standard hearing test and the prescription of the conventional hearing aid with the standard pure tone audiogram require decision making and subjective responses back from the patients, it can be hard and even impossible in cases of children and infants. The ABR is undoubtedly useful and the procedures and normative standards have been established and are clinically used today [5]-[6]. The characterization of the auditory system and auditory diagnosis through the auditory cortical response can result in the assessment of the underlying mechanism and

function of the auditory nervous system deeper along the auditory pathway which is more likely to be associated with the speech interpretation and hearing process of the brain and can yield even more improved assistive device. However, the procedures required for obtaining and evaluating the cortical responses are more complex and time consuming. Also, there is more variability of the response characteristics between patients and within the same patient and also effects from the stimulus for which the evaluation of the hearing system function and diagnosis of disorder can be more difficult.

Appendix A of Chapter 5

Designed Circuits of the Corrector System

The circuits of the corrector system from the proposed correction method are designed and presented in this section. The corrector system consists of the system of normal hearing function and the derived system that is the inverse of the hearing aid's user ear type system as already discussed in earlier chapters. The example of the investigation is given on the models set up from the patient with hearing impairment detected through an ABR measured with the stimulus to the left ear. For this case, the normal system (*Normal*) is referred to the ear type system set up through the right sided response and the inverse system (*InvofBad*) is referred to the ear type system set up through the left sided response. The top level circuit for the proposed hearing aid is given in Fig.A.0 of which detailed sub-circuits are subsequently shown as indicated as the names under the blocks.

From Fig.A.0, the sub-circuit of *Normal* is shown in Fig.A.1 which is the

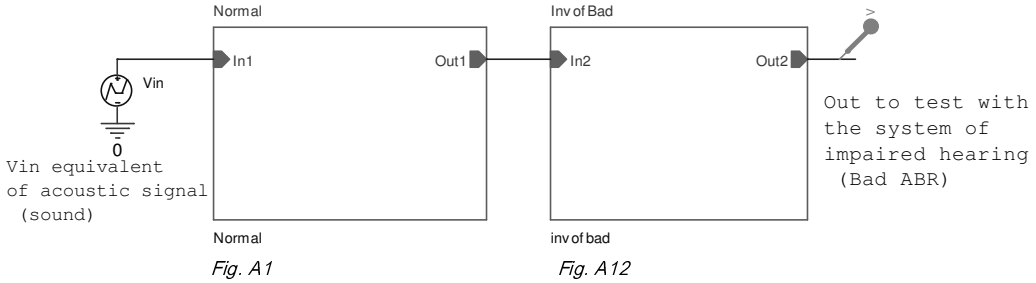

Figure A.0. The top level circuit for the proposed hearing aid

circuit representative ear type system of the right sided response with the mathematical representative equations with scaled parameters suitable for VLSI circuit implementations shown earlier as (5.32)-(5.34) and reprinted as

$$\tilde{\mathbf{E}}_R\,(d\mathbf{x}_R\,(t)/dt) = \tilde{\mathbf{A}}_R\,\tilde{\mathbf{v}}_R\,(t) + \tilde{\mathbf{G}}_R + \tilde{\mathbf{B}}_R\,u_R\,(t),\;\; \mathbf{x}_R\,(0) = x_{R0} \qquad (A.1)$$

$$\tilde{\mathbf{v}}_R(t) = k_{R3} \times \tanh(\mathbf{x}_R(t)) \qquad (A.2)$$

$$y_R\,(t) = \tilde{\mathbf{C}}_R\,\tilde{\mathbf{v}}_R\,(t) + d_R \qquad (A.3).$$

The circuit realization of this system is already described in Section 5.1.1. The schematic is presented in Fig.A2 with the sub-circuits subsequently given. The names of the circuits are presented corresponding to the system variables. For example, the first row element of (A.1) is equal to $e_R dx_{R1}(t)/dt = [a_{11}\ a_{21}\ a_{31}\ a_{41}\ a_{51}\ a_{61}]v_{R1}(t) + G_1 + B_1 u_R(t)$ of which its schematic representation is expressed as $e_1 dx_{R1}/dt = Av1 + I\_G1 + B1u_R(t)$. The similar expressions are applied to the rest of the system variables.

For the system that is inverse to the ear type system identifying the hearing impairment, the mathematical representative equations with scaled parameters shown earlier as (5.35)-(5.37) and reprinted as

$$\begin{aligned}\tilde{\mathbf{E}}_L\,(d\mathbf{x}_{\mathbf{Linv}}\,(t)/dt) = {} & \{\tilde{\mathbf{A}}_L - \tilde{\mathbf{B}}_L\,(\tilde{\mathbf{C}}_L[\partial f_{xL}\ \mathbf{I}]\tilde{\mathbf{B}}_L/\tilde{e}_L)^{-1}(\tilde{\mathbf{C}}_L[\partial f_{xL}\ \mathbf{I}]\tilde{\mathbf{A}}_L/\tilde{e}_L)\}\tilde{\mathbf{v}}_{Linv}\,(t) \\ & + \tilde{\mathbf{G}}_L - \tilde{\mathbf{B}}_L\,(\tilde{\mathbf{C}}_L[\partial f_{xL}\ \mathbf{I}]\tilde{\mathbf{B}}_L/\tilde{e}_L)^{-1}(\tilde{\mathbf{C}}_L[\partial f_{xL}\ \mathbf{I}]/\tilde{e}_L)\tilde{\mathbf{G}}_L \\ & + \tilde{\mathbf{B}}_L\,(\tilde{\mathbf{C}}_L[\partial f_{xL}\ \mathbf{I}]\tilde{\mathbf{B}}_L/\tilde{e}_L)^{-1}u_{Linv}\,(t)\end{aligned} \qquad (A.4)$$

$$\tilde{\mathbf{v}}_{Linv}(t) = k_{L3} \times f(\mathbf{x}_{Linv}(t)) \qquad (A.5)$$

$$\begin{aligned}\mathbf{y}_{\mathbf{Linv}}\,(t) = {} & -(\tilde{\mathbf{C}}_L[\partial f_{xL}\ \mathbf{I}]\tilde{\mathbf{B}}_L/\tilde{e}_L)^{-1}(\tilde{\mathbf{C}}_L[\partial f_{xL}\ \mathbf{I}]\tilde{\mathbf{A}}_L/\tilde{e}_L)\}\tilde{\mathbf{v}}_{Linv}\,(t) \\ & - (\tilde{\mathbf{C}}_L[\partial f_{xL}\ \mathbf{I}]\tilde{\mathbf{B}}_L/\tilde{e}_L)^{-1}(\tilde{\mathbf{C}}_L[\partial f_{xL}\ \mathbf{I}]/\tilde{e}_L)\tilde{\mathbf{G}}_L \\ & + (\tilde{\mathbf{C}}_L[\partial f_{xL}\ \mathbf{I}]\tilde{\mathbf{B}}_L/\tilde{e}_L)^{-1}u_{Linv}\,(t)\end{aligned} \qquad (A.6).$$

From Fig.A.0, the sub-circuit of this inverse system (*InvofBad*) is shown in Fig.A.12 with the respective sub-circuits as listed from Fig.A.13-A.31. The system is derived from the ear type system with the effects from the sensorineural hearing loss detected through the ABR with the stimulus sound to the left ear. The names of the circuits of this inverse system are also given corresponding to the system variables with the term '*ofBad*' referring to the parameters of the ear type system with the hearing loss and disorder effects in need of the hearing aid

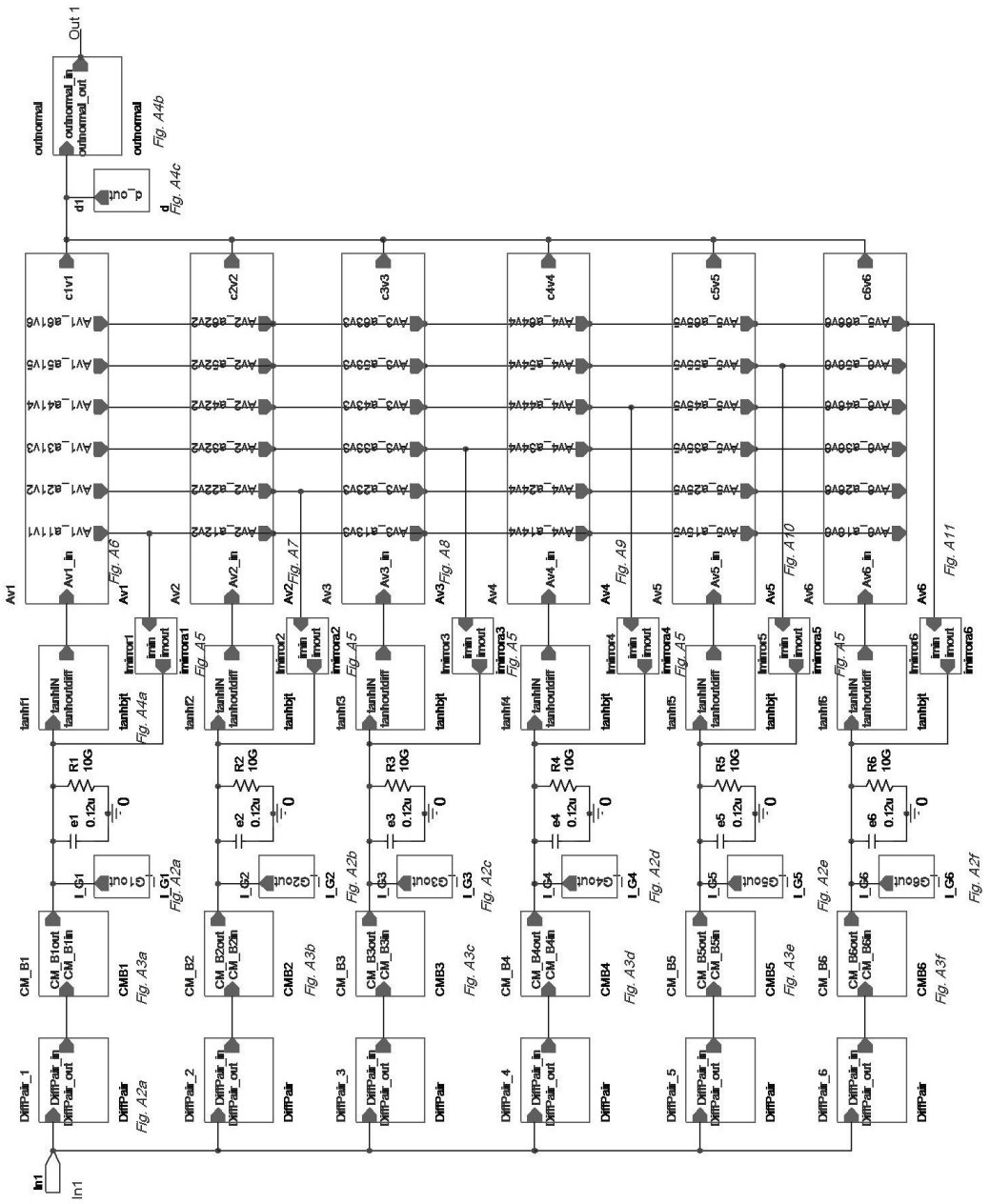

Figure A1. Schematics: *Normal*

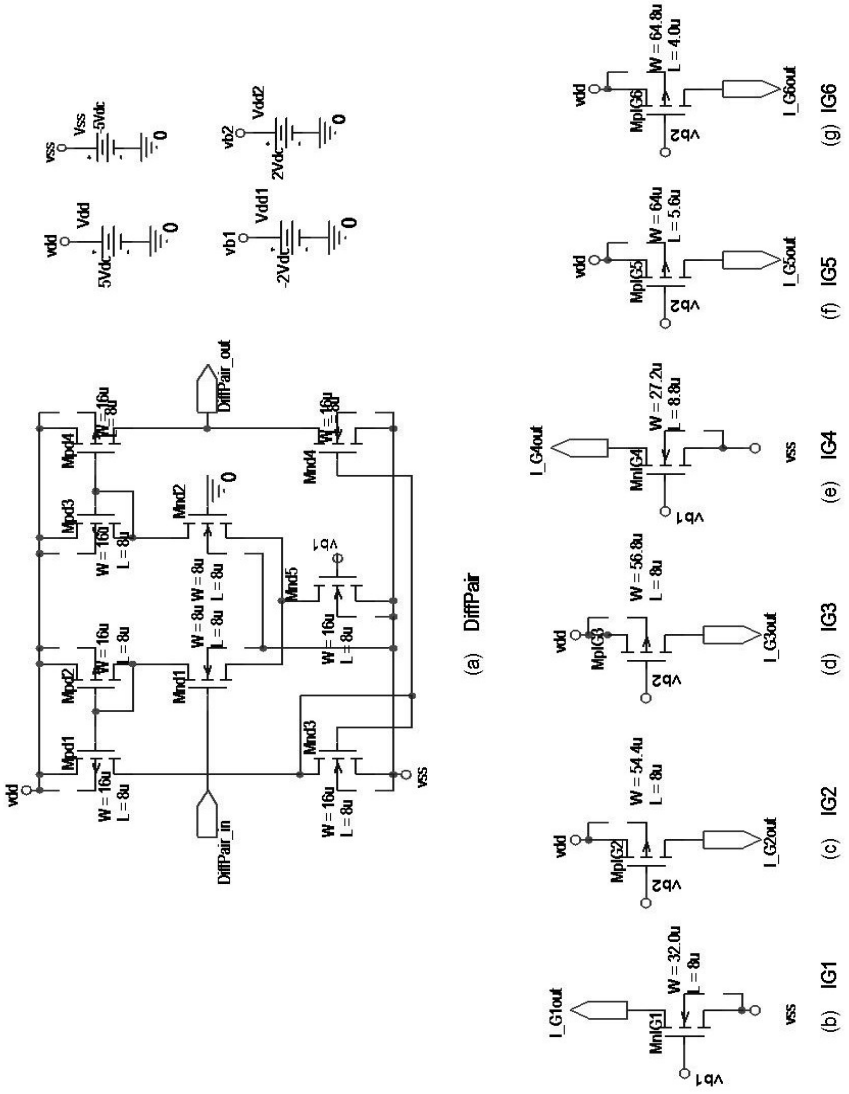

Figure A2. Schematics*: DiffPair*, *IG1*, *IG2*, *IG3*, *IG4*, *IG5*, *IG6*.

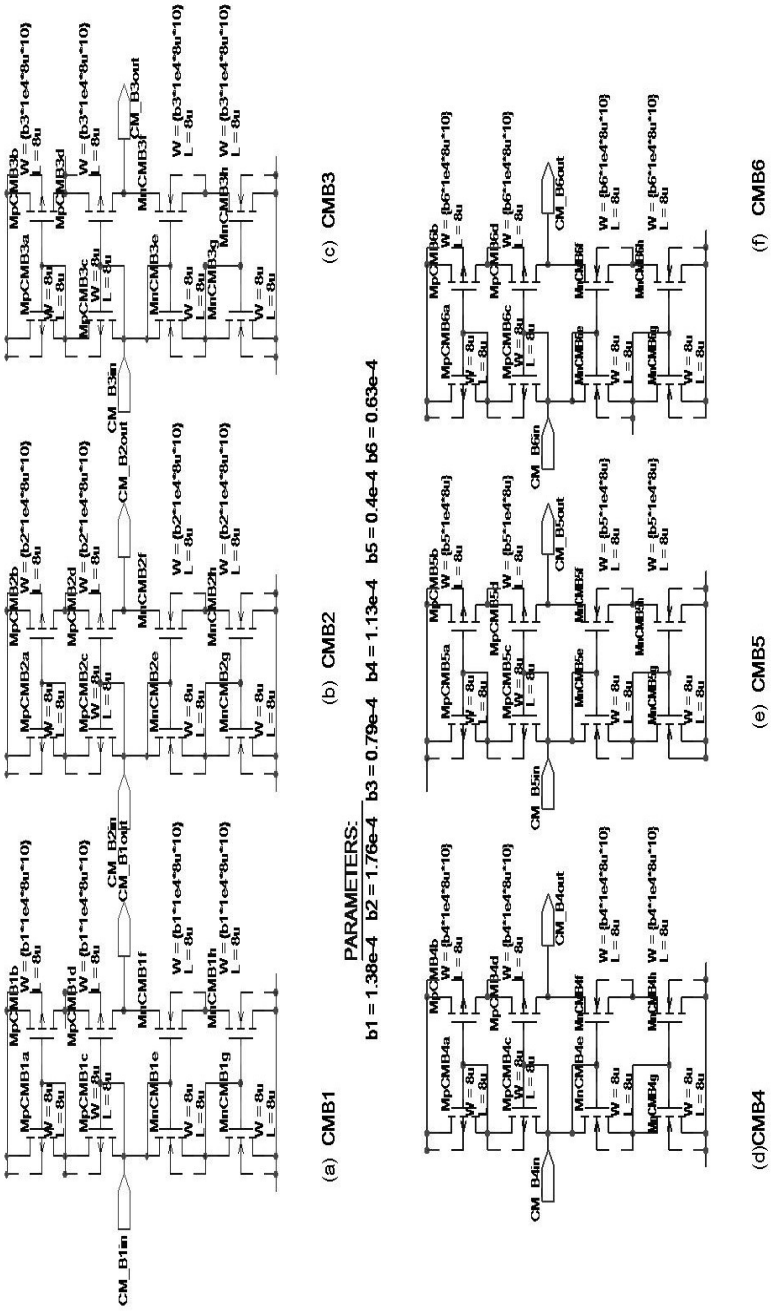

Figure A3. Schematics: *CMB1, CMB2, CMB3, CMB4, CMB5, CMB6*

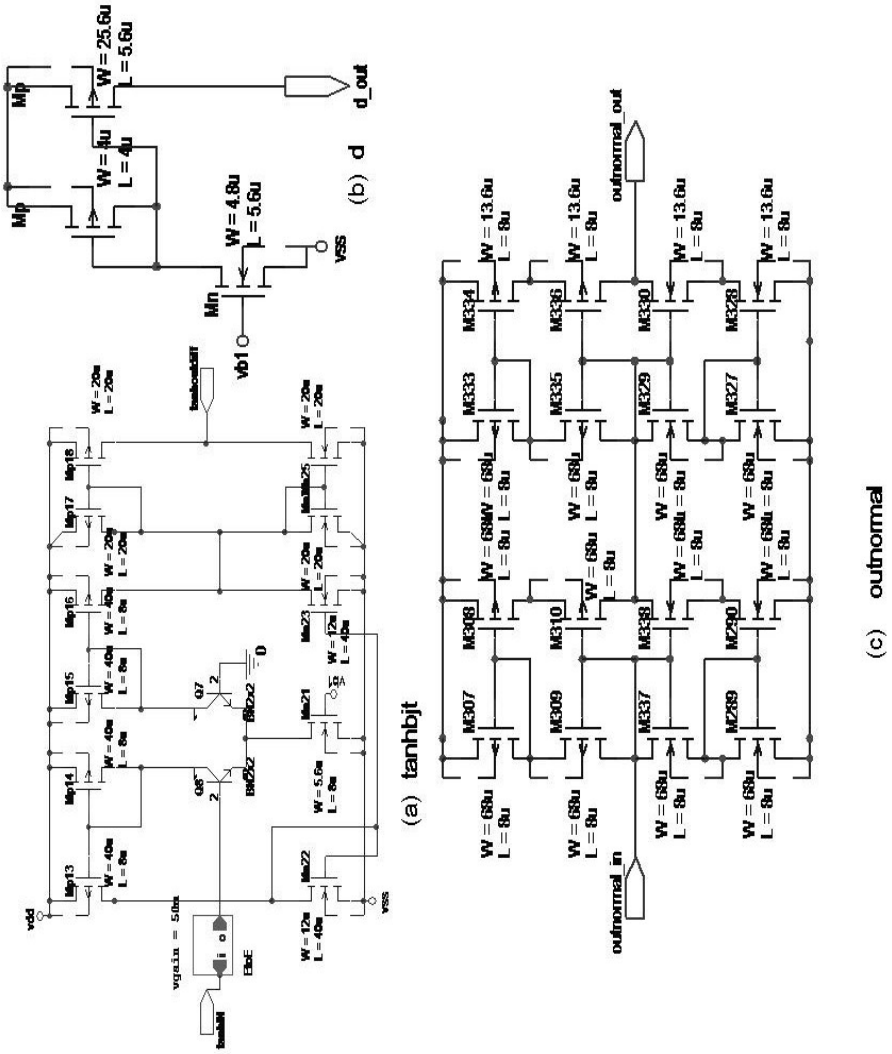

Figure A4. Schematics*: tanhbjt, d, outnormal*

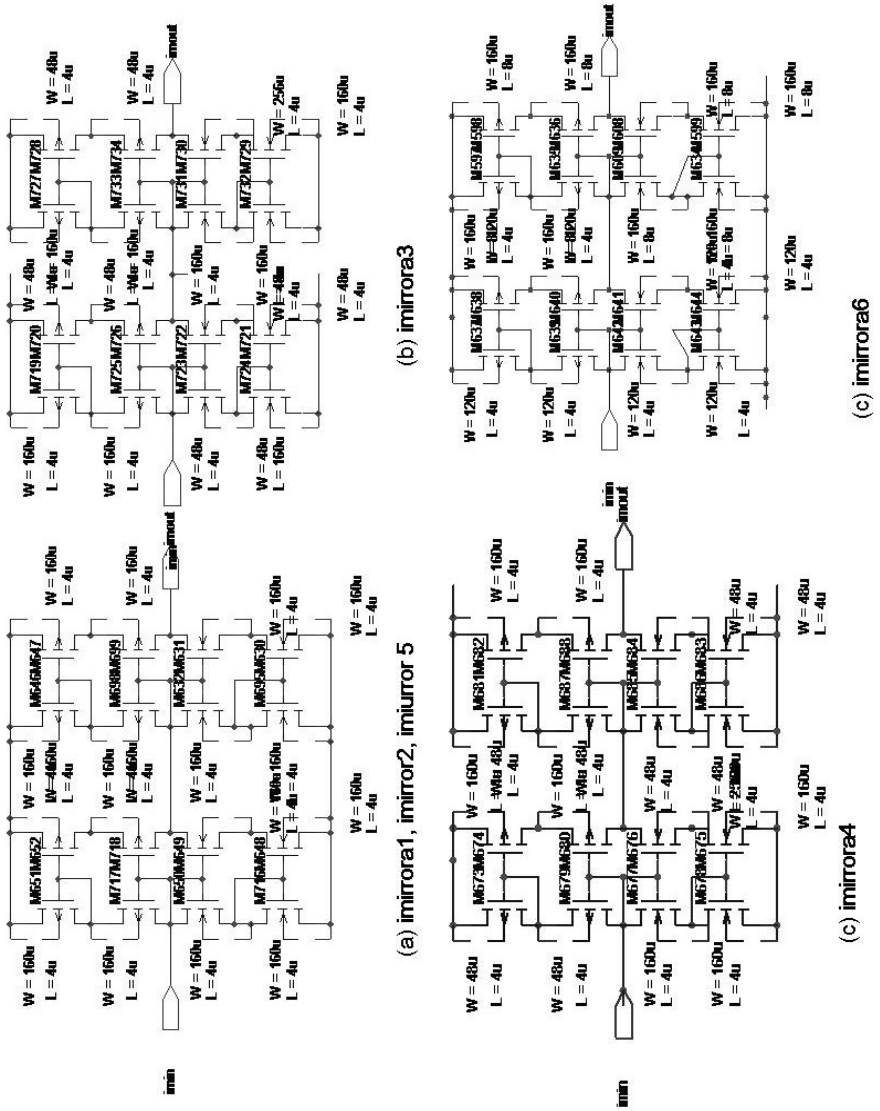

Figure A5. Schematics*: imirrora 1,2,3,4,5,6*

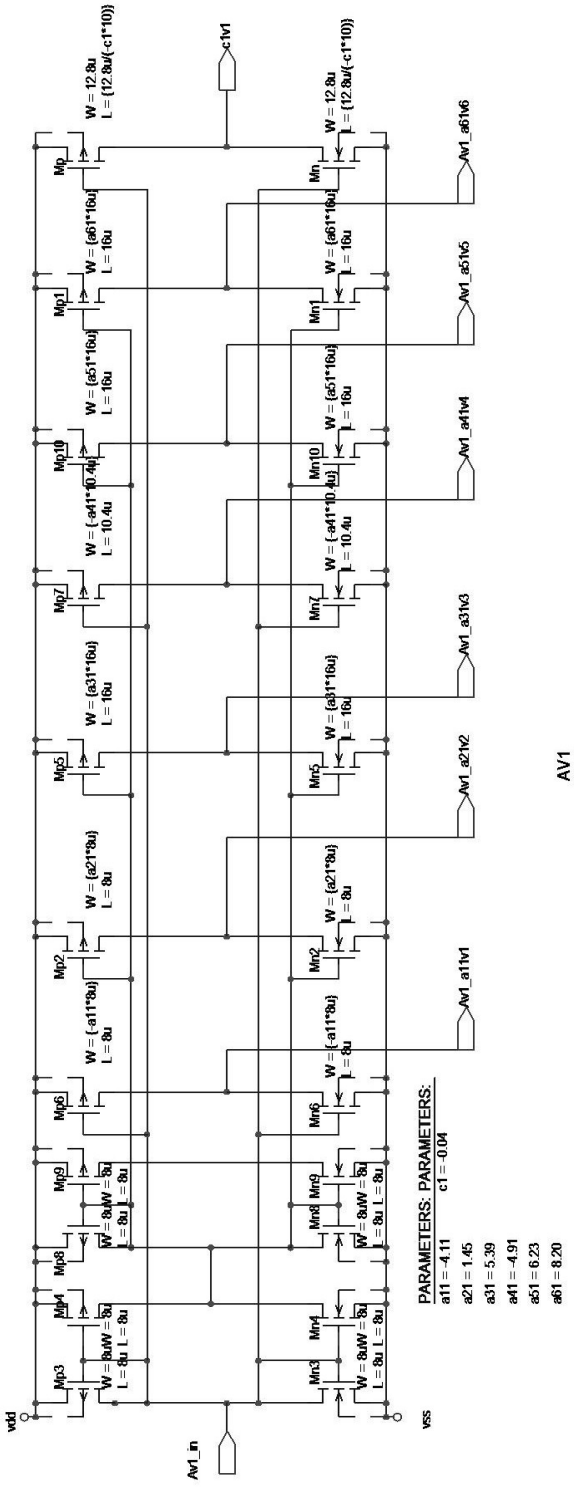

Figure A6. Schematics: *Av1*

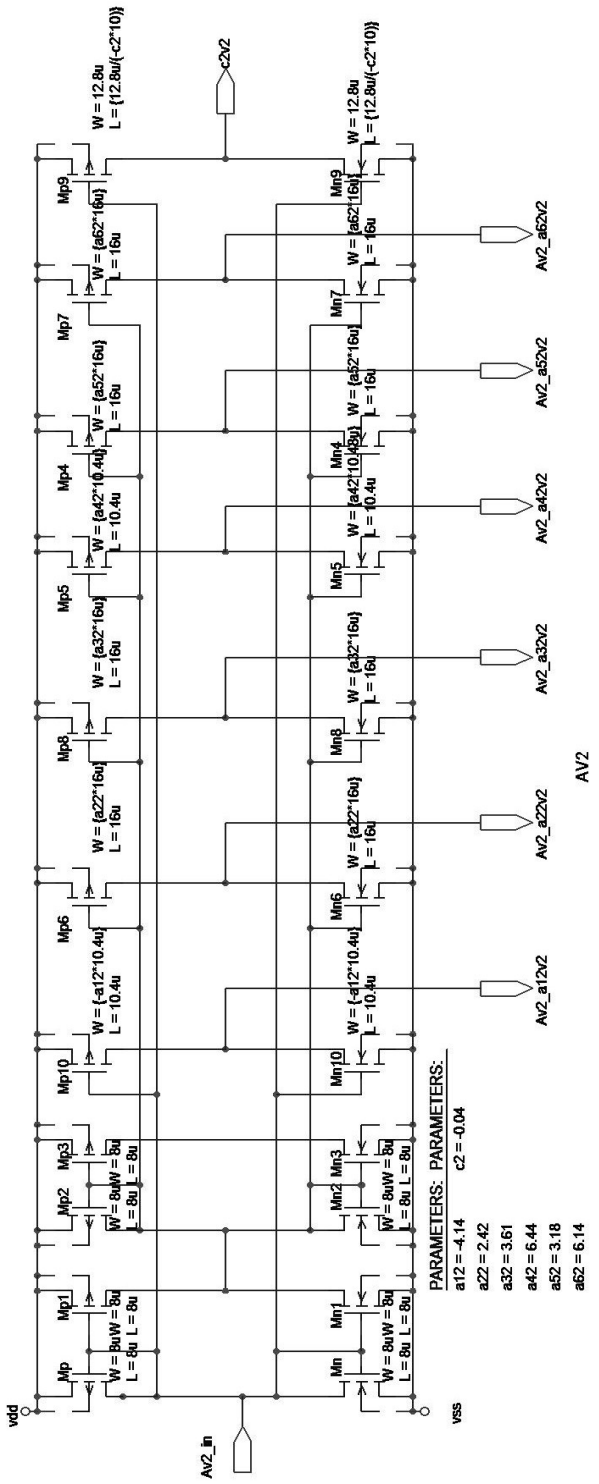

Figure A7. Schematics: *Av2.*

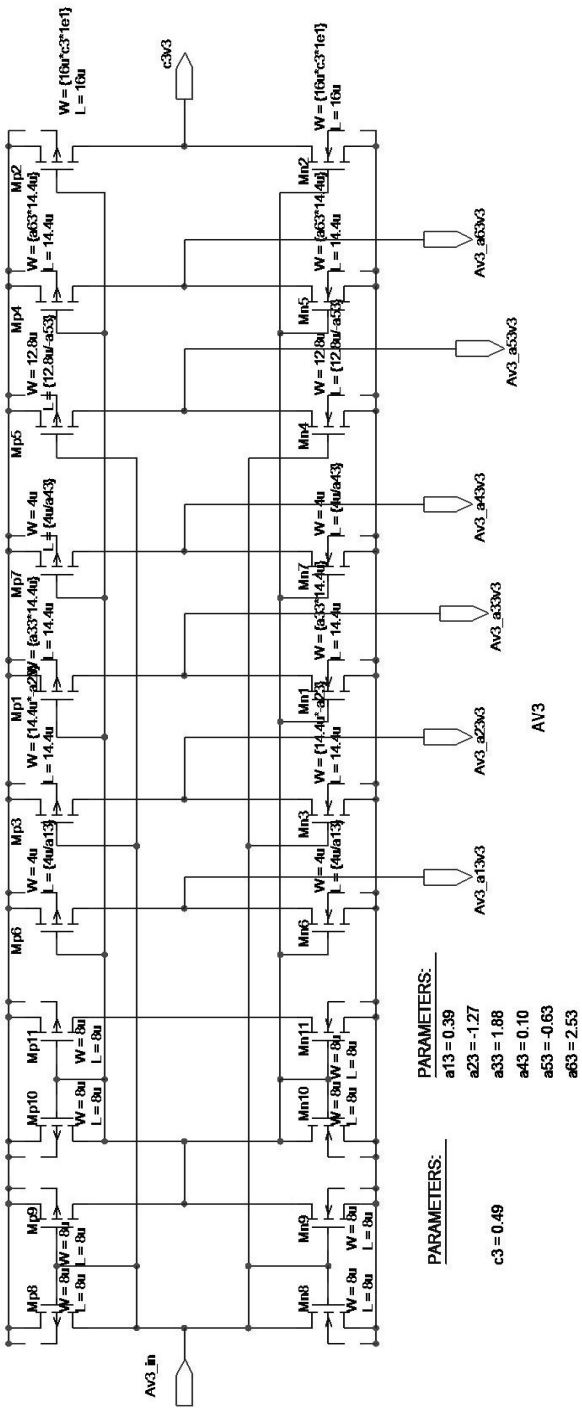

Figure A8. Schematics: *Av3*

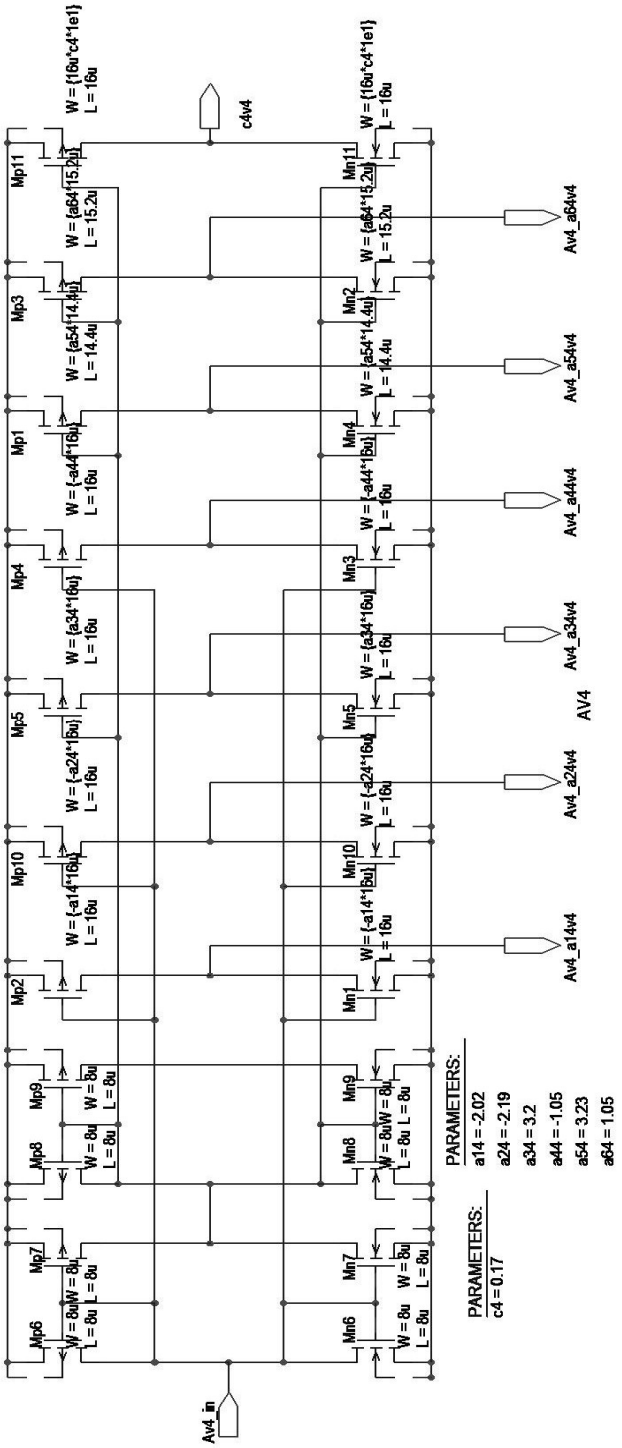

Figure A9. Schematics: *Av4*

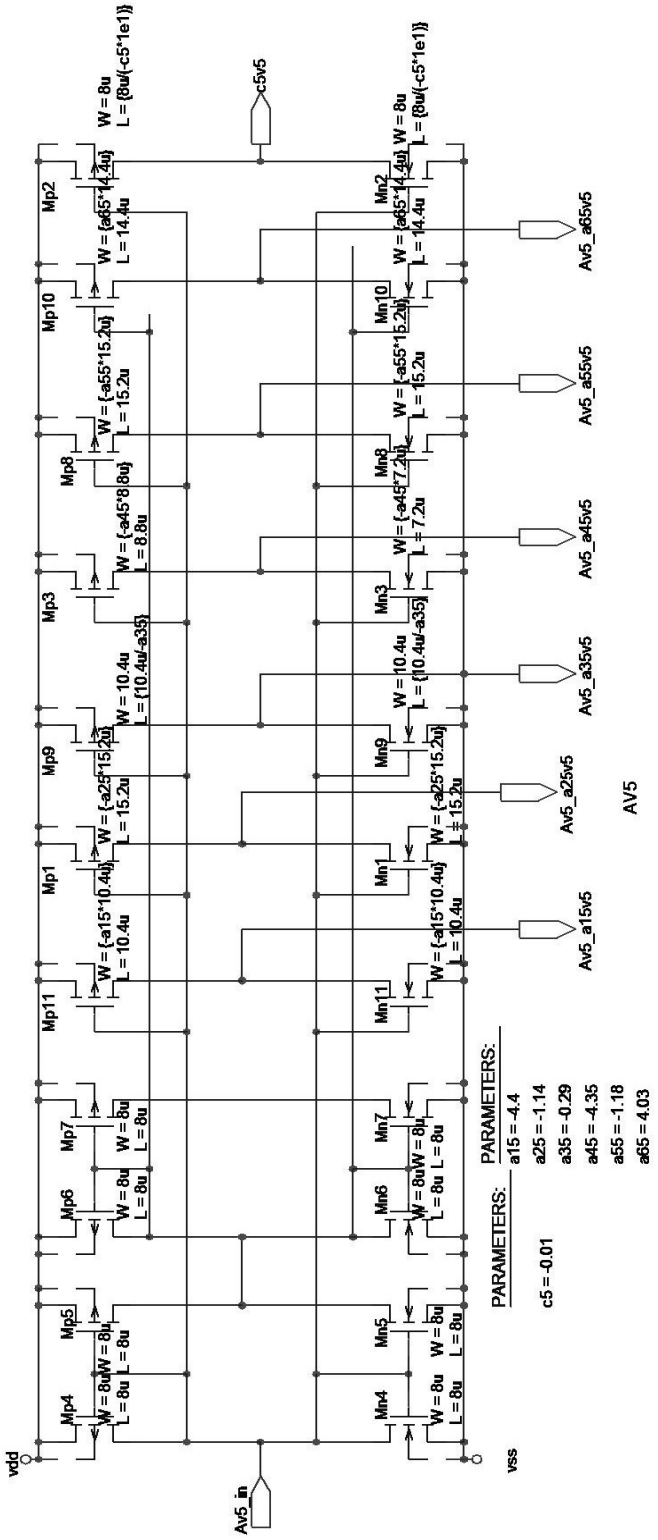

Figure A10. Schematics: *Av5*

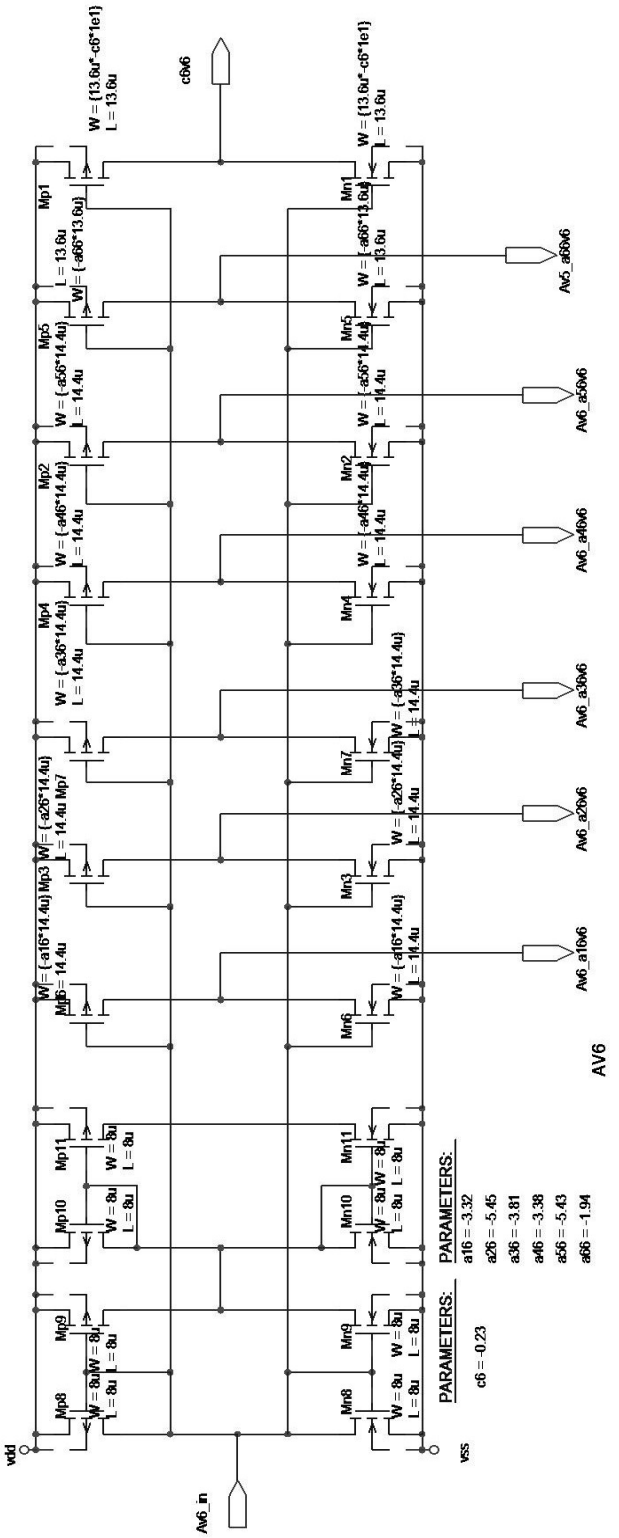

Figure A11. Schematics: *Av6*

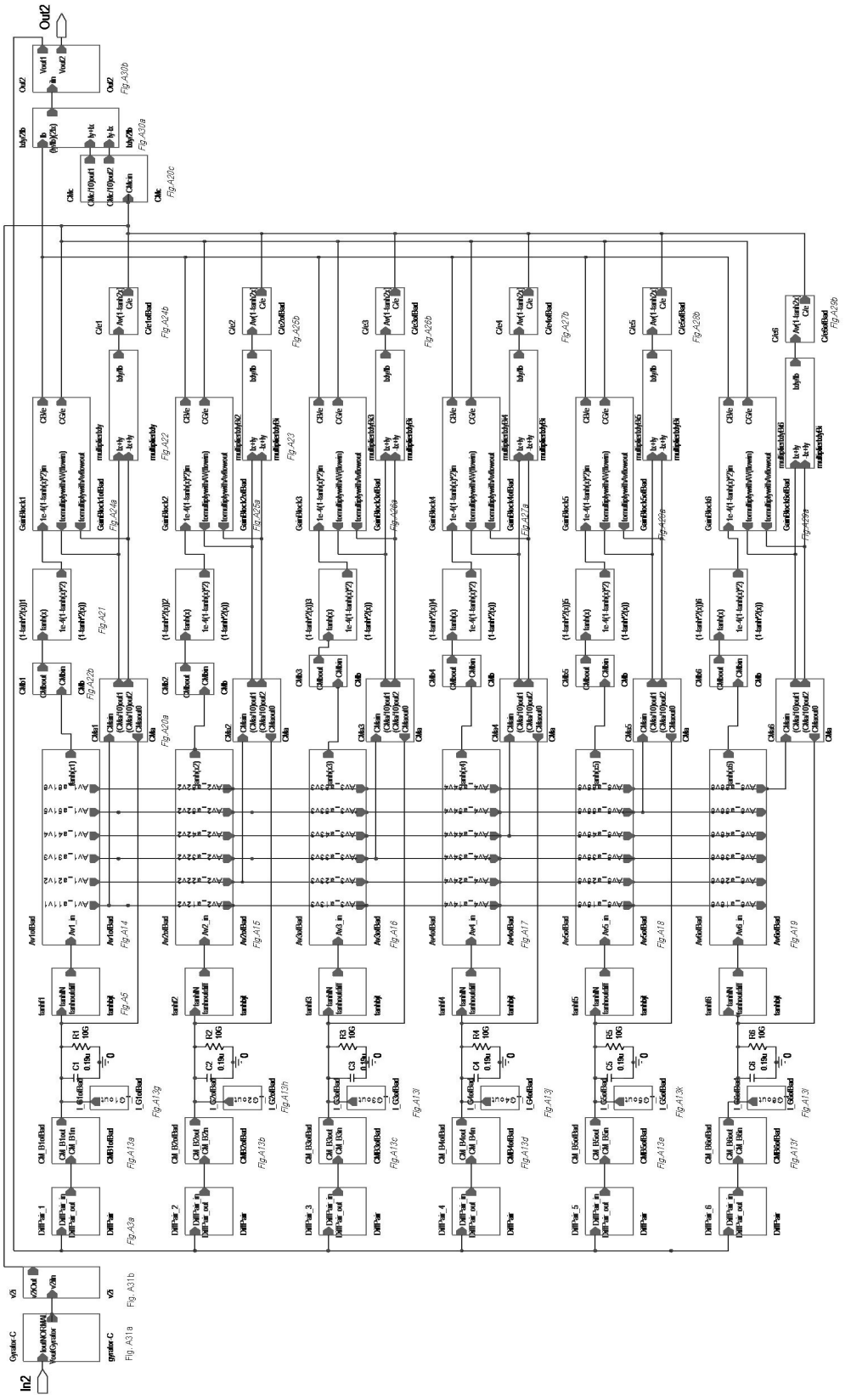

Figure A12. Schematics: *invofbad*

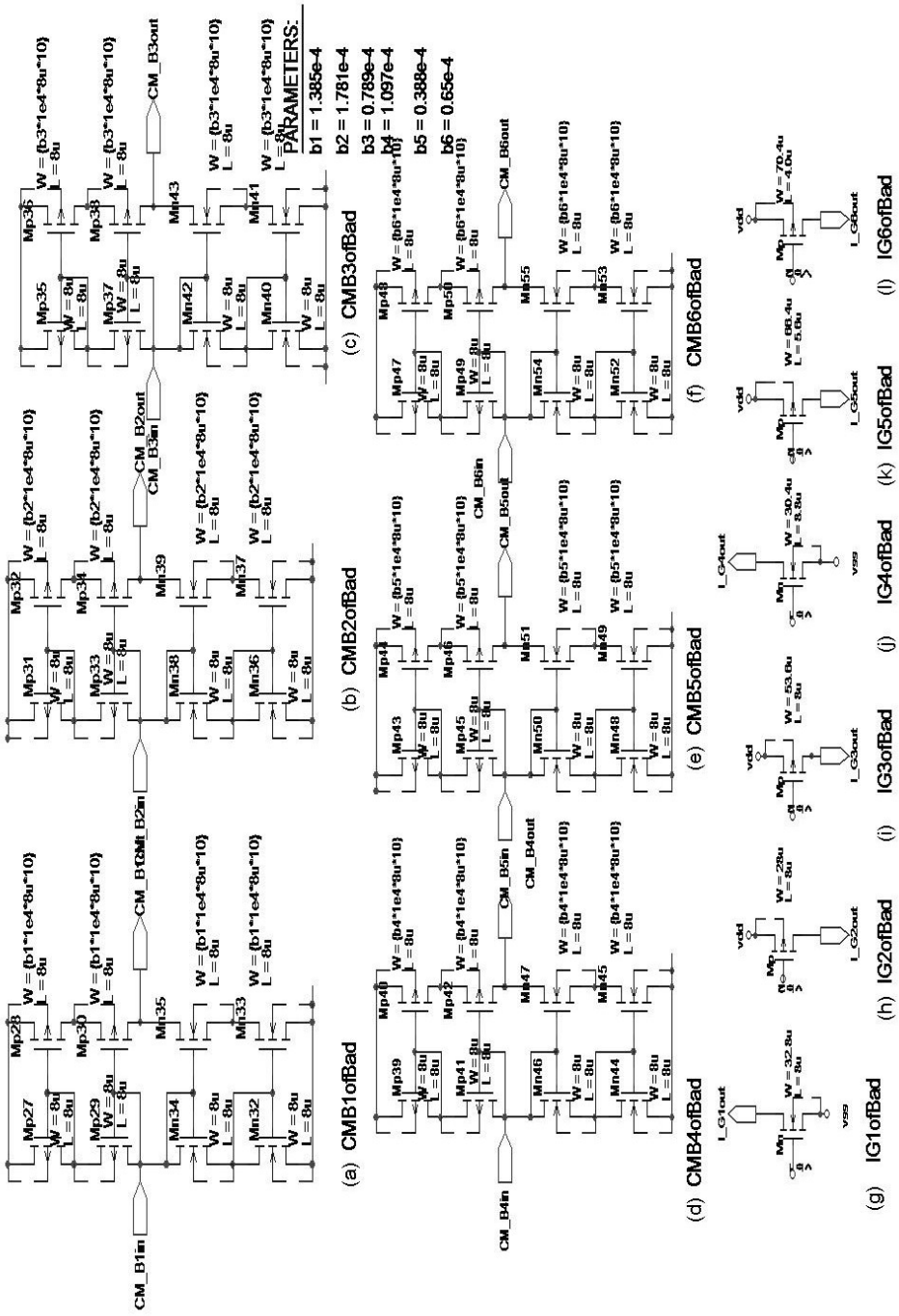

Figure A13. Schematics: *CMB(1-6)ofbad, IG(1-6)ofBad*

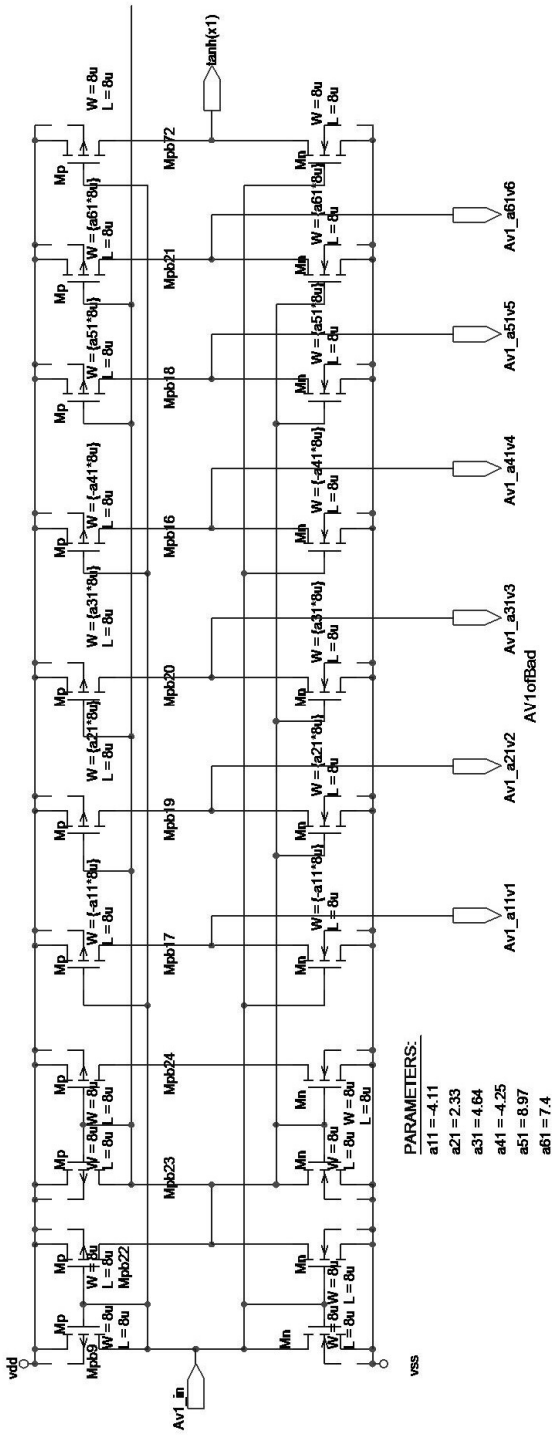

Figure A14. Schematics: *Av1ofbad*

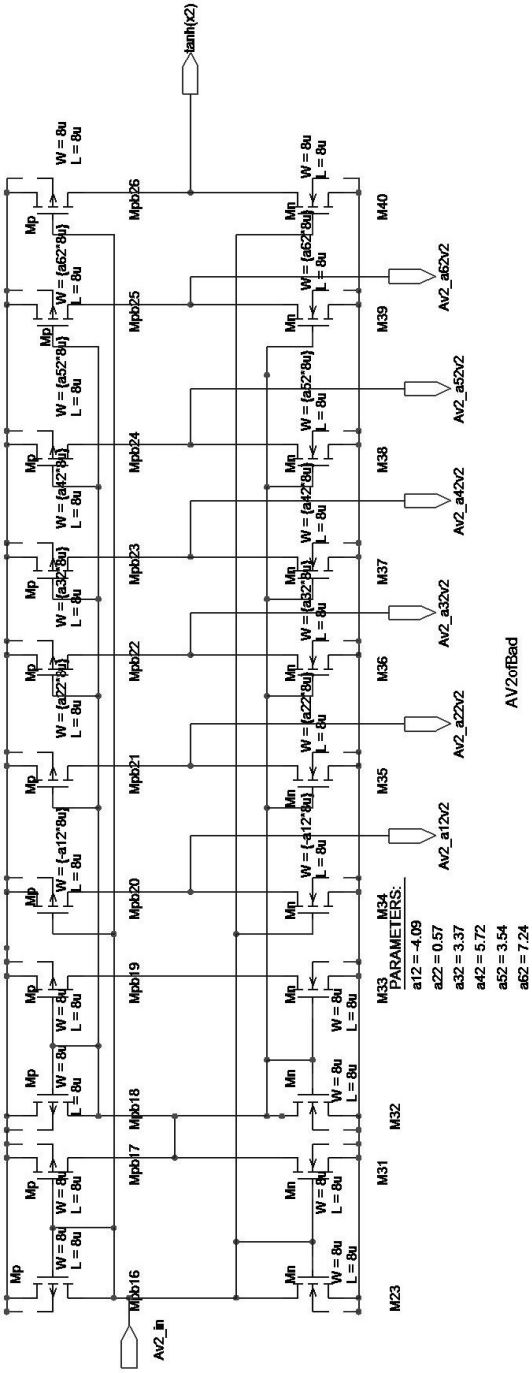

Figure A15. Schematics: *Av2ofbad*

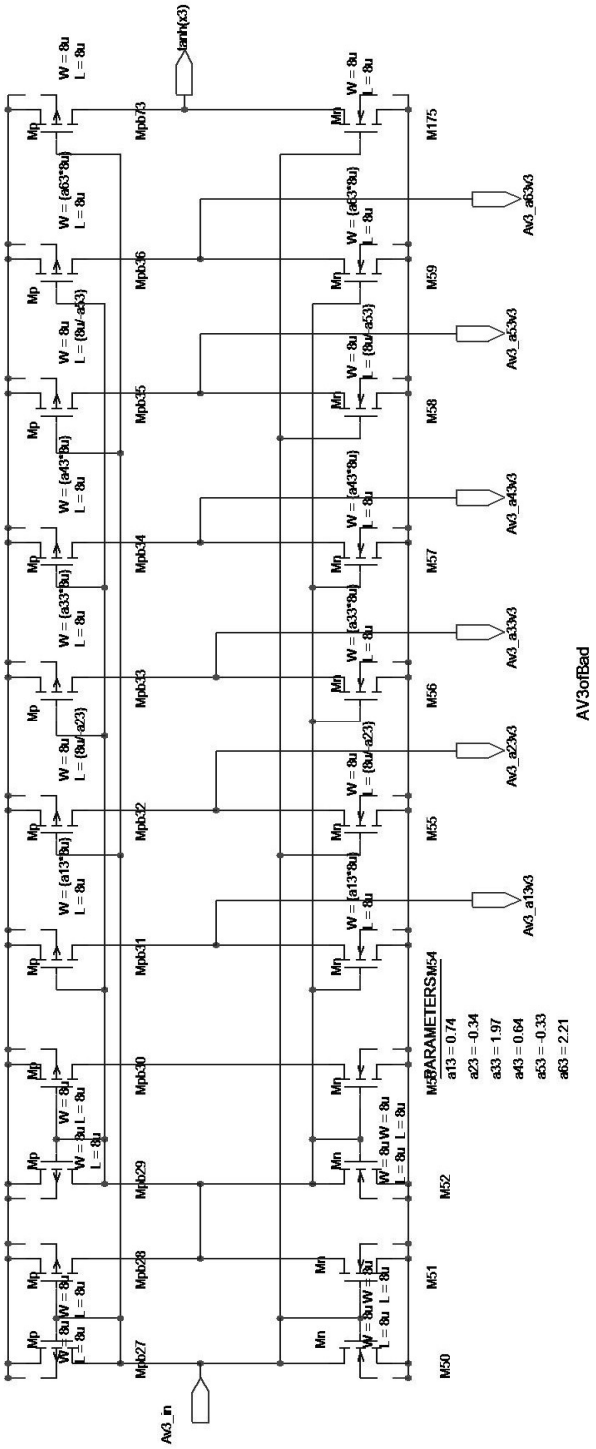

Figure A16. Schematics: *Av3ofbad*

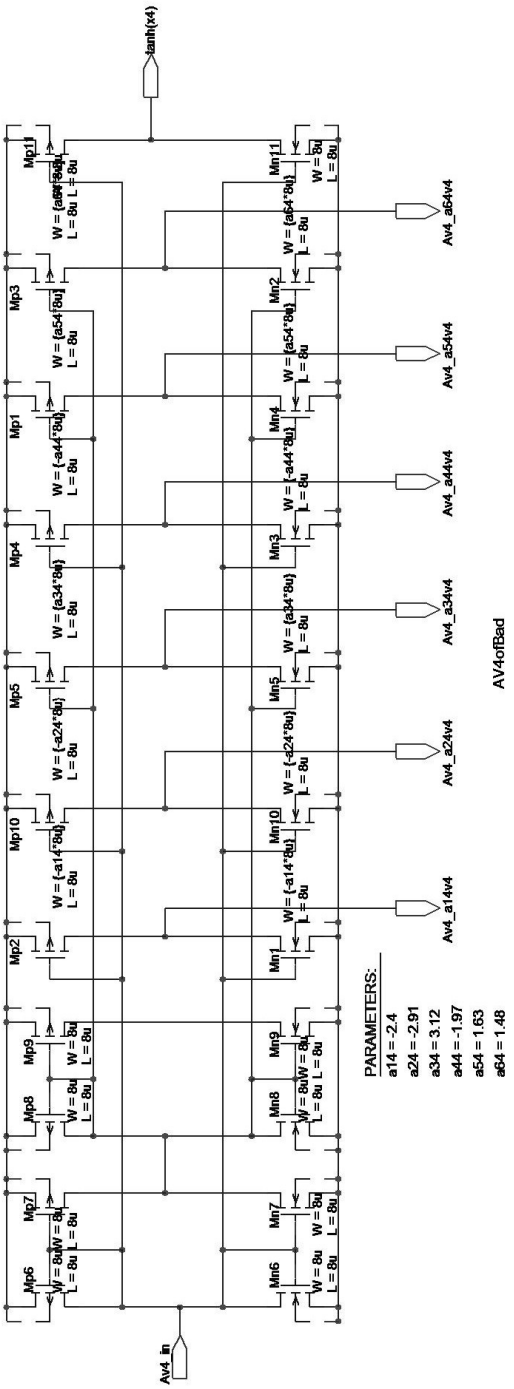

Figure A17. Schematics: *Av4ofbad*

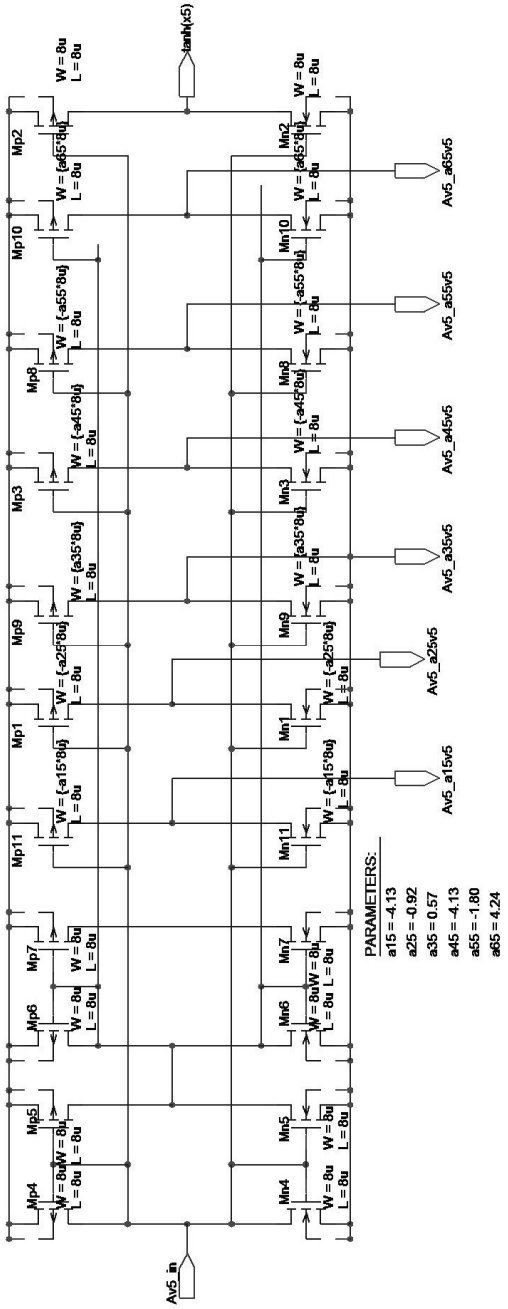

Figure A18. Schematics: *Av5ofbad*

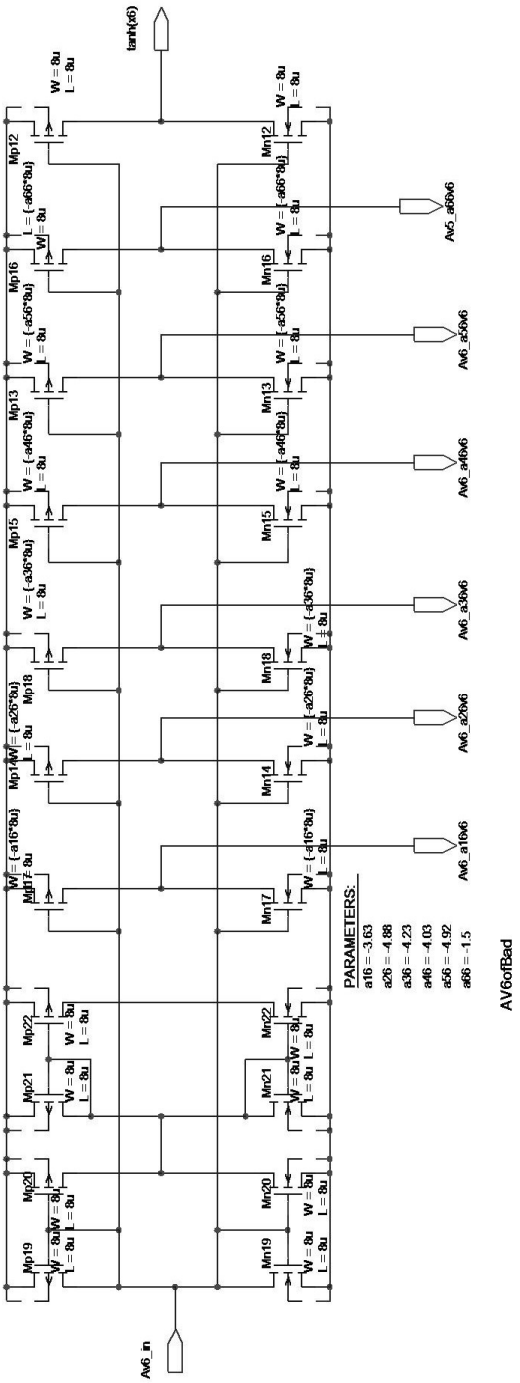

Figure A19. Schematics: *Av6ofbad*

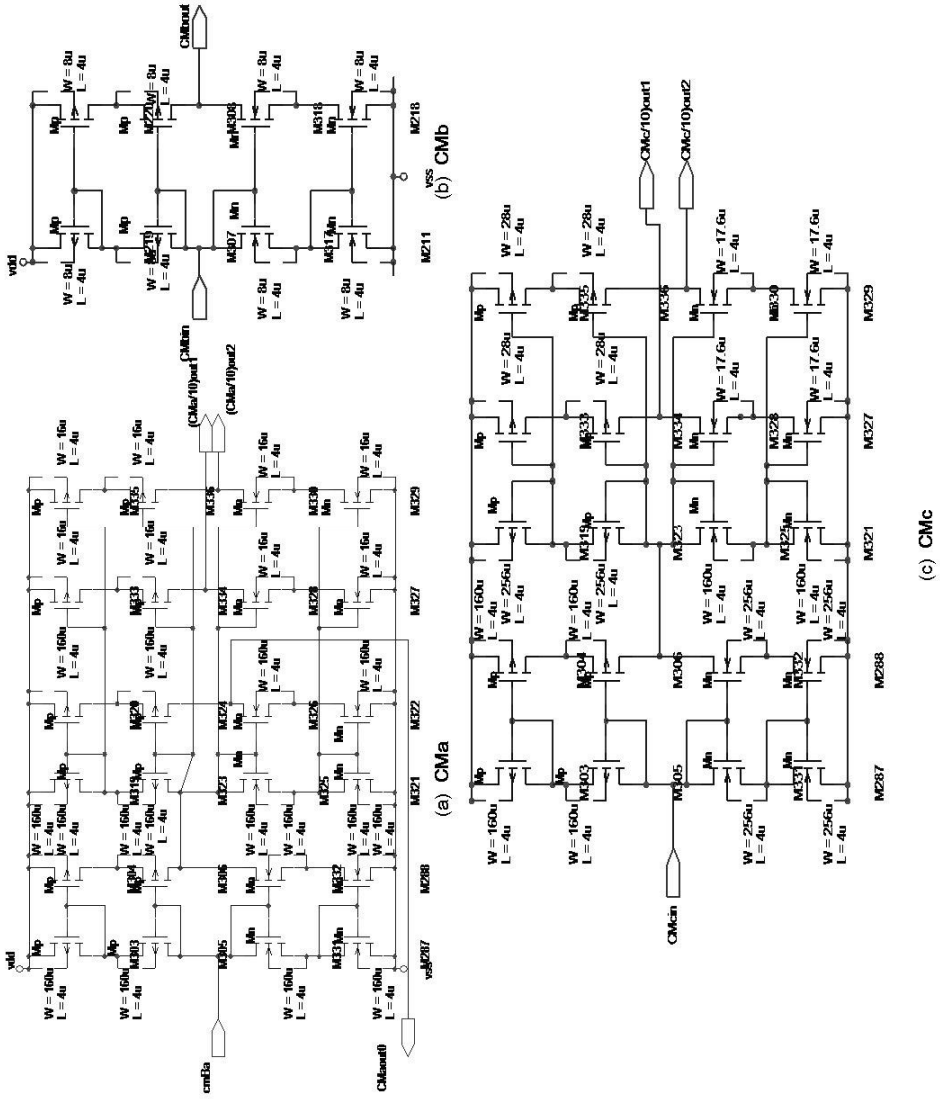

Figure A20. Schematics: *CMa*, *CMb*, *CMc*

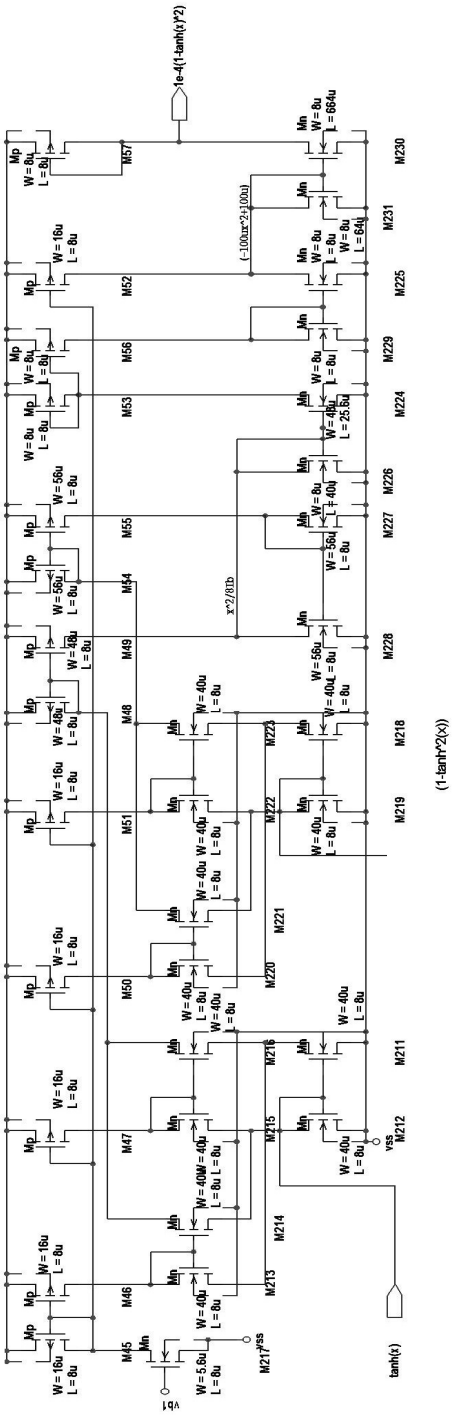

Figure A21. Schematics: *(1-tanh2(x))*

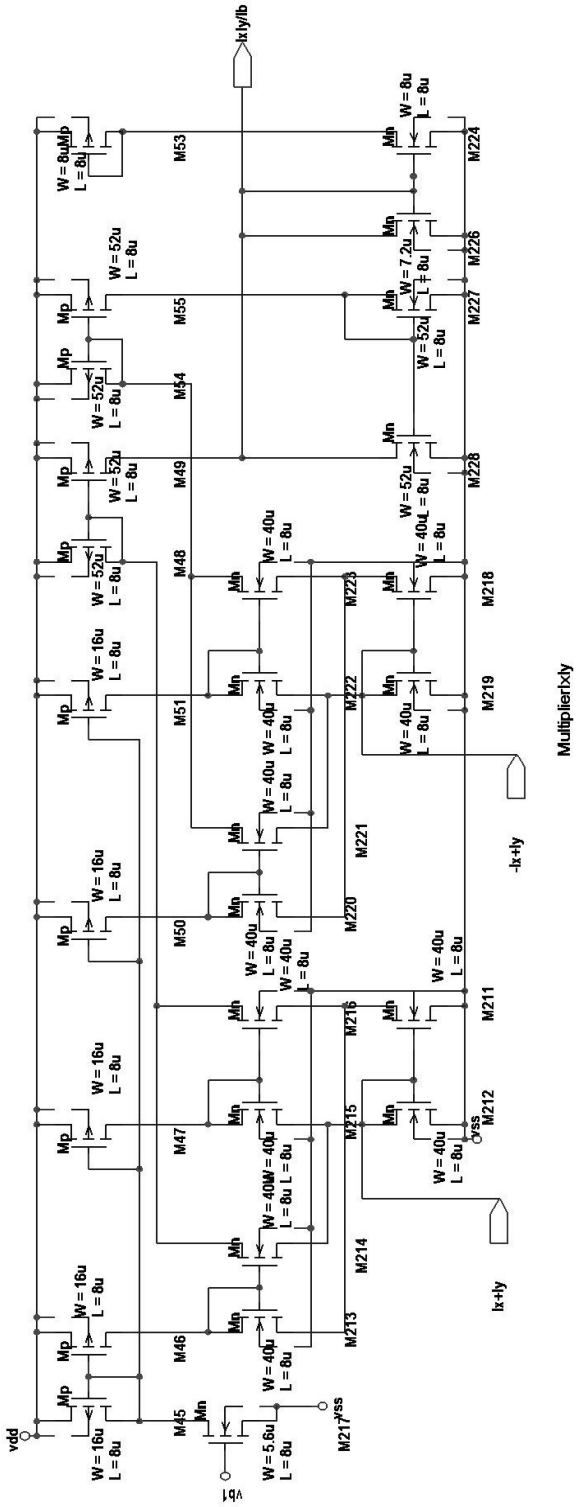

Figure A22. Schematics: *MultiplierIxIy*

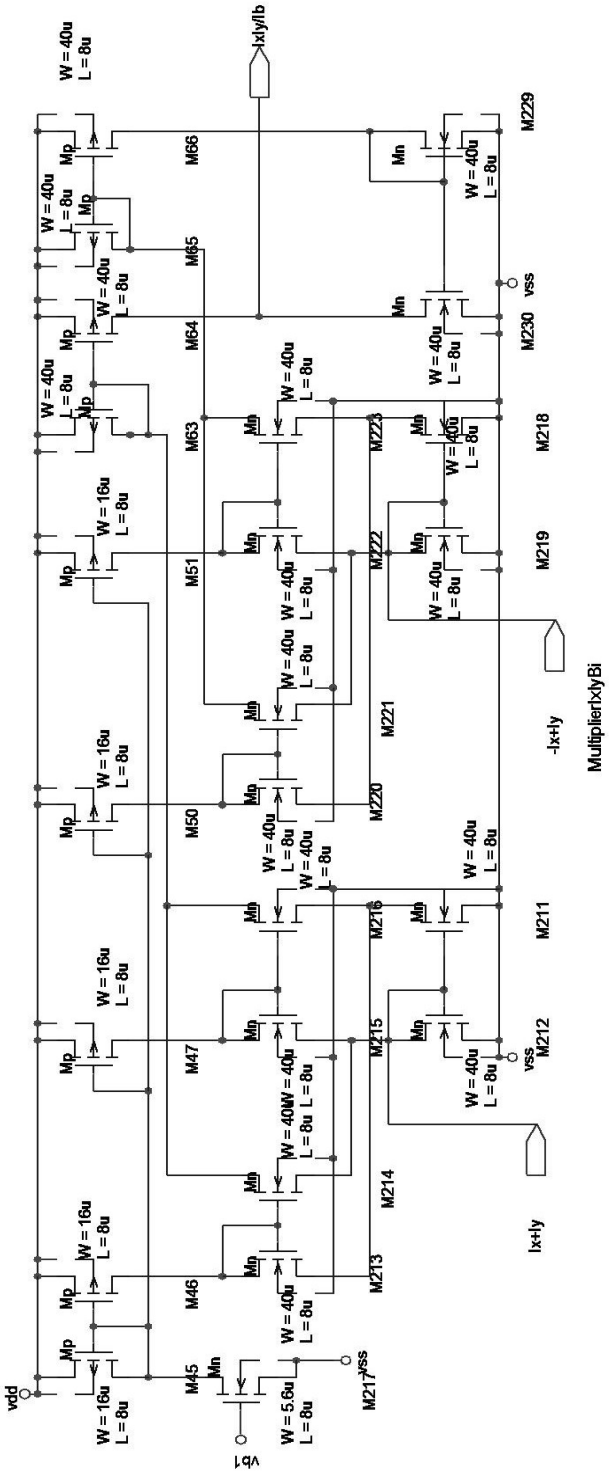

Figure A23. Schematics: *MultiplierIxIyBi*

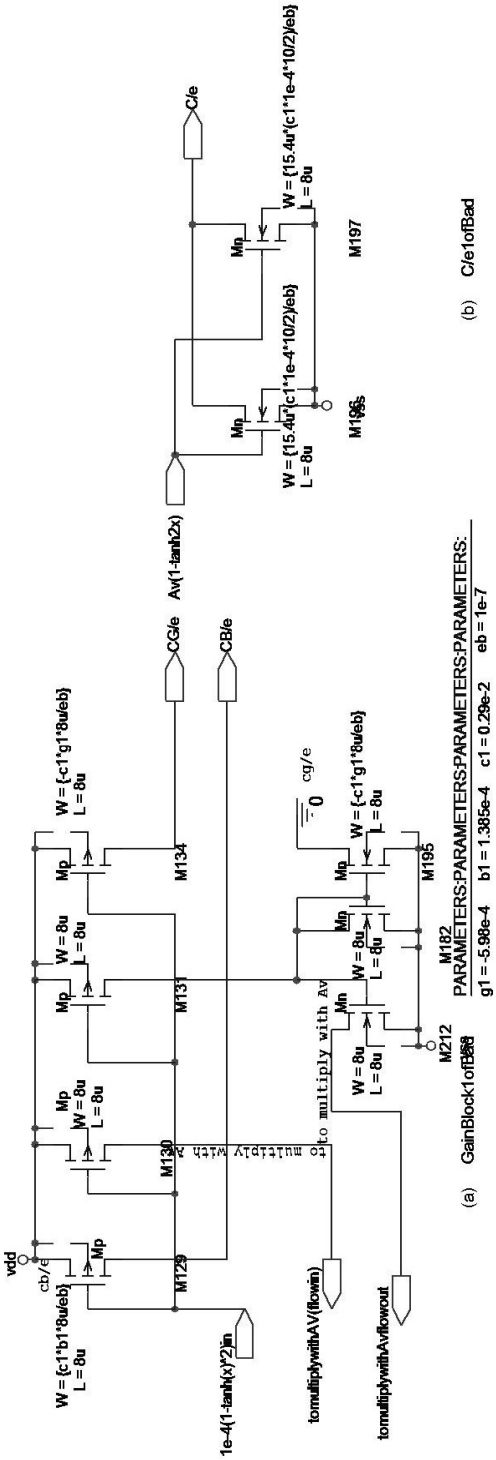

Figure A24. Schematics: *Gainblock1ofBad*, *C/e1ofBad*

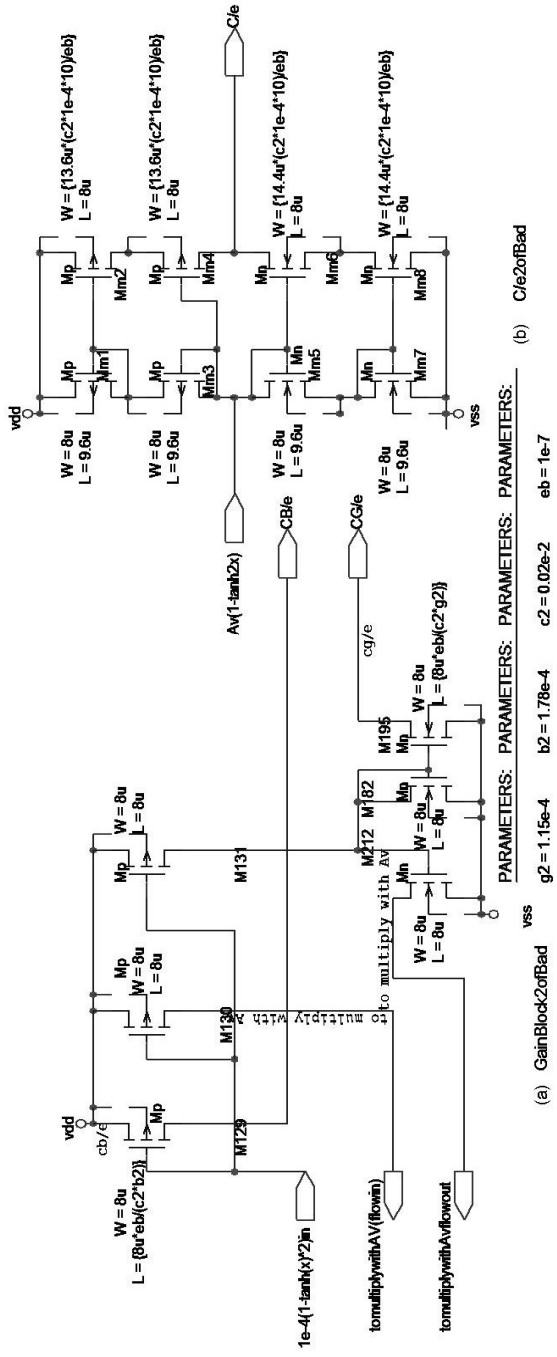

Figure A25. Schematics: *Gainblock2ofBad*, *C/e2ofBad*

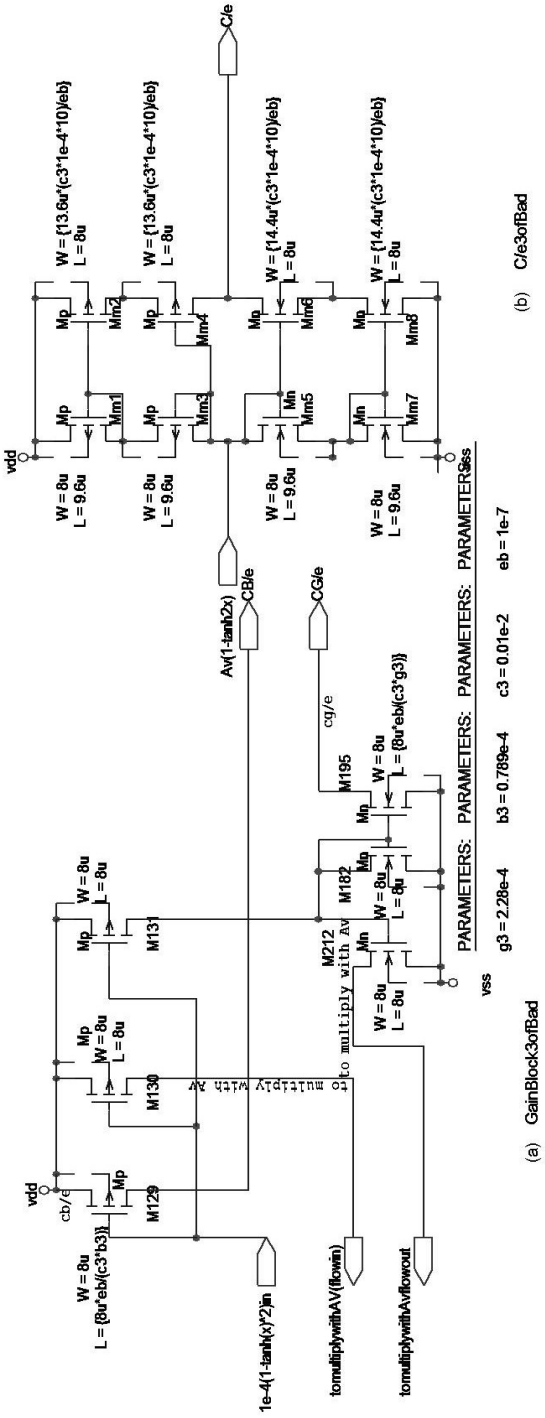

Figure A26. Schematics: *Gainblock3ofBad*, *C/e3ofBad*

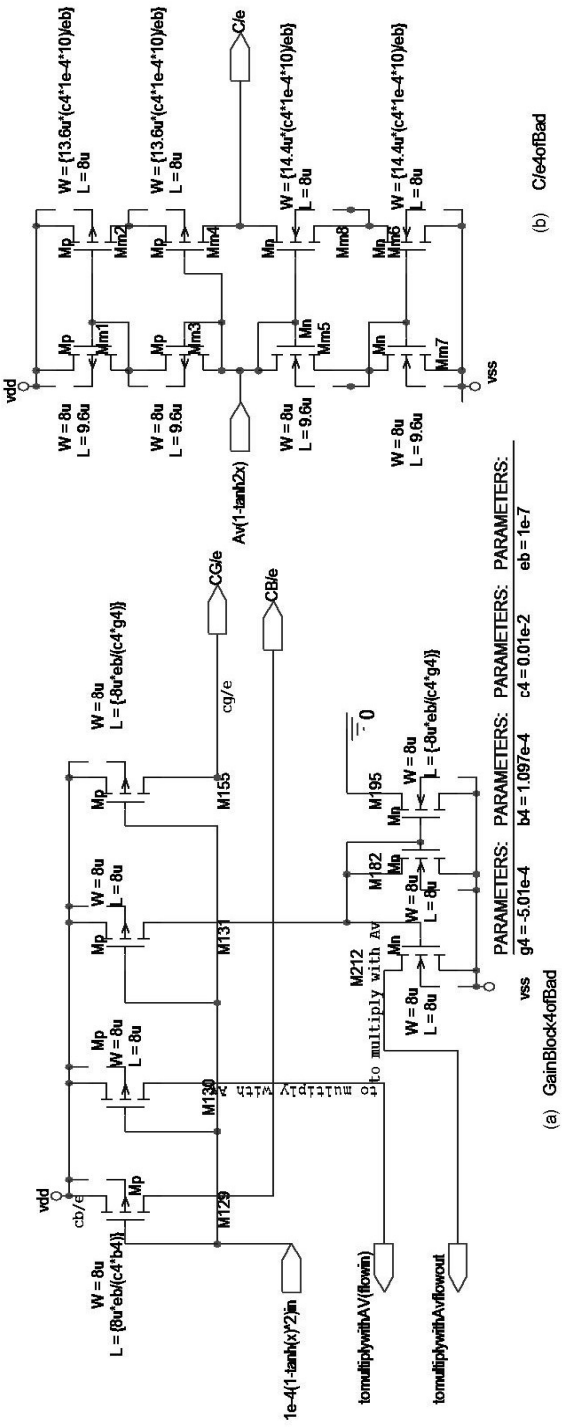

Figure A27. Schematics: *Gainblock4ofBad*, *C/e4ofBad*

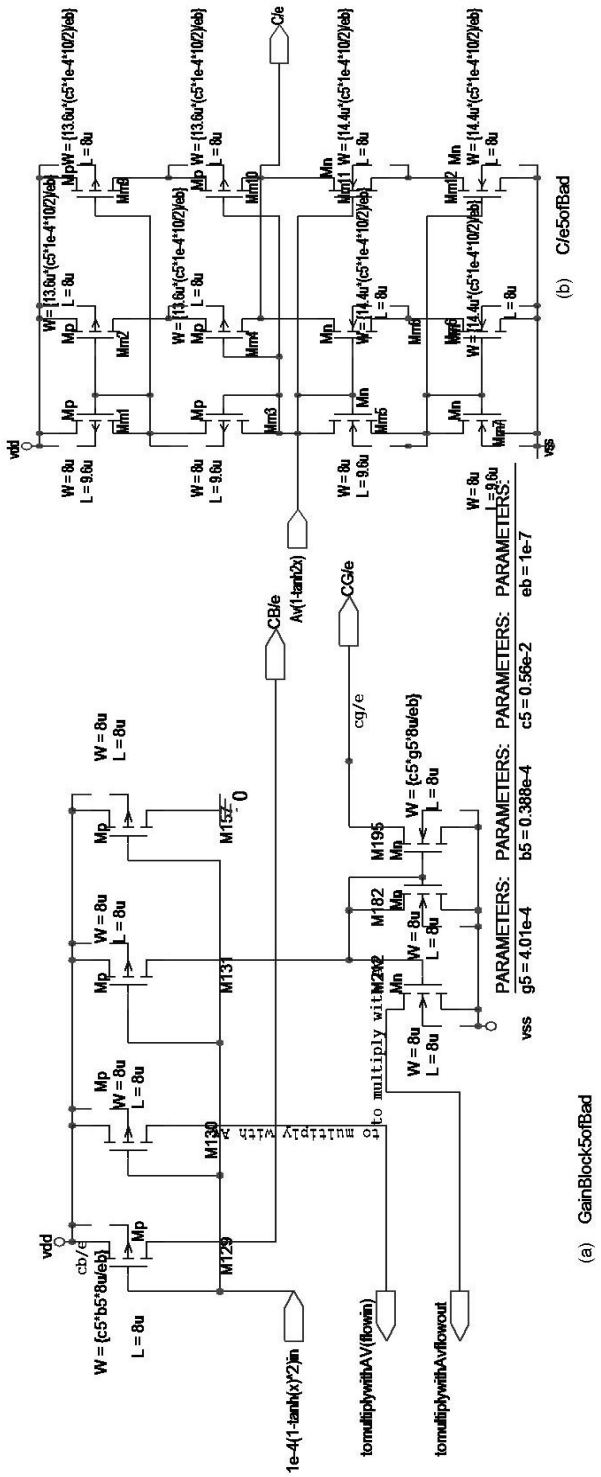

Figure A28. Schematics: *Gainblock5ofBad*, *C/e5ofBad*

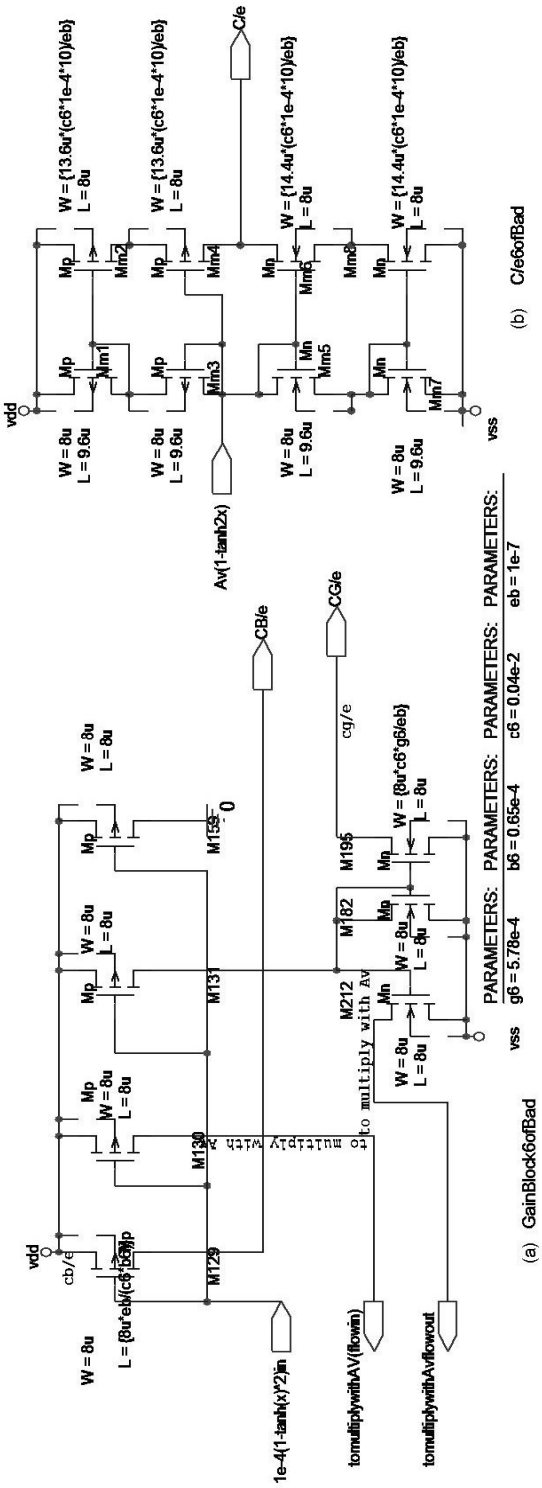

Figure A29. Schematics: *Gainblock6ofBad*, *C/e6ofBad*

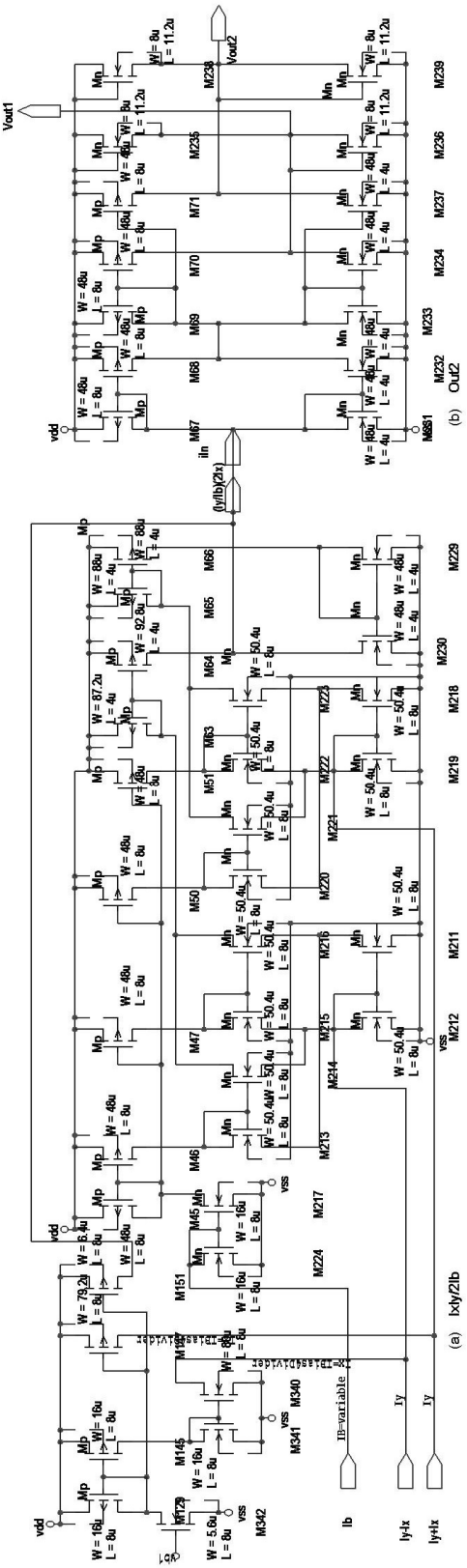

Figure A30. Schematics: *IxIy/2Ib*, *Out2*

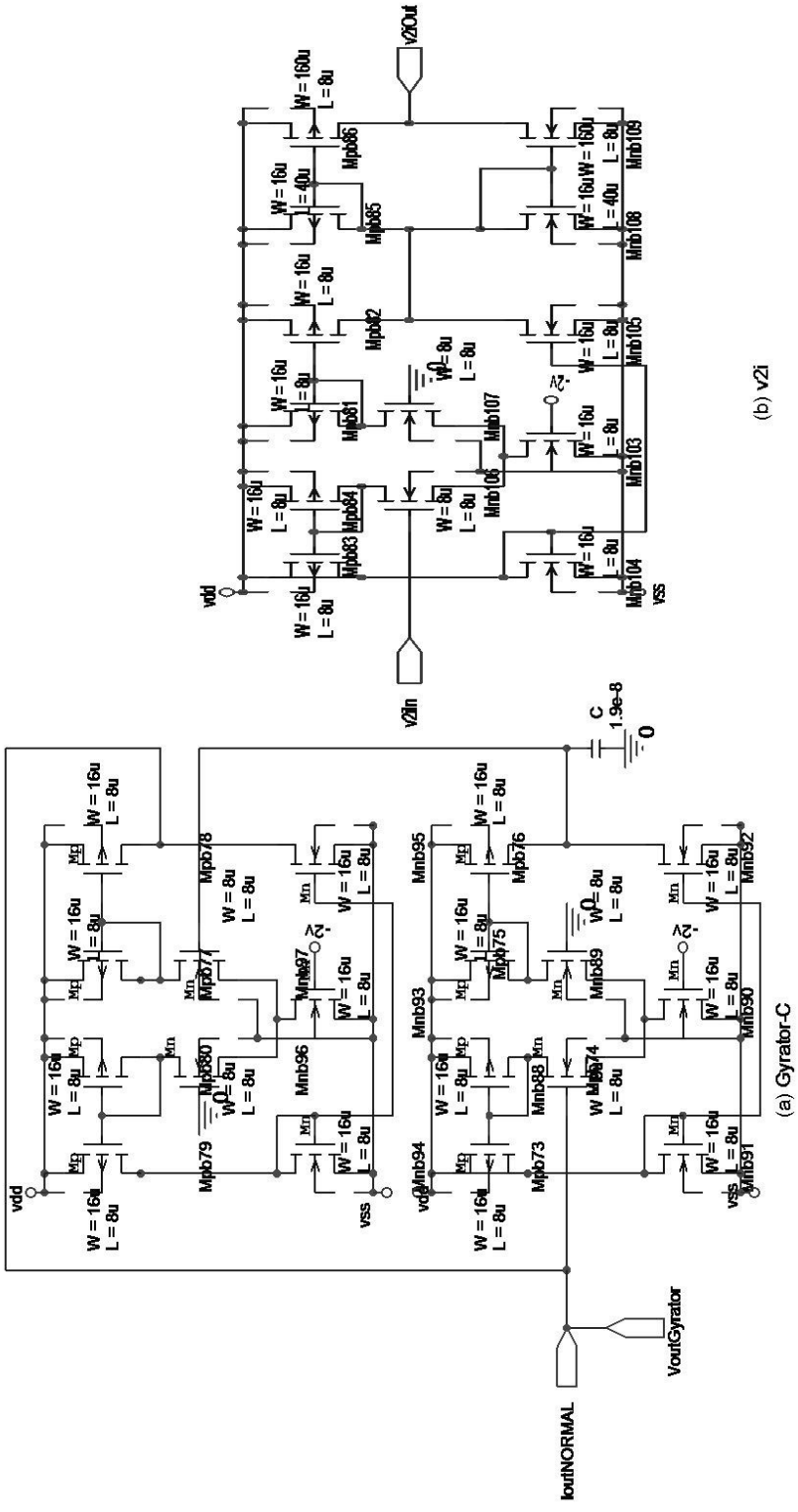

Figure A31. Schematics: *Gyrator-C*, *v2i*

Bibliography

[1] P. Gomez, V. Rodellar, and R. Newcomb, "A PARCOR characterization of the ear for hearing aids," Proceedings of the IEEE, Vol. 70, No. 12, pp. 1464 – 1466, December 1982.

[2] L. Sellami and R. W. Newcomb, "Ear-Type analog and digital systems," Recent Research Developments in Circuits and Systems Vol. 1 edited by S. G. Pandalai, Trivandrum, India: Research Signpost, pp. 59 – 83, 1996.

[3] D. T. Kemp, "Stimulated acoustic emissions from within the human auditory system," Journal of Acoustical Society of America, Vol. 64, No. 5, pp. 1368 – 1391, November 1978.

[4] D. T. Kemp, "Otoacoustic emissions, their origin in cochlear function, and use," British Medical Bulletin, Vol. 63, No. 1, pp. 223 – 241, October 2002.

[5] U. S. National Institutes of Health, "Early identification of hearing impairment in infants and young children," NIH Consensus Development Conference Statement, Vol. 11, No. 1, pp. 1-24, Bethesda, Maryland, USA, March 1993.

[6] J.I. Benito-Orejas, B. Ramı´rez, D. Morais, A. Almaraz, and J.L. Ferna´ndez-Calvo, "Comparison of two-step transient evoked otoacoustic emissions (TEOAE) and automated auditory brainstem response (AABR) for universal newborn hearing screening programs," International Journal of Pediatric Otorhinolaryngology, Vol. 72, No. 8, pp. 1193 – 1201, August 2008.

[7] B. O. Olusanya, L. M. Luxon, and S. L. Wirz, "Benefits and challenges of newborn hearing screening for developing countries," International Journal of Pediatric Otorhinolaryngology, Vol. 68, No. 4, pp. 287 – 305, March 2004.

[8] J. A. Mason and K. R. Herrmann, "Universal infant hearing screening by automated auditory brainstem response measurement," Pediatrics, Vol. 101, No.2, pp. 221 – 228, February 1998.

[9] A. S. Wrightson, "Universal newborn hearing screenings," Journal of the American Academy of Family Physicians, Vol. 75, No.9, pp.1349 – 1356, May 2007.

[10] A. Starr and A. E. Hamilton, "Correlation between confirmed sites of neurological lesions and abnormalities of far-field auditory brainstem responses," Electroencephalography and Clinical Neurophysiology, vol. 41, no. 6, pp. 595 – 608, December 1976.

[11] D. L. Jewett and J. S. Williston, "Auditory evoked far fields averaged from the scalp of humans," Brain, Vol. 94, No. 4, pp. 681 – 696, January 1971.

[12] J. T. Jacobson, "An overview of the auditory brainstem response," in J. T. Jacobson, The auditory brainstem response. San Diego, USA: College Hill Press, Chapter1, pp. 1 – 13, 1985.

[13] J. W. Hall III, New handbook of auditory evoked responses. Boston, USA: Pearson Education, 2007.

[14] M. Don and B. Kwong, "Auditory brainstem response: differential diagnosis," in J. Katz, L. Medwetsky, R. Burkard, and L. Hood, Handbook of clinical audiology. Baltimore, USA: Lippincott Williams and Wilkins, Chapter 13, pp. 265 – 292, 2009.

[15] S. A. Arnold, "The auditory brain stem response," in R. J. Roeser, M. Valente, and H. Hosford-Dunn, Audiology diagnosis. New York, USA: Thieme, Chapter 19, pp. 451 – 470, 2000.

[16] S. Silman and C. A. Silverman, Auditory diagnosis: principles and applications. California, USA: Academic Press, 1991.

[17] A. R. Moller, Hearing: anatomy, physiology, and disorders of the auditory system. London, United Kingdom: Academic Press, 2006.

[18] Y. S. Sininger, "Establishing clinical norms for auditory brainstem response," American Journal of Audiology, Vol. 1, No. 1, pp. 16 – 28, July 1992.

[19] S. D. Scollie, R. C. Seewald, L. E. Cornelisse, and L. M. Jenstad, "Validity and repeatibility of level-independent HL to SPL transforms," Ear and Hearing, Vol. 19, No. 5, pp. 407 – 413, May 1998.

[20] K. T. Kavanach, W. D. Domico, P. L. Crews, and V. A. Mccormick, "Comparison of the intrasubject repeatability of auditory brain stem and middle latency responses elicited in young children," The Annals of Otology, Rhinology & Laryngology, Vol. 97, No. 3, Part 1, pp. 264 – 471, May-June 1988.

[21] J. L. Lauter and R. G. Karzon, "Individual differences in auditory electric responses: comparisons of between-subject and within subject variability. IV. Latency-variability comparisons in early, middle, and late response," Scandinavian Audiology, Vol. 19, No. 4, pp. 175 – 182, October 1990.

[22] F. E. Musiek and K. M. Gollegly, "ABR in eighth nerve and low brainstem lesions," in J. T. Jacobson, The auditory brainstem response. San Diego, USA: College Hill Press, Chapter 10, pp. 181 – 202, 1985.

[23] G. E. Lynn and N. P. Verma, "ABR in upper brainstem lesions," in J. T. Jacobson, The auditory brainstem response. San Diego, USA: College Hill Press, Chapter 11, pp. 203 – 217, 1985.

[24] P. A. Despland and R. Galambos, "The auditory brainstem response (ABR) is a useful diagnostic tool in the intensive care nursery," Pediatric Research, Vol. 14, No. 2, pp. 154 – 158, February 1980.

[25] W. H. Martin and Y. Shi, "Intraoperative neurophysiology: monitoring auditory evoked potentials," in J. Katz, L. Medwetsky, R. Burkard, and L. Hood, Handbook of clinical audiology. Baltimore, USA: Lippincott Williams and Wilkins, Chapter 16, pp. 351 - 372, 2009.

[26] A. R. Moller, "Intraoperative neurophysiological monitoring," in R. J. Roeser, M. Valente, and H. Hosford-Dunn, Audiology diagnosis. New York, USA: Thieme, Chapter 23, pp. 545 – 570, 2000.

[27] K. A. Beauchaine, M. P. Gorga, J. K. Reiland, and L. L. Larson, "Application of ABRs to the hearing-aid selection process: Preliminary data," Journal of Speech and Hearing Research, Vol. 29, No. 1, pp. 120 – 128, March 1986.

[28] J. Kiessling, “Hearing aid selection by brainstem audiometry,” Scandinavian Audiology, Vol. 11, No. 4, pp. 269 – 275, July 1982.

[29] T. M. Mahoney, “Auditory brainstem response hearing aid applications,” in The auditory brainstem response. edited by J. T. Jacobson, San Diego, USA: College Hill Press, Chapter 19, pp. 349 – 370, 1985.

[30] K. E. Hecox, “Role of auditory brain stem response in the selection of hearing aids,” Ear and Hearing, Vol. 4, No. 1, pp. 51 – 55, January/February 1983.

[31] M. Hämäläinen, R. Hari, R. J. Ilmoniemi, J. Knuutila, and O.V. Lounasmaa, “Magnetoencephalography. Theory, instrumentation, and applications to the noninvasive study of human brain function,” Reviews of Modern Physics, Vol. 65, No.2, pp. 413 – 398, April 1993.

[32] J. L. Lauter, P. Herscovitch, C. Formby, and M. E. Raichle, “Tonotopic organization in human auditory cortex revealed by positron emission tomography,” Hearing Research, Vol. 20, No. 3, pp. 199 – 205, August 1985.

[33] L. Jancke, N. Gaab, T. Wustenberg, H. Scheich, and H.-J. Heinze, “Short-term functional plasticity in the human auditory cortex: an fMRI study,” Cognitive Brain Research, Vol. 12, No.3, pp. 479 – 485, December 2001.

[34] E. Budinger, A. Laszcz, H. Lison, H. Scheich, and F. W. Ohl, “Non-sensory cortical and subcortical connections of the primary auditory cortex in Mongolian gerbils: Bottom-up and top-down processing of neuronal information via field AI,” Brain Research, Vol. 1220, No. 1, pp. 2 – 32, July 2008.

[35] A. R. Moller and P. J. Jannetta, “Neural generators of the auditory brainstem response,” in J. T. Jacobson, The auditory brainstem response. San Diego, USA: College Hill Press, Chapter 2, pp. 13 - 32, 1985.

[36] H. Dillon, Hearing aids. Turramurra, Australia: Boomerang Press, 2000.

[37] A. Schaub, Digital hearing aids. New York, USA: Thieme Medical Publishers, Inc., 2008.

[38] P. C. Loizou, “Introduction to cochlear implants,” IEEE Engineering in Medicine and Biology Magazine, Vol. 18, No. 1, pp. 32 – 42, January/February 1999.

[39] J. N. Fayad, S. R. Otto, R. V. Shannon, and D. E. Brackmann, “Cochlear and brainstem auditory prostheses “Neural interface for hearing restoration: Cochlear and brain stem implants”” Proceedings of the IEEE, Vol. 96, No. 7, pp. 1085 – 1095, July 2008.

[40] A. R. Moller, “Neurophysiologic basis for cochlear and auditory brainstem implants,” American Journal of Audiology, Vol. 10, No.2, pp. 68 – 77, December 2001.

[41] K. B. Jackson, G. Mark, J. Helms, J. Mueller, and R. Behr, “An auditory brainstem implant system,” American Journal of Audiology, Vol. 11, No.2, pp. 128 – 133, December 2002.

[42] H. H. Lim, T. Lenartz, G. Joseph, R. D. Battmer, A. Samii, M. Samii, J. F. Patrick, and M. Lenarz, “Electrical stimulation of the midbrain for hearing restoration: Insight into the functional organization of the human central auditory

system," The Journal of Neuroscience, Vol. 27, No. 49, pp. 13541 – 13551, December 2007.

[43] B. L. Mersky, "Method and apparatus for endodontically augmenting hearing," US Patent 5,033,999, July 31, 1991.

[44] E. Aharon, "Israel's Audiodent invents hearing aid for the mouth," edited by N. Blackburn, ISRAEL21c Technology, www.israel21c.com, April, 2007.

[45] S. Gelfand, Essentials of audiology. New York, USA: Thieme Medical Publishers, Inc., 2009.

[46] R. Burkard and K. McNerney, "Introduction to auditory evoked potentials," in J. Katz, L. Medwetsky, R. Burkard, and L. Hood, Handbook of clinical audiology. Baltimore, USA: Lippincott Williams and Wilkins, pp. 222 - 241, 2009.

[47] M. P. Gorga, J. K. Reiland, and K. A. Beauchaine, "Auditor brainstem responses in a case high frequency conductive hearing loss," Journal of Speech and Hearing Disorders, Vol. 50, No.1, pp. 346 – 350, November 1985.

[48] J. W. Hall and P. J. Antonelli, "Assessment of peripheral and central auditory function," in B. J. Bailey, J. T. Johnson, and S. D. Newlands, Head & neck surgery – otolaryngology. Maryland, USA: Lippincott Williams & Wilkins, pp.1927 - 1942 2006.

[49] H. Levitt, "A historical perspective on digital hearing aids: how digital technology has changed modern hearing aids," Trends in amplification, vol. 11, no. 1, pp. 7 – 24, March 2007.

[50] A. M. Tharpe, L. Eiten, and S. A. Gabbard, "Hearing technology," Seminars in Hearing, Vol. 29, No. 2, pp. 169 – 177, May 2008.

[51] J. J. DiGiovanni, Hearing aid handbook 2008-2009. New York, USA: Delmar, 2008.

[52] D. M. Chabries, D. V. Anderson, T. G. Stockham, and R. W. Christiansen, "Application of a human auditory model to loudness perception and hearing compenstion," IEEE International Conference on Acoustics, Speech, and Signal Processing, Vol. 5, pp. 3527 – 3530, Detroit, Michigan, USA, May 1995.

[53] D. V. Anderson, R. W. Harris, and D. M. Chabries, "Evaluation of a hearing compensation algorithm," IEEE International Conference on Acoustics, Speech, and Signal Processing, Vol. 5, pp. 3531 - 3533, Detroit, Michigan, USA, May 1995.

[54] J. Bondy, S. Becker, I. Bruce, L. Trainor, and S. Haykin, "A novel signal processing strategy for hearing-aid design: neurocompensation," Signal Processing, Vol. 84, No. 7, pp. 1239 – 1253, July 2004.

[55] L.H. Carney, "A model for the responses of low frequency auditory-nerve fibers in cat," Journal of the Acoustical Society of America, Vol. 99, No.1, pp. 401–417, January 1993.

[56] D. Byrne and H. Dillon, "The National Acoustic Laboratories (NAL) new procedure for selecting the gain and frequency responses of a hearing aid", Ear and Hearing, Vol. 7, No. 4, pp. 257 – 265, August 1986.

[57] M. Valente, Strategies for selecting and verifying hearing aid fittings. New York, , USA: Thieme, 2002.

[58] R. E. Sandlin, Textbook of hearing aid amplification: Technical and clinical considerations. Kentucky, USA: Cengage Learning, 2000.

[59] H. Tobin, Practical hearing aid selection and fitting. Baltimore, Maryland, USA: Veteran Health Administration, 1997.

[60] MAICO Diagnostic, Operation instruction MB21. Berlin, Germany: MAICO Diagnostic GMBH, 2003.

[61] J. J. Hopfield, "Neurons with graded response have collective computational properties like those of two-state neurons," Proceedings of the National Academy of Sciences of the United States of America, Vol. 81, No. 10, pp. 3088 – 3092, May 1984.

[62] J. J. Hopfield and D. W. Tank, "Neural computations of decisions in optimization problems," Biological Cybernetics, Vol. 52, No. 1, pp. 141 – 152, 1985.

[63] A. E. Gelperin, J. J. Hopfield, and D. W. Tank, "The logic of Limax learning," in : Model neural networks and behavior. edited by A. Selverston, New York, USA: Plenum Press, 1985.

[64] D. V. Tank and J. J. Hopfield, "Simple "neural" optimization networks: An A/D converter, signal decision circuit, and a linear programming circuit," IEEE Transactions on Circuits and Systems, Vol. 33, No. 5, pp. 533 – 542, May 1986.

[65] M. Saggar, T. Mericli, S. Andoni, and R. Miikkulainen, "System identification for the Hodgkin-Huxley model using artificial nerural networks," Proceedings of International Joint Conference on Neural Networks, Orlando, Florida, USA, pp. 2239 – 2244, August 2007

[66] K. S. Narendra and K. Parthasarathy, "Identification and control of dynamical systems using neural networks," IEEE Transactions on Neural Networks, Vol. 1, No. 1, pp. 4 – 27, March 1990.

[67] C. Q. Zhang and M. Sami Fadali, "Nonlinear system identification using a Gabor/Hopfield Network," IEEE Transactions on Systems, Man, and Cybernetics-Part B: Cybernetics, Vol. 26, No. 1, pp. 124 – 135, February 1996.

[68] K. Funahashi and Y. Nakamura, "Approximation of dynamical systems by continous time recurrent neural networks," Neural Networks, Vol. 6, No. 6, pp. 801 – 806, August 1993.

[69] J. J. Paulos and P. W. Hollis, "Neural networks using analog multipliers," IEEE International Symposium on Circuits and Systems, Vol. 1, pp. 499 – 502, June 1988.

[70] R. W. Newcomb and J. D. Lohn, "Analog VLSI for neural networks," in Handbook of brain theory and neural networks. edited by M. Arbib, Massachusetts, USA: Bradford Books, MIT Press, 1995.

[71] C. Mead, Analog VLSI and neural systems. Massachusetts, USA: Addison Wesley Publishing Company, 1989.

[72] H. Demuth, M. Beale, and M. Hagan, Neural network toolbox – User's guide. Massachusetts, USA: The Mathworks Inc., 2009.

[73] M. Hagan, H. Demuth, and M. Beale, Neural network design. Colorado, USA: University of Colorado Bookstore, 2002.

[74] L. Ljung, System identification toolbox – User's guide. Massachusetts, USA: The Mathworks Inc., 2009.

[75] V. Z. Marmarelis, Nonlinear dynamic modeling of physiological systems. New Jersey, USA: John Wiley & Sons, Inc., 2004.

[76] L. Ljung, System identification 2nd edition: Theroy for the user, New Jersey, USA: Prentice Hall, 1999.

[77] T. Soderstorm and P. Stoica, System identification. Hertfordshire, UK: Prentice Hall International Series in Systems and Control Engineering edited by M. J. Grimble, 1989.

[78] O. Nelles, Nonlinear system identification: From classical approaches to neural networks and fuzzy models. New York, USA: Springer, 2000.

[79] X. He and H. Asada, "A new method for identifying orders of input-output models for nonlinear dynamic systems," Proceedings of the American Control Conference, pp. 2520 – 2523, California, USA, June 1993.

[80] L. Stragner and G. Horvath, "Improved model order estimation for nonlinear dynamic systems," IEEE International Workshop on Intelligent Data Acquisition and Advanced Computing Systems: Technology and Applications, Lviv Ukraine, pp. 266 – 271, September 2003.

[81] M. Norgaard, O. Ravn, N. K. Poulsen, L. K. Hansen, Neural networks for modeling and control of dynamic systems. New York, USA: Springer, 2001.

[82] M. Norgaard, Neural network based system identification toolbox, Technical report. Copenhagen, Denmark: Department of Automation, Technical University of Denmark, 2000.

[83] V. Rouss, W. Charon, and A. Desflots, "Characterisation of mechanical non-linearities in a proton exchange membrane fuel cell using raw data," International Journal of Hydrogen Energy, Vol. 34, No. 5, pp. 2377 – 2386, March 2009.

[84] J. S. Wang, Y. L. Hsu, H. Y. Lin, and Y. P. Chen, "Minimal model dimension/order determination algorithms for recurrent neural networks," Pattern Recognition Letters, Vol. 30, No. 9, pp. 812 – 819, July 2009.

[85] B. O'Brien, J. Dooley, A. Zhu, and T. J. Brazil, "Estimation of memory length for RF power amplifier behavioral models," Proceedings of the 36th European Microwave Conference, pp. 680 – 682, Manchestor, UK: September 2006.

[86] J. E. Dennis Jr. and R. B. Schnabel, Numerical methods for unconstrained optimization and nonlinear equations. New York, USA: Prentice-Hall, 1983.

[87] R. Fletcher, Practical methods of optimization. New York, USA: John Wiley & Sons, 1987.

[88] T. F. Coleman and Y. Zhang, Optimization toolbox – User's guide. Massachusetts, USA: The Mathworks Inc., 2009.

[89] A. Hodge, W. Zhen, and R. W. Newcomb, "On the inverse of Hopfield-type dynamical neural networks," Proceedings of the 29th Asilomar Conference on Signals, Systems, and Computers, Pacific Groves, CA, USA, pp. 881 – 884, October, 1995.

[90] L. Sellami and R. W. Newcomb, "An inverse Hollis-Paulos artificial neural network," IEEE Transaction on Neural Networks, Vol. 9, No. 5, pp. 979 – 986, September 1998.

[91] L. A. Zadeh and C. A. Desoer, Linear system theory The state space approach, New York, USA: McGraw Hill Inc., pp. 67 – 120, 1963.

[92] R. M. Hirschorn, "Invertibility of nonlinear control system," Society for Industrial and Applied Mathmaticas (SIAM) Journal of Control and Optimization, Vol. 17, No. 2, pp. 289 – 297, March 1979.

[93] G. Strang, Introduction to linear algebra. Massachusetts, USA: Wellesley Cambridge, 2003.

[94] D. R. Stapells, A. Herdman, S. A. Small, A. Dimitrijevic, and J. Hatton, "Current status of the auditory steady state response and tone evoked auditory brainstem response for estimating an infant's audiogram," A sound foundation through early amplification: Proceedings of an international conference 2004 edited by R. C. Seewald, and J. M. Bamford, Chicago, Illinois, USA: Phonak AG, Chapter 3, pp. 43 – 59, November 2004.

[95] M. P. Stueve and C. O'Rourke, "Estimation of hearing loss in children: comparison of auditory statedy-state response, auditory brainstem response, and behavioral test methods," American Journal of Audiology, Vol. 12, No. 2, pp. 125 – 136, December 2003.

[96] S. C. Purdy, R. Katsch, H. Dillon, L. Storey, M. Sharma, and K. Agung, "Aided Cortical auditory evoked potentials for hearing instrument evaluation in infants," in A sound foundation through early amplification: Proceedings of an international conference 2004 edited by R. C. Seewald, and J. M. Bamford, Chicago, Illinois, USA: Phonak AG, Chapter 3, pp. 115 – 127, November 2004.

[97] P. E. Souza and K. L. Tremblay, "New perspectives on assessing amplification effects," Trends in amplification, vol. 10, no. 3, pp. 119 – 143, September 2006.

[98] K. L. Tremblay, "Hearing aids and the brain: What's the connection?", The Hearing Journal, Vol. 59, No. 8, pp. 10 – 17, August 2006.

[99] P. R. Kileny and M. G. Magathan, "Predictive value of ABR in infants and children with moderate to profound hearing impairment," Ear and Hearing, Vol. 8, No. 4, pp. 217 – 220, August 1987.

[100] H. Dillon, "So, baby, how does it sound? Cortical assessment of infants with hearing aids," The Hearing Journal, Vol. 58, No. 10, pp. 10 – 17, October 2005.

[101] Phonak, Product brochure and technical data: Audeo YES behind-the-ear hearing aid. Illinois, USA: Phonak, Inc. 2009.

[102] Phonak, Product brochure and technical data: Exelia Art Micro Petite behind-the-ear hearing aid. Illinois, USA: Phonak, Inc. 2009.

[103] H. H. Jaspers, "The ten-twenty electrode system of the internation federation," Internal Federation of Clinical Neurophysiology: Recommendations for the practice of clinical electroencephalography edited by G. Deuschl and A. Eisen, Amsterdam, Germany: Elsevier, pp. 3-10, 1983

[104] R. Oostenveld and P. Praamstra, "The five percent electrode system for high-resolution EEG and ERP measurements," Clinical Neurophysiology, Vol. 112, No. 4, pp. 713 – 719, April 2001.

[105] E. Liebenthal, M. L. Ellingson, M. V. Spanaki, T. E. Prieto, K. M. Ropella, and J. R. Binder, "Simultaneous ERP and fMRI of the auditory cortex in a passive oddball paradigm," NeuroImage, Vol. 19, No. 4, pp. 1395 – 1404, August 2003.

[106] C. J. Scarff, A. Reynolds, B. G. Goodyear, C. W. Ponton, J. C. Dort, and J. J. Eggermont, "Simultaneous 3-T fMRI and high density recording of human auditory evoked potentials," NeuroImage, Vol. 23, No. 3, pp. 1129 – 1142, November 2004.

[107] J. A. Kaltenbach, J. Zhang, and P. Finlayson, "Tinnitus as a plastic phenomenon and its possible neural underpinnings in the dorsal cochlear nucleus," Hearing Research, Vol. 206, No. 1-2, pp. 200 – 226, August 2005.

[108] T. Tzounopoulos, "Mechanisms of synaptic plasticity in the dorsal cochlear nuclues: Plasticity-induced changes that could underlie tinnitus," American Journal of Audiology, Vol. 17, No. 2, pp. S170 – S175, December 2008.

[109] J. A. Kaltenbach and D. A. Godfrey, "Dorsal cochlear neclues hyperactivity and tinnitus: Are they related?," American Journal of Audiology, Vol. 17, No. 2, pp. S148 – S161, December 2008.

[110] W. Muhlnickel, T. Elbert, E. Taub, and H. Flor, "Reorganization of auditory cortex in tinnitus," Proceedings of the National Academy of Sciences, Vol. 95, pp. 10340 – 10343, August 1998

[111] S. M. Bowyer, M. Seidman, K. Elisevich, D. De Ridder, K. M. Mason, J. Dria, Q. Jiang, and I. Darrat, "MEG localization of the putative cortical generators of tinnitus," International Congress Series, Vol. 1300, pp. 33 – 36, June 2007.

[112] T. Yoshiura, S. Ueno, K. Iramina, and K. Masuda, "Source localization of middle latency auditory evoked responses using MEG and MRI techniques," IEEE Engineering in Medicine and Biology Society, Vol. 1, pp. 606 – 607, Baltimore, Maryland, USA, November 1994.

[113] F. Fregni, R. Marcondes, P. S. Boggio, M. A. Marcolin, S. P. Rigonatti, T. G. Sanchez, M. A. Nitsche, and A. Pascual-Leone, "Transient tinnitus suppression induced by repetitive transcranial magnetic stimulation and transcranial direct current stimulation," European Journal of Neurology, Vol. 13, No. 9, pp. 996 – 1001, September 2006.

[114] T. Wagner, A. Valero-Cabre, A. Pascual-Leone, "Noninvasive human brain stimulation," The Annual Review of Biomedical Engineering, Vol. 9, pp. 527 – 565, August 2007.

[115] D. M. Baguley, "Tinnitus: recent insights into mechanism, models, and therapies," The Hearing Journal, Vol. 59, No. 5, pp. 10 – 15, May 2006.

[116] J. W. Hall, S. H. Morgan, J. Mackey-Hargadine, E. A. Aguilar, and R. A. Jahrsdoerfer, "Neuro-otologic applications of multi-channel auditory brainstem response recordings," Laryngoscope, Vol. 94, No. 7, pp. 883 – 889, July 1984.

[117] M. H. Choudhury and A. Barreto, "A recording system for the study of tinnitus through auditory evoked potentials," IEEE Engineering in Medicine and

Biology Society Conference on Neural Engineering, pp. 675 – 678, Washington D.C., USA, March 2005.

[118] W. H. Hayt and J. E. Kemmerly, Engineering circuit analysis. New York, USA: McGraw-Hill Inc., 1993.

[119] J. G. Tront, PSpice for basic circuit analysis. New York, USA: McGraw-Hill Inc., 2005.

[120] M. Bialko and R. W. Newcomb, "Generation of all finite linear circuits using the integrated DVCCS", IEEE Transactions on Circuit Theory, Vol. 18, No. 6, pp. 733 – 736, November 1971.

[121] A. M. Hodge and R. W. Newcomb, "Semistate theory and analog VLSI design," IEEE Circuits and Systems Magazine, Vol. 2, No. 2, pp. 30 – 51, Second Quarter 2002.

[122] A. S. Sedra and K. C. Smith, Microelectronic Circuits, 4th edition. New York, USA: The Oxford Series in Electrical and Computer Engineering, Oxford University Press, 1987.

[123] Z. Wang, "2-MOSFET transresistor with extremely low distortion for output reaching supply voltage," Electronic Letter, Vol. 26, No. 13, pp. 951 – 952, 1990.

[124] R. J. Wiegerink, "A CMOS four quadrant analog current multiplier," IEEE International Symposium on Circuits and Systems, Vol. 4, pp. 2244 – 2247, Singapore, June 1991.

[125] G. Palmisano and S. Pennisi, "New CMOS tunable transconductor for filtering applications," IEEE International Symposium on Circuits and Systems, Vol.1, pp. 196-199, Sydney, Australia, May 2001.

[126] Y. Tsividis, Operation and modeling of the MOS transistor, 2nd edition, New York, USA: McGraw-Hill, 1999.

[127] W. J. Wilson, M. Winter, C. Nohr, and F. Aghdasi, "Signal processing of the auditory brainstem response: clinical effects of variations in fast fouriere transform analysis," Proceedings of the 1998 South African Symposium on Communication and Signal Processing, pp. 23 – 28, Rondebosch, September 1998.

[128] N. Russo, T. Nicol, G. Musacchia, and N. Kraus, "Brainstem responses to speech syllables," Clinical Neurophysiology, Vol. 115, No. 9, pp. 2021 – 2030, September 2004.

[129] I. Akhoun, S. Gallego, A. Moulin, M. Menard, E. Veuillet, C. Berger-Vachon, L. Collet, and H. Thai-Van, "The temporal relationship between speech auditory brainstem reponses and the acoustic pattern of the phoneme /ba/ in normal hearing adults," Clinical Neurophysiology, Vol. 119, No. 4, pp. 922 – 933, April 2008.

[130] C. King, C. M. Warrier, E. Hayes, and N. Kraus, "Deficits in auditory brainstem pathway encoding of speech sounds in children with learning problems," Neuroscience Letters, Vol. 319, No. 2, pp. 111 – 115, February 2002.

[131] K. Gordon, B. Papsin, and R. Harrison, "Auditory brainstem activity and development evoked by apical versus basal cochlear implant electrode stimulation in children," Clinical Neurophysiology, Vol. 118, No. 8, pp. 1671 – 1684, August 2007.

[132] C. Pantev, B. Ross, A. Wollbrink, M. Riebandt, K. W. Delank, E. Seifert, and A. Lamprecht-Dinnesen, “Acoustically and electrically evoked responses of the human cortex before and after cochlear implantation,” Hearing Research, Vol. 171, No. 1-2, pp. 191 – 195, September 2002.